

DISS. ETH NO. 28822

WEARABLE INERTIAL SENSORS TO ASSESS ACTIVITIES OF DAILY LIVING IN INDIVIDUALS UNDERGOING NEUROREHABILITATION

A thesis submitted to attain the degree of
DOCTOR OF SCIENCES of ETH ZURICH
(Dr. sc. ETH Zurich)

presented by

Charlotte Sophie Werner

M.Sc. in Mechanical Engineering
ETH Zurich

born 26.07.1994
citizen of Germany

accepted on the recommendation of
Prof. Dr. Robert Riener
Prof. Dr. med. Armin Curt
Dr. Olivier Lamercy
Prof. Dr. Thomas Seel

2022

“It would be possible to describe everything scientifically, but it would make no sense.

It would be a description without meaning —
as if you described a Beethoven symphony as a variation of wave pressure.”

— Albert Einstein

Acknowledgements

This work would not have been possible without the continuous support from my supervisors, colleagues, collaborators, friends and family to whom I would like to express my genuine gratitude and appreciation.

First of all, I would like to thank my thesis committee: Robert Riener, Armin Curt, Olivier Lambercy, and Thomas Seel. Many thanks to Robert Riener, for taking over the role as the official ETH supervisor and his precious feedback during the last steps of my PhD. Further, I am extremely grateful to Armin Curt, for granting me the opportunity to pursue my PhD, for his genuine interest in my work, and for challenging me with his clinical perspective. I would like to extend my gratefulness to Olivier Lambercy, for his extensive support both personally and scientifically over the past years, especially given the extraordinary circumstances. Thanks to Thomas Seel, for letting me gain new perspectives on my work during my time spent at his laboratory and the profound insights on sensor technology.

Further, I would like to thank my immediate colleagues. Many thanks to László Demkó for always offering help over the past years. I deeply thank Irina Lerch and Anita Linke for their tremendous support on data collection and their precious therapist perspectives on my work. Further, I would like to thank all of my collaborators. Special thanks goes to Chris Awai Easthope, for believing in my work from the beginning, for opening up new avenues for projects and for your continuous support. Thanks to Fabian Rast, I am grateful that I had the opportunity to be involved in his exciting project. Thanks to Josef Schönhammer, Freschta Zipser-Mohammadzada, Jan Meyer, Romina Willi, Marc Bollinger, Björn Zörner, Wiebe de Vries, Prisca Eser, and Catherine Jutzeler for providing a collaborative and open-minded research environment. In addition, I would like to thank my students Sarah Hermann, Riccardo Femiano, Selina Weber, Lea Cebulla, Ugne Kari, Sabrina Amrein, and Meltem Gönel. It was a pleasure working with all of you.

I thank all members of the Spinal Cord Injury Center and the Rehabilitation Engineering Laboratory for providing an inspiring working environment. Thank you for the many fruitful scientific discussions during the research seminars or the 'competence group assessment' meetings. Also, I truly enjoyed spending time with you during extended lunch breaks or at countless social events. A very special thanks goes to Roger Gassert for incorporating me in his lab environment, for his great supervision, and for being an inspiring person in many ways. I

Acknowledgements

am further deeply thankful to Sophie Schneider, for fascinating me for this exciting project and for supporting me on my way and throughout my doctorate.

A big thank you to all the people who participated in the measurements. Further, I am grateful for the financial support, which was mainly given by the International Foundation for Research in Paraplegia (IRP) and the Swiss State Secretariat for Education, Research and Innovation (Seri, Horizon 2020).

Finally, I wish to thank my friends, for always listening to my troubles and celebrating my achievements. A special thanks goes to Dorian Henning, for the confidence you give me, the unconditional support and for having an ear for me in challenging and joyful moments. I would like to extend my deepest gratitude to my family, especially my parents, who have always encouraged and supported me to realize my aspirations.

I thank everyone who made this thesis possible!

Zurich, October 2022

Charlotte Werner

Abstract

The main long-term rehabilitation goal of patients with a neurological injury is to achieve the highest possible functional independence with respect to the level of the patient's impairments. On the way to achieve this goal, clinical decision making is often difficult due to the complex symptoms and the diverse outcome possibilities. This implies that therapy programs must be tailored for each patient. A comprehensive assessment helps to better understand the status of the patient, the effect of clinical interventions, and can provide guidelines for individualized rehabilitation goals. In today's standard clinical practice, the therapists and clinicians perform assessments continuously during rehabilitation by choosing standardized tests. Limitation of these conventional assessments include ceiling or flooring effects, poor sensitivity, and subjectiveness. Besides other devices, wearable inertial sensors offer a solution to address these issues. The small and affordable sensors can be attached to the body to provide objective digital metrics on movements of interest. Hence, inertial measurement units offer the unique possibility to unobtrusively assess activities of daily living not limited to a standardized setting. Nevertheless, the widespread adaptation of such setups for technological-aided assessments in the clinical routine has yet to be realized.

The aim of this thesis is to provide digital health metrics from a sparse inertial sensor setup to assess daily life-like activities for patients undergoing neurorehabilitation. These metrics are expected to extend conventional assessments by providing more objective and detailed measures on the movement profiles. Hence, limitations in performing these activities can be assessed more precisely than using conventional methods which is highly relevant regarding the patient's mobility and independence. Three key activities of daily living, namely walking, wheeling and grasping, were selected and a suitable inertial sensor setup was chosen for each activity. Novel algorithms were developed to extract digital metrics related to each activity. Further, these metrics are used in combination with machine learning methods to characterize patients and to propose roadmaps to integrate these metrics into clinical routine and decision making by suggesting therapy goals.

A sensor-based gait analysis has been developed specifically for individuals with an incomplete spinal cord injury. These patients often suffer from diverse gait deficits depending on the location and severeness of the injury but in the current clinical routine walking function is only assessed by simple timed gait tests. The sensor-based gait analysis would allow a more comprehensively characterization of walking for a more targeted therapy approach and better

Acknowledgements

estimation of walking recovery. The algorithm derives typical spatio-temporal gait metrics from shank-mounted inertial sensors robustly for various gait profiles walking at slow (0.3m/s) and preferred (0.76 ± 0.17 m/s) walking speeds. The robustness was achieved by automatically adapting thresholds of the algorithm to the individual gait profiles. This sensor-based gait analysis was used on a dataset of 66 spinal cord injury patients and 20 healthy controls performing a standardized walking test. Using unsupervised machine learning, distinct clusters with similar gait profiles were identified. Abnormal gait metrics were derived for each cluster, their composition was characterized with respect to clinical scores, and recommendations for a targeted physiotherapy were given. Further, including sensor-derived metrics in a prediction model, improved the performance of the predictor by 10% on estimating whether a patient will improve his walking capacity in the future or not.

Overuse injuries and pain in the upper extremities is a common problem in wheelchair users and can be linked to the wheeling technique. In order to objectively measure the propulsion technique, a novel wheeling algorithm was developed to estimate wheeling propulsion patterns from a sparse inertial sensor setup. The algorithm was applied to data of 41 wheelchair-bound individuals. In line with current research, four dominant wheeling patterns could be identified, which are associated with different risks of developing upper limb injuries. Further, more experienced wheelers showed more efficient and less harmful wheeling patterns.

The Action Research Arm test is the most prominent tool to assess grasping function, but is tedious to perform and requires trained personnel. A method was presented to instrument this assessment by estimating the clinical scores from wrist-bound inertial sensor data. A dataset of 21 individuals with stroke was used to train an ordinal classifier for estimating the task scores, achieving an accuracy of around 80%. The method showed a clear potential to pave the way towards minimally supervised assessments.

In conclusion, this thesis contributes to establishing technological-aided assessments for neurorehabilitation by providing clinically meaningful, accurate, and reproducible metrics derived from an affordable setup. Finally, the proposed system and methodologies offer the possibility to assess activities of daily living in an unrestricted setting. Previously, this was only possible in standardized setting and dependent on therapist ratings. In the future, comprehensive clinical outcome measures of treatments or therapies could be provided either under minimal supervision or even in their own habitual environment.

Zusammenfassung

Das wichtigste langfristige Rehabilitationsziel für Patienten mit einer neurologischen Verletzung ist das Erreichen der größtmöglichen Unabhängigkeit unter Berücksichtigung des Grades der Beeinträchtigung des Patienten. Allerdings ist die klinische Entscheidungsfindung aufgrund der komplexen Symptome und der unterschiedlichen Ergebnismöglichkeiten oft schwierig. Dies bedeutet, dass die Therapieprogramme auf jeden einzelnen Patienten zugeschnitten sein müssen. Ein umfassendes Assessment hilft, den Zustand des Patienten und die Wirkung klinischer Maßnahmen besser zu verstehen, und kann Leitlinien für individuelle Rehabilitationsziele liefern. In der heutigen klinischen Praxis führen Therapeuten und Kliniker während der Rehabilitation kontinuierlich Assessments mithilfe standardisierter Tests durch. Zu den Einschränkungen dieser konventionellen Tests gehören Ceiling- oder Flooringeffekte, geringe Empfindlichkeit und Subjektivität. Inertialsensoren bieten neben anderen Tools eine Lösung für diese Probleme. Die kleinen und bezahlbaren Sensoren können am Körper befestigt werden und liefern objektive digitale Metriken über die Bewegungen von Interesse. Inertiale Sensoren bieten daher die einzigartige Möglichkeit, Aktivitäten des täglichen Lebens unauffällig und nicht auf ein standardisiertes Umfeld beschränkt zu bewerten. Die breite Anwendung solcher Geräte für technologiegestützte Assessments in der klinischen Routine steht jedoch noch aus.

Das Ziel dieser Arbeit ist es, digitale Gesundheitsmetriken aus einem spärlichen Sensor-Setup bereitzustellen, um alltagsnahe Aktivitäten für Patienten in der Neurorehabilitation zu bewerten. Diese Metriken sollen die herkömmlichen Assessments erweitern, indem sie objektivere und detailliertere Messungen der Bewegungsprofile liefern. So können die Einschränkungen bei der Durchführung dieser Aktivitäten genauer als mit herkömmlichen Methoden bewertet werden, was für die Mobilität und Unabhängigkeit des Patienten von großer Bedeutung ist. Drei Schlüsselaktivitäten des täglichen Lebens, nämlich Gehen, Rollstuhlfahren und Greifen, wurden ausgewählt und für jede Aktivität wurde ein geeignetes Sensor-Setup gewählt. Es wurden neuartige Algorithmen entwickelt, um digitale Metriken für jede Aktivität zu extrahieren. Darüber hinaus wurden diese Metriken in Kombination mit Methoden des maschinellen Lernens verwendet, um Patienten zu charakterisieren und um Pläne vorzuschlagen, diese Metriken in die klinische Routine und Entscheidungsfindung zu integrieren.

Eine sensorbasierte Ganganalyse wurde speziell für Personen mit einer inkompletten Rückenmarksverletzung entwickelt. Diese Patienten leiden je nach Ort und Schwere der Verletzung

Acknowledgements

oft unter verschiedenen Gangstörungen. Doch in der derzeitigen klinischen Routine wird die Gehfunktion nur durch einfache Gehtests beurteilt. Die sensorbasierte Ganganalyse würde eine umfassendere Charakterisierung des Gehens für einen gezielteren Therapieansatz und eine bessere Abschätzung der Geherholung ermöglichen. Der Algorithmus leitet typische Gangmetriken von am Knöchel montierten Inertialsensoren robust für verschiedene Gangprofile bei langsamen ($0,3\text{m/s}$) und bevorzugten ($0,76 \pm 0,17\text{m/s}$) Gehgeschwindigkeiten ab. Die Robustheit wurde durch automatische Anpassung der Schwellenwerte des Algorithmus an die einzelnen Gangprofile erreicht. Diese sensorbasierte Ganganalyse wurde auf einen Datensatz von 66 Patienten mit Rückenmarksverletzungen und 20 gesunden Kontrollpersonen angewendet, die einen standardisierten Gehtest absolvierten. Mithilfe von unüberwachtem maschinellem Lernen wurden verschiedene Cluster mit ähnlichen Gangprofilen identifiziert. Für jedes Cluster wurden abnormale Gangmetriken abgeleitet, ihre Zusammensetzung wurde im Hinblick auf klinische Scores charakterisiert, und es wurden Empfehlungen für eine gezielte Physiotherapie gegeben. Die Einbeziehung der Sensormetriken in ein Vorhersagemodell verbesserte die Genauigkeit um 10% bei der Einschätzung, ob ein Patient seine Gehfähigkeit in Zukunft verbessern wird oder nicht.

Überlastungsverletzungen und Schmerzen in den oberen Extremitäten sind ein häufiges Problem bei Rollstuhlfahrern und konnten mit der Fahrtechnik in Verbindung gebracht werden. Um die Antriebstechnik objektiv zu messen, wurde ein neuartiger Algorithmus zur Schätzung der Antriebstechnik von Rollstuhlfahrern anhand eines spärlichen Inertialsensor-Setup entwickelt. Der Algorithmus wurde auf die Daten von 41 Rollstuhlfahrer angewendet. Im Einklang mit der aktuellen Forschung konnten vier dominante Antriebstechniken identifiziert werden, die mit unterschiedlichen Risiken für Verletzungen der oberen Gliedmaßen verbunden sind. Außerdem zeigten erfahrenere Rollstuhlfahrer effizientere und weniger schädliche Fahrmuster.

Der Action-Research-Arm-Test ist das bekannteste Instrument zur Beurteilung der Greiffunktion. Er ist jedoch mühsam in der Durchführung und erfordert geschultes Personal. Es wurde eine Methode vorgestellt, mit der dieses Assessment durch Schätzung der klinischen Werte aus Daten von Inertialsensoren, die am Handgelenk befestigt sind, erfolgen kann. Anhand eines Datensatzes von 21 Personen mit Schlaganfall wurde ein ordinaler Klassifikator für die Schätzung der klinischen Werte trainiert. Eine Genauigkeit von etwa 80% wurde dabei erreicht. Die Methode zeigte ein deutliches Potenzial, den Weg zu minimal überwachten Assessments zu ebnen.

Diese Arbeit trägt dazu bei, technologiegestützte Assessments für die Neurorehabilitation zu etablieren, indem sie klinisch aussagekräftige, genaue und reproduzierbare Metriken liefert. Schließlich bieten das Sensorsetup und die Algorithmen die Möglichkeit, Aktivitäten des täglichen Lebens in einer uneingeschränkten Umgebung zu beurteilen. Bisher war dies nur in einer standardisierten Umgebung möglich und von den Bewertungen der Therapeuten abhängig. In Zukunft könnten umfassende klinische Assessments entweder unter minimaler Aufsicht oder sogar in der gewohnten Umgebung durchgeführt werden.

Contents

Acknowledgements	v
Abstract (English/Deutsch)	vii
1 Introduction	1
1.1 Sensorimotor deficits due to injuries of the central nervous system	1
1.2 The importance of assessments for neurorehabilitation	2
1.3 Limitations of conventional assessments	3
1.4 Wearable sensors as an opportunity for technology-aided assessments	3
1.5 Motion tracking using inertial measurement units	5
1.6 Open challenges of using inertial sensors for assessing activities of daily living .	5
1.7 Objectives and outline of this theses	6
2 Towards a Mobile Gait Analysis for Patients with a Spinal Cord Injury: A Robust Algorithm Validated for Slow Walking Speeds	9
2.1 Abstract	10
2.2 Introduction	11
2.3 Methods	12
2.4 Results	17
2.5 Discussion	25
2.6 Conclusion	27
3 Data-Driven Characterization of Walking after a Spinal Cord Injury using Inertial Sensors	29
3.1 Abstract	30
3.2 Introduction	31
3.3 Methods	32
3.4 Results	36
3.5 Discussion	41
3.6 Conclusion	44
4 Estimating Wheeling Propulsion Patterns using a Sparse Inertial Sensor Setup	47
4.1 Abstract	48
4.2 Introduction	49

Contents

4.3	Methods	50
4.4	Results	55
4.5	Discussion	59
4.6	Conclusion	61
5	Using Wearable Inertial Sensors to Estimate Clinical Scores of Upper Limb Movement Quality in Stroke	63
5.1	Abstract	64
5.2	Introduction	65
5.3	Methods	66
5.4	Results	70
5.5	Discussion	71
5.6	Conclusion	75
6	General Discussion	77
6.1	Synthesis of results with respect to objectives	77
6.2	Contributions to the field, outlook, and clinical impact	80
6.3	Overall conclusion	81
A	Appendix	83
A.1	Supplementary Material	83
A.2	Walking Report	88
A.3	Wheeling Report	91
	Bibliography	94
	Complete List of Publications	111

1 Introduction

Wearable inertial sensors in the form of activity trackers are a widely accepted and used tool in the lifestyle and fitness industry. Usually, the physical activity is quantified by simple metrics such as the number of steps per day. The sensors incorporated in these activity trackers started to gain interest in the research and medical field for motion analysis of patients with a movement disorder.

1.1 Sensorimotor deficits due to injuries of the central nervous system

Injuries to the central nervous system are amidst the leading causes of acquired adult disability [Ma et al., 2014, Katan and Luft, 2018, WHO, 2006]. CNS injuries cause heterogenous and complex symptoms depending on the location and severity. The CNS composes primarily the brain and the spinal cord, which connects the peripheral nervous system with the brain. Ascending and descending spinal pathways carry sensory or motor information, respectively. Mechanical traumas or non-traumatic injuries can cause damage to the spinal cord by interrupting these pathways [Dietz and Fouad, 2014]. This results in symptoms such as loss of muscle function, sensation and/or autonomic function depending on which spinal tracts were damaged and at which level of the spinal cord [Tator, 1995]. Injuries to the brain can also be caused due to a trauma, a so called traumatic brain injury (TBI), or non-traumatic with the most prominent example of stroke. Similar to a damage of the spinal cord, the symptoms of these injuries strongly depend on the affected locations of the CNS.

Functional recovery after a neurological injury is a combination of both neuronal recovery and behavioural compensation [Levin et al., 2009, Ramer et al., 2014]. The acute phase after the injury is characterized by immediate care, surgical interventions and the avoidance of secondary complications [Bourguignon et al., 2022]. The following chronic phase consists of a multidisciplinary treatment including physiotherapy, occupational therapy, psychologists, and more [Albert and Kesselring, 2012]. The most important goal during the chronic phase is to achieve the highest possible degree of independence and mobility for that patient in order

to reintegrate the patient back into society [Nas, 2015, WHO, 2006]. Besides the severity of the injury, factors such as age, weight, the general health status prior to the injury, motivation and spasticity influence achieving this goal. Even though an extensive rehabilitation program enables the patient to regain function, it often leads to lifelong disabilities that need to be considered when the patients is leaving the hospital [Katan and Luft, 2018, WHO, 2006]. Besides the socioeconomic burden, an injury of the CNS and the resulting disabilities impede the ability of the patient to perform activities of daily living and thus have a strong impact on the persons quality of life [Lawrence et al., 2001, Gooch et al., 2017, Ma et al., 2014, WHO, 2006].

1.2 The importance of assessments for neurorehabilitation

The extensive heterogeneity of patients with a CNS injury makes clinical decisions often difficult due to the complexity of symptoms and the diverse outcome possibilities [Nas, 2015]. Standardized assessments are used to identify the patients deficits [Albert and Kesselring, 2012]. More specifically, deficits are either assessed on the level of loss of body function and structures, activity limitations, or participation restriction according to the WHO framework of the International Classification of Functioning, Disability and Health (ICF) [WHO, 2001]. As an example for an assessment of loss of body function and structures, the impairment scale of the American Spinal Injury Association (AIS) captures the remaining sensor and motor function of different body parts by rating of a clinician [Kirshblum et al., 2011]. An example for an assessment of activity limitations is the Action Research Arm Test (ARAT), which consists of several reaching and grasping tasks that are rated by a therapist focusing on the task duration, task completion and observed movement quality [Yozbatiran et al., 2008]. A second example for an assessment of activity limitation are simple gait tests, such as the six-minute walking test, where the distance is measured that the patient is able to walk within 6 minutes [Hedel et al., 2005]. Restrictions in participation are often assessed by self-reported questionnaires, e.g. with the Stroke Specific Quality of Life Scale (SS-QOL) [Salter et al., 2005].

The heterogeneity of patients with a CNS injury implies that a one-fits-all treatment plan during rehabilitation is not applicable and therapy programs must be tailored for each patient [WHO, 2006]. The clinical decision-making process starts with identifying the deficits of the patients with a selection of suitable assessments [Albert and Kesselring, 2012]. This initial assessment helps to form a hypothesis on the patient recovery profile and to set realistic rehabilitation goals [Ryerson, 2009]. During the course of rehabilitation, patients are regularly re-assessed to revise treatment plans to the specific needs and progress of the patients [Bernhardt and Hill, 2005]. In summary, assessments should be ongoing, accurate, consistent and reproducible in order to be a helpful tool for clinical decision making [WHO, 2001]. In addition, health insurances include these clinical assessments outcomes into their decision on which kind of therapies and aids will be covered. And in research, assessments are typically used as primary outcome measures in clinical studies to evaluate the efficacy of novel intervention methods or as inclusion criteria [Stieglitz et al., 2021, Iolanda et al., 2018].

1.3 Limitations of conventional assessments

Conventional clinical assessments have several benefits [WHO, 2006, WHO, 2001]. The assessments are developed to be simple and intuitive to administer such that clinicians and therapists can easily learn and apply them to their patients. Conventional assessments are often time-based tasks or use an ordinal scale either dependent on a therapist's rating or by self-reporting of the patient with a questionnaire [Burrige et al., 2019]. Both, time-based tasks and ordinal scales, inherently have low inter-rater variability. Further, for most assessments, little or cheap material is needed, making it affordable for the clinics and fast to set up. In a research setting, conventional assessments are often preferred because normative data of healthy individuals or specific patient cohorts from other studies exist, which enables comparisons across cohorts and between interventions [Gladstone et al., 2002].

Conventional assessments have limitations not only in their application within the clinical routine but also in research settings [Lambercy et al., 2016]. For instance, any assessment takes time to perform and is thus conflicting with the tight schedule of clinicians and therapists. Therapists rather spend their time training the patient instead of performing an assessment, which is usually also in the patient's interest. Moreover, clinicians preferably rely on their experience when evaluating the patient's deficits and estimating the patient's recovery profile than on assessment-based outcome measures. Furthermore, while providing only a few or single outcome measures, most assessments fail to capture a complete view of the complex deficits of patients with a CNS injury [Burrige et al., 2019]. Consequently, assessments are only performed selectively and not as often as desired within the clinical routine. In a research setting, assessments with ordinal rating scales are often insufficient due to ceiling and/or flooring effects resulting in poor responsiveness for patients with low or high function [Gladstone et al., 2002]. Further, coarse rating scales result in overall poor sensitivity, making it difficult to track the subtle changes due to a novel intervention in these heterogeneous patient cohorts [Pollock et al., 2014]. Also, self-reported questionnaires suffer from recollection bias [Oung et al., 2015]. Given the limitations of conventional assessments, novel complementary tools are needed to provide a more comprehensive and accurate description of the patient's deficits [Shirota et al., 2019, Kanzler et al., 2020, Schwarz et al., 2019].

1.4 Wearable sensors as an opportunity for technology-aided assessments

Technological devices, such as sensors or other computational tools, could potentially address the limitations conventional assessments possess [Shirota et al., 2019, Kanzler et al., 2020]. They provide so-called digital health metrics as outcome measures, defined as measures extracted from a digital tool [Coravos et al., 2019, Goldsack et al., 2020, Vasudevan et al., 2022]. Digital health metrics have the potential to be more objective, rich, and sensitive outcome measures [Oung et al., 2015, Balasubramanian et al., 2012]. These metrics are typically derived by computing statistical features of the time series sensor data. Features are usually derived

Chapter 1. Introduction

from the time or frequency spectrum of the data. Given the plethora of feature options, numerous metrics can be extracted under the assumption to provide a more comprehensive picture of the patient's deficits than conventional assessments, which often rely on single measures. For example, standard clinical assessment could be instrumented with sensors to complement the assessment outcome [Storm et al., 2020]. Further, these digital metrics provide measures from a continuous scale, which is an advantage compared to the often used ordinary scales in conventional assessments. In general, continuous scales are more sensitive and suffer less from ceiling and flooring effects because they are not bounded. Finally, digital health metrics are more objective than assessment scores depending on therapist ratings. Examples of technological devices that can be used to assess movement disorders are robotic platforms, camera-based or marker-based motion tracking, and wearable sensors [Lambercy et al., 2016].

The key benefit of using robotic platforms for technological-aided assessments is the quality of the metrics they provide. Since the assessment itself is independent of a therapist and the movements are highly standardized or controlled, objective and precise metrics can be extracted [Kanzler et al., 2020]. However, drawbacks of robotic platforms are the related costs and the complexity of the systems. Further, the platforms are usually restricted to assess only specific body parts or tasks and thus have a low application flexibility and provide a very narrow description of the patients deficits.

Motion capture, either marker- or camera based, is paramount for assessing task specific movement quality. The methods offer a complete kinematic description of the whole body, including all joint angles of interest. Marker-based motion capture systems are in research widely accepted as the gold standard for biomechanical analysis [Patrick, 2003]. The accuracy of camera-based systems improved in the past years significantly and started to gain ground for the application in movement analysis [Steinert et al., 2020]. Even though both systems can provide accurate whole body kinematics, the application within the clinical routine is difficult for different reasons. Marker-based systems require long set-up times and expensive laboratories, which implies that measurements are restricted in space and time. Camera-based systems are easier to set up, but the measurement is still restricted in space by the field of view and video recordings within a clinical routine are controversial due to data and privacy protection guidelines.

Wearable sensors are devices an individual wears to continuously measure physiological parameters [Jalloul, 2018]. With technological advances in miniaturization, sophistication, and proliferation in the past decades, the sensors became smaller, more accessible, affordable, and thus increasingly interesting for healthcare applications [Johansson et al., 2018, Maetzler et al., 2013, Sasaki et al., 2017, Garofalo, 2012]. The main advantage of wearable sensors is that they are unobtrusive measurement tools. The sensors are small, light devices that can be attached to different body parts depending on the application [Rast and Labruyère, 2020]. Further, the devices usually measure for longer time periods, up to several days, and are not bound to any laboratory setting, which provides the possibility to perform measurements in

real-world environments. Moreover, wearable sensors can be used to instrument established conventional assessments unobtrusively with to goal to complement these assessment with more objective and detailed metrics. Examples of wearable sensors are optical, pressure, chemical, and inertial sensors, whereas the latter are the most dominant for assessing movement disorders [Jalloul, 2018, Cervantes and Porretta, 2010].

1.5 Motion tracking using inertial measurement units

The gold standard for movement tracking is marker-based motion capture, which requires expensive equipment and extensive infrastructure. These systems provide accurate and comprehensive descriptions of biomechanical kinematics. However, considering the costs of such systems and the trained personnel needed to operate them, motion capture laboratories are rare in clinical environments and, thus, not accessible to most patients. Hence, mobile, unobtrusive measurement systems have a considerable advantage over motion capture laboratories. Even though a motion analysis based on wearable inertial sensors might lack comprehensiveness and accuracy compared to the gold standard, inertial sensors still outperform in terms of ease of deployment for the clinical setting.

Inertial sensors usually comprise a tri-axial accelerometer and a tri-axial gyroscope, which are summarized as the inertial measurement unit (IMU). The accelerometer measures the combination of the change in velocity and a gravity-related acceleration, pointing in the vertical direction. The gyroscope measures angular velocity, which is a change of orientation. Some inertial measurement units further include a magnetometer, which measures the strength and direction of the magnetic field. Since magnetic fields are often distorted indoors due to ferromagnetic materials or electronic devices, magnetometer-free sensor fusion approaches are preferred for biomechanical applications [Laidig et al., 2019]. In microelectromechanical systems (MEMS), the sensors are rigidly connected in so-called strapdown systems, and sensor fusion is needed to derive the orientation and position of the IMU for motion tracking applications [Madgwick et al., 2011, Seel and Ruppel, 2017, Nilsson et al., 2014]. Processing IMU data into orientation, displacement, and velocity data has the advantage that more intuitive digital health metrics can be extracted than from the raw sensor data [Tunca et al., 2017].

1.6 Open challenges of using inertial sensors for assessing activities of daily living

In the past decade, clinicians and researchers shifted their focus from assessing body function and impairments toward assessments of the level of activity and participation [Lemmens et al., 2012]. This is a shift towards the level that is of interest to the patient, who is typically asking questions regarding their potential to walk, eat, or getting dressed again on their own. Furthermore, it has been shown that assessments on the impairment level do not necessarily correlate with performance in assessments on the activity level [Arnould et al., 2007, Burrige

et al., 2009]. Since wearable inertial sensors offer the unique possibility to assess activities not only in a standardized setting but also in a real-world environment, research activity in this field has increased in the past years to provide solutions for that matter [Gilmore and Jog, 2017].

The widespread clinical use of wearable inertial sensors for monitoring movement disorders has yet to be realized [Shirota et al., 2019, Maetzler et al., 2013]. First, sensor setups, including number and attachment sites, must be established; a trade-off needs to be found between complex body sensor networks and single sensor setups that differ in their comprehensiveness and ease of use [Sasaki et al., 2017]. This implies, that attachment sites need to be identified that are suitable for the specific application [Dobkin, 2013]. Second, signal processing algorithms must be improved to work robustly across individuals with multiple and diverse movement disorders and validated for the target population [Rast and Labruyère, 2020]. Third, the main reason for the difficulty in translating the technology into the clinical routine is that a plethora of digital metrics can be extracted from the sensors, but their individual clinical meaningfulness is often still unclear [Johansson et al., 2018, Shirota et al., 2019].

1.7 Objectives and outline of this theses

The overarching goal of this thesis is to provide digital health metrics from a sparse inertial sensor setup to assess daily life-like activities in the context of neurorehabilitation. These metrics are expected to extend conventional assessments by providing more objective and detailed measures on the movement profiles. More specifically, the sensor-derived metrics would allow to differentiate and track movement patterns of patients during daily life-like activities, which cannot be achieved through the conventional assessments only.

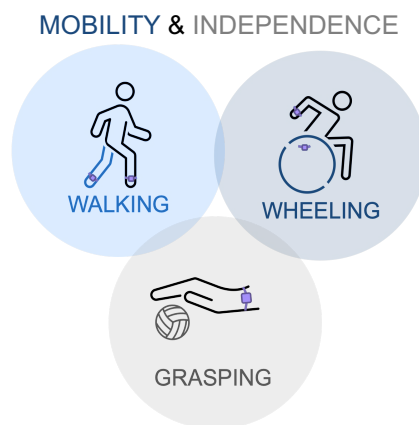


Figure 1.1: Three key activities of daily living relevant for the individual's mobility and independence.

To demonstrate this benefit, walking, wheeling, and grasping were selected as three exemplary but key activities of daily living for this thesis and are shown in Figure 1.1. The main

requirement for the selection was that the activities must be highly relevant for the individual in terms of mobility and independence. Further, the activities should include functional movements which involve either the upper or lower limbs, as these body parts typically show sensorimotor deficits after a CNS injury. Walking is the main form of human locomotion. Given the complexity of the movement, a comprehensive gait analysis can give insights into underlying deficits. As a proportion of patients with a CNS injury rely on a wheelchair for locomotion, wheeling was selected for this cohort as an analogous activity. Further, grasping, a movement highly relevant for performing many different tasks such as eating, getting dressed, or cleaning, was selected to include an activity from the domain of independence.

The underlying objectives of this thesis were as follows:

Objective 1: Identify a modular, sparse sensor setup to assess key activities of daily living

Objective 2: Development and validation of novel algorithms to assess these activities

Objective 3: Bring extracted metrics in context with clinical characterization of patients

This thesis attempts to consider these three objectives independently for each of the three activities. First, a modular but sparse sensor setup was selected with the trade-off of capturing relevant information about the underlying movement while still being a suitable tool for the clinical routine. Second, algorithms to extract digital health metrics from the raw sensor data were developed and validated ideally in the target population. Existing algorithms found in the literature were modified, extended, and improved for the target population and application with the intention of developing algorithms that work robustly across a wide range of movement deficits. Third, the algorithms were applied to data of the target population, and the extracted metrics were brought into context with the established clinical characterization of the individuals. Especially the latter extends the work found in literature where usually the focus lies on developing and validating algorithms to extract sensor-based measures without interpreting the derived metrics.

This cumulative thesis consists of four chapters, which are based on journal publications that are either published, under evaluation, or in preparation for submission. I am the (shared-) first and corresponding author of these publications. The core part of this thesis is followed by a general discussion.

Chapter 2 presents a sensor-based gait analysis specifically developed and validated for the population of patients with a SCI. The robustness of the algorithm was tested on patients with diverse gait deficits and from slow to preferred walking speeds.

Chapter 3 demonstrates the application of this sensor-based gait analysis to an extensive dataset of patients with a SCI. A data-driven approach is presented to derive non-redundant and relevant metrics that can characterize and predict walking after a SCI.

Chapter 1. Introduction

Chapter 4 includes a novel algorithm to extract wheeling propulsion patterns from a sparse sensor setup. Further, the applicability for wheelchair-bound patients with a SCI is investigated by identifying the core wheeling propulsion patterns of that cohort.

Chapter 5 presents a method to estimate clinical scores of an assessment for upper limb function based on a single wrist sensor as a step toward a therapist-independent or minimally supervised assessment.

Chapter 6 draws an overall conclusion on the work presented with respect to the objectives and the contributions to the field.

2 Towards a Mobile Gait Analysis for Patients with a Spinal Cord Injury: A Robust Algorithm Validated for Slow Walking Speeds

Charlotte Werner, Chris Awai Easthope, Armin Curt, and László Demkó
Sensors, 2021

Charlotte Werner was leading the study design, data analysis, and writing of the manuscript, and was involved in the data collection.

Chapter 2. Towards a Mobile Gait Analysis for Patients with a Spinal Cord Injury: A Robust Algorithm Validated for Slow Walking Speeds

2.1 Abstract

Background Spinal cord injury (SCI) patients suffer from diverse gait deficits depending on the severity of their injury. Gait assessments can objectively track the progress during rehabilitation and support clinical decision making, but a comprehensive gait analysis requires far more complex setups and time-consuming protocols that are not feasible in the daily clinical routine. As using inertial sensors for mobile gait analysis has started to gain ground, this work aimed to develop a sensor-based gait analysis for the specific population of SCI patients that measures the spatio-temporal parameters of typical gait laboratories for day-to-day clinical applications.

Methods The proposed algorithm uses shank-mounted inertial sensors and personalized thresholds to detect steps and gait events according to the individual gait profiles. The method was validated in nine SCI patients and 17 healthy controls walking on an instrumented treadmill while wearing reflective markers for motion capture used as a gold standard.

Results The sensor-based algorithm (i) performed similarly well for the two cohorts and (ii) is robust enough to cover the diverse gait deficits of SCI patients, from slow (0.3 m/s) to preferred walking speeds.

Conclusion The proposed algorithm is a suitable method to unobtrusively monitor walking of patients with a SCI and is a step towards a more objective measurement of gait deficits. This provides two potential clinical applications: standardized clinical walking test could be complemented using sensor-derived measures and walking performance outside of therapy could be assessed towards a next-generation continuum of care.

2.2 Introduction

Spinal cord injury (SCI), either caused by a trauma (e.g., accident) or disease (e.g., tumors), leads to permanent changes in the central nervous system. Depending on the severity and location of the injury, the symptoms vary widely: the patients might have a partial or complete loss of sensory function and motor control in the legs, arms, or whole body [WHO, 2013]. In particular, an incomplete SCI refers to remaining sensorimotor functions below the injury level, which can allow some patients to regain walking function despite their injury [Krawetz and Nance, 1996]. As independence in mobility is a crucial factor for performing daily life activities and for participating in society, regaining walking function is a common goal in most rehabilitation programs for these patients [Nas, 2015].

An accurate gait assessment during rehabilitation can give an insight into the recovery of motor functions and help with clinical decision making due to impairment specific training [van Middendorp et al., 2011]. However, in a typical clinical routine, only simple gait tests such as the six-minute walking test are performed [Hedel et al., 2005]. The outcome of these tests is the distance covered or the time to perform the test. Therefore, only the average walking speed of the patient is assessed. On the other hand, in research, a detailed gait analysis is conducted in gait laboratories, which are usually equipped with complex setups such as force plates and motion capture systems [Patrick, 2003]. Here, the outcome is a comprehensive analysis of the gait kinematics and joint kinetics. However, these gait laboratories are costly, postprocessing of the data is time-consuming, and the measurements are restricted in both space and duration.

Wearable inertial sensors could potentially be a balance between simple but less detailed clinical assessments and costly but highly informative gait analyses in laboratories. An advantage of the inertial measurement units compared to gait laboratories is that the sensors are small, affordable, and can be attached to different body parts according to the use case [Lambercy et al., 2016]. A potential application of these inertial sensors is to complement the aforementioned clinical gait tests by providing, in addition to the walking speed, information on the gait pattern and thus gait deficits of the patient. The benefit of using inertial sensors during the six-minute walking test has already been demonstrated for neurological diseases including multiple sclerosis [Shema-Shiratzky et al., 2019, Engelhard et al., 2016, Gong et al., 2016, Brodie et al., 2016], Parkinson's disease [Atrsaei et al., 2021] and stroke [Zhang et al., 2018]. Furthermore, wearable sensors carry the promise for long-term monitoring of gait speed and quality outside of laboratory settings, opening the potential to target remote interventions for individual patients.

In the past decade, a considerable amount of algorithms arose to investigate gait deficits with inertial sensors, focusing on the gait of elderly, stroke, multiple sclerosis, or Parkinson's disease [Dandu et al., 2018, Trojaniello et al., 2014b, Salarian et al., 2004, Rampp et al., 2015]. The typical approach of such algorithms is to detect gait events like initial and final foot contact, then estimating the sensor trajectory for each stride. Based on this, spatio-temporal parameters like step duration, gait phases, and walking speed can be calculated. Various methods exist to extract these parameters, which differ in terms of complexity, robustness, and computational effort [Panebianco et al., 2018, Yang and Li, 2012].

To the best of our knowledge, up to now, no validated algorithm exists to reliably extract these spatio-temporal gait parameters of SCI walking from shank-mounted inertial sensors. Jasiewicz et al. [Jasiewicz et al., 2006] presented a method to extract only the initial and final foot contact, and Tong et al. [Tong and Granat, 1999] validated their algorithm solely for one single patient, which is not representative of the wide variety of gait patterns found in this patient population. A possible reason for the lack of algorithms for SCI patients could be that the prevalence of SCI is lower compared to, e.g., stroke.

Chapter 2. Towards a Mobile Gait Analysis for Patients with a Spinal Cord Injury: A Robust Algorithm Validated for Slow Walking Speeds

Furthermore, people with SCI do not have a pathognomonic walking pattern like, for example, patients with Parkinson's disease. On the contrary, the gait deficits of SCI patients vary widely depending on the degree and level of the injury [Barbeau et al., 1999] often inducing compensatory movement patterns. Thus, algorithms that rely on fixed thresholds are prone to fail for these pathological gait patterns.

Furthermore, algorithms are often validated only for normal walking speeds of around 1 m/s. However, severely affected patients that are only able to walk indoors under supervision usually have a much slower average walking speed of ~0.34 m/s [Hedel, 2009]. Therefore, it is necessary to validate such algorithms for slow walking speeds so that they can be used reliably in a clinical setting for patients with low functional ambulation.

We here propose a sensor-based gait analysis for SCI that derives typical spatio-temporal gait parameters from inertial sensors attached to both ankles. Our goal was to focus on a minimal but still clinically accurate setup that is non-obtrusive for daily life applications, easy to handle, and can have the potential to be integrated into the daily clinical routine. In contrast to typical sensor-based gait analysis found in literature, where the detection of steps relies on fixed thresholds, we here propose a method that adapts these thresholds based on individual gait profiles. We hypothesize, that our algorithm is more robust against variable gait patterns and variable walking speeds. By validating the sensor-derived gait parameters with a gold standard, we demonstrate that the proposed algorithm is robust enough to be applied for the diverse gait deficits of SCI patients, from slow to preferred walking speeds.

2.3 Methods

2.3.1 Subjects

This study's participants (>18 years old) were either patients with a chronic SCI or neurologically unimpaired subjects. The patients were recruited from the patient database of the University Hospital Balgrist. Patients with all neurological levels of injury were included if they (i) were able to stand without physical assistance for more than 120 s, and (ii) had preserved segmental and cutaneo-muscular reflexes in the lower limbs. Patients with current orthopedic problems, psychological disorders, or neurological impairments other than SCI were excluded from the study. Participants for the control cohort could be included if they did not have any orthopedic problems affecting gait. In total, ten SCI patients and 17 healthy controls were recruited for this study.

Each participant was informed about the study procedure and risks before they participated in this study. The study was conducted in accordance with the Declaration of Helsinki, and the protocol was approved by the ethical committee of the canton Zurich (KEK-ZH No. 2017-01780) and by the Research ethics committee of ETH Zurich (EK No. 2018-N-80).

2.3.2 Study Protocol and Data Collection

For the SCI subjects, a clinician assessed the American Spinal Injury Association Impairment score (AIS score) [Maynard et al., 1997]. This AIS score includes assessing motor function in terms of the upper (UEMS) and lower (LEMS) extremity motor score and sensory function in terms of pin prick and light touch sensation. A combination of the sensory and motor function determines the neurological level of injury (NLI). In addition, the Spinal Cord Independence Measure (SCIM) was assessed [Itzkovich

et al., 2007]. For this study, we focused on the mobility domain of the SCIM, including ‘room and toilet mobility’ and ‘indoors and outdoors mobility’, resulting in a maximum achievable score of 40. Demographic information like age, height, body mass index (BMI), and sex were collected for all participants. Furthermore, the walking pattern of the patient was qualitatively described by a physiotherapist.

Two inertial sensors were attached to the participants’ ankles above the lateral malleolus with flexible straps as shown in Figure 4.1A. The sensor modules used for the study have been developed as part of the ZurichMOVE project [Popp et al., 2019]. The main components of the modules ($35 \times 35 \times 12$ mm, 18 g) include a tri-axial accelerometer, a tri-axial gyroscope, and a tri-axial magnetometer recording with a sampling rate of 200 Hz. As the magnetic field is often distorted indoors, the magnetometer data was omitted from the data analysis. The local coordinate system of the sensor module is depicted in Figure 4.1B.

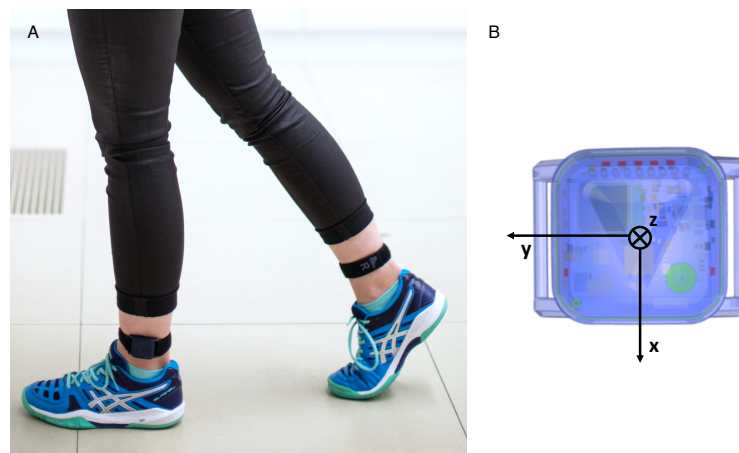


Figure 2.1: Subject wearing sensor modules attached laterally above each ankle (A). Schematics of the sensor module with its coordinate system (B).

The measurements were performed in the Gait Real-time Analysis Interactive Lab (GRAIL, Motekforce Link, The Netherlands), widely accepted as a gold standard for gait analysis. The GRAIL is a compact experimental lab for gait analysis with a treadmill, a motion capture system, and three stationary cameras. The instrumented dual-belt treadmill (V-Gait Dual Belt, Motekforce Link, The Netherlands) has two integrated force plates, which measure the ground reaction forces in three dimensions with a sampling frequency of 1000 Hz. One reflective marker was placed on each sensor and was tracked by ten cameras (Vero, Vicon Motion Systems, United Kingdom) at a sampling frequency of 100 Hz.

Synchronization between the GRAIL and inertial sensors was achieved by placing an additional sensor module on top of a piezo element, which was connected to the trigger line of the motion capture system. The trigger induced vibration of the piezoelectric material during the measurements, which was captured by the additional sensor module. Time synchronization between the three sensor modules was achieved by a master-slave configuration using Bluetooth Low Energy.

Before the first measurement, each participant became familiar with the test environment and the procedure by walking on the treadmill for about 5 min as recommended by Meyer et al. [Meyer et al., 2019]. During this familiarization phase, the speed levels increased starting from 0.3 m/s in steps of 0.1 m/s to determine the preferred walking speed of the patient. The patient had to give feedback as soon

Chapter 2. Towards a Mobile Gait Analysis for Patients with a Spinal Cord Injury: A Robust Algorithm Validated for Slow Walking Speeds

as the speed level exceeded his preferred walking speed. For SCI patients, the data of three different speed levels have been collected: preferred walking speed, 0.5 m/s, and 0.3 m/s. The measurement of each speed level lasted for 180s. These levels cover a broad range of walking speeds, including slow walking. More specifically, the speed ranges were selected to represent sub-community and community ambulators, and to ensure that all participants would be able to complete the task. Healthy participants were only measured at the speed of 0.5 m/s for 180 s to have a comparable condition between the two cohorts of the study. All participants wore their normal street shoes for the experiment.

2.3.3 Gait Analysis

Definition of Gait Parameters

Walking is typically segmented into individual gait cycles and further described by temporal gait parameters, which are depicted in Figure 2.2. A gait cycle corresponds to one stride, which starts with the initial contact (IC) of one foot and ends when the same foot contacts the ground again (following IC). The stride can be divided into a stance phase, where the foot is in contact with the ground, and a swing phase, where the foot is not in contact with the ground. The transition from stance to swing phase is initiated with toe-off. As some patients do not have a typical toe-off, we refer to this gait event by the final foot contact (FC). The double support phase corresponds to the period when both feet are on the ground, namely, from the IC of one side to the FC of the other side. The step duration starts with the IC of one side and ends with the IC of the other side. Other gait events relevant for the analysis are mid-swing (MSW) and mid-stance (MST), defined as the midpoint of the swing phase and stance phase, respectively.

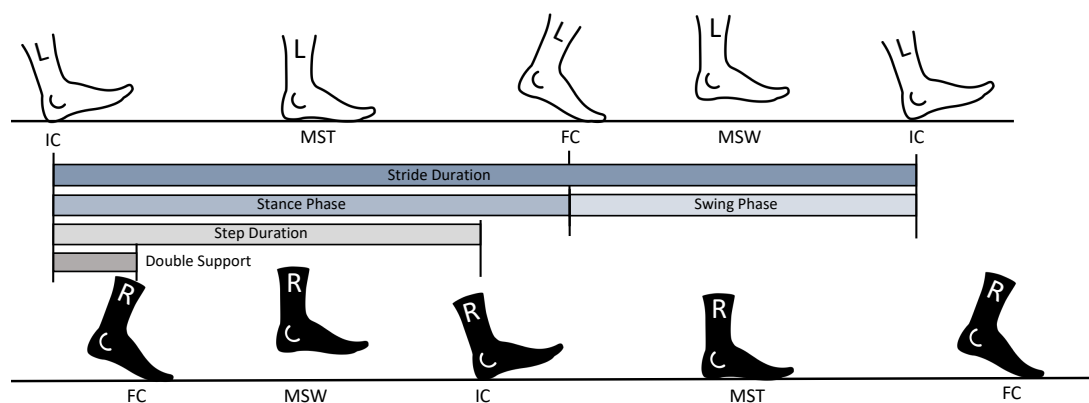


Figure 2.2: Schematic of the gait events initial contact (IC), final contact (FC), mid-swing (MSW), and mid-stance (MST) of a complete gait cycle and the corresponding gait phases.

Spatial parameters describe the displacement of the foot during a gait cycle and are depicted in Figure 2.3. The stride length is defined as the maximum displacement of one foot in the movement direction within a stride. The stride width and stride height correspond to the lateral and vertical displacement range during a gait cycle, respectively.

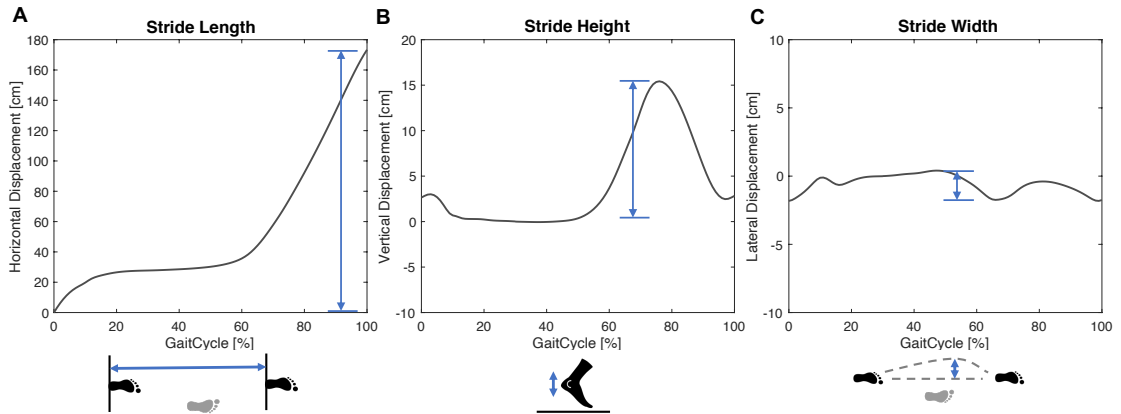


Figure 2.3: Schematic of the spatial parameter - stride length (A), height (B), and width (C) for one gait cycle, which is defined from initial contact to initial contact of the same side.

Sensor-Derived Gait Parameters

The following data processing workflow has been developed to extract typical spatio-temporal gait parameters from the 3D accelerometer and gyroscope data of the shank-mounted inertial sensors.

First, the data are segmented into individual gait cycles. For this purpose, a fast Fourier transform (FFT) is applied to the angular velocity perpendicular to the sagittal plane (ω_z) to obtain the frequency spectrum. The first main frequency component (f_{max}) corresponds to the periodicity of the cyclic movement of walking. Thus, the inverse of f_{max} corresponds to the average gait cycle duration (T_{cycle}):

$$T_{cycle} = \frac{1}{f_{max}} \quad \text{with} \quad f_{max} = \max(\text{FFT}(\omega_z)) \quad (2.1)$$

Individual gait cycles are identified as prominent local peaks of ω_z , corresponding to mid-swing (MSW). Instead of using fixed thresholds for the minimum peak height and the minimum distance between two consecutive peaks, these thresholds are adapted for each measurement for algorithm robustness across different walking speeds and cadences. The minimum peak height is defined as 20% of the 99th percentile of ω_z and the minimum peak distance as 50% of T_{cycle} .

Accurate identification of initial foot contact (IC) and final foot contact (FC) is paramount for further calculating gait parameters, as these serve as anchors for the temporal parameter definition. These gait events are detected by local peaks of the acceleration data in the anterior-posterior direction (a_y) and ω_z . Similarly, as before, the window in which to search for these peaks is adapted based on T_{cycle} . Because the IC typically occurs at 20% of the gait cycle after MSW, IC is defined as the local maximum in a_y within 5% to 45% of T_{cycle} after MSW. The FC is defined as the midpoint between the minimum in ω_z and the maximum in a_y within -35% to -5% of T_{cycle} before MSW. Finally, mid-stance (MST) is identified as the maximum of ω_z within the IC and the following FC. The temporal gait parameters are then computed as defined in Section 2.3.3.

The spatial parameters were computed from the 3D trajectory of the sensor during each stride. To obtain this trajectory, the orientation of the sensor in space was estimated by the magnetometer-free orientation estimation algorithm developed by Seel et al. [Seel and Ruppel, 2017]. Using this estimated

Chapter 2. Towards a Mobile Gait Analysis for Patients with a Spinal Cord Injury: A Robust Algorithm Validated for Slow Walking Speeds

orientation, the acceleration data were transformed from the local coordinate system of the sensor, which rotates with the movement of the sensor, into a fixed coordinate system. This is necessary because the acceleration data consists of both movement and gravitational acceleration. In the fixed coordinate system, the gravitational component could be easily removed from the vertical axis, which corresponds to the direction of earth's gravity. After receiving the pure movement acceleration, the acceleration data is integrated for each stride from MST to MST with a trapezoidal integration. As the sensor data is contaminated with noise, an integration of this thermo-mechanical noise results in a first order drift for the velocity and a second order drift for the displacement. Therefore, the following boundary conditions were introduced to correct for this drift: Instead of the often used zero-velocity update, the initial and final velocity values of each stride are estimated from the angular velocity at MST multiplied by the distance between the sensor and the ankle joint as proposed by Li et al. [Li et al., 2010]. This distance is estimated to be 10 cm. In addition, for abnormally long strides (>2.5 s), a first-order high-pass Butterworth filter with a cut-off frequency of 0.0002 Hz has been introduced to reduce the effect of drift. Moreover, without using the magnetometer data, the heading direction is undetermined and would result in a drift around the vertical axis. Therefore, the heading angle was chosen to be fixed to the main movement direction, which is estimated for each stride according to Trojaniello et al. [Trojaniello et al., 2014a, Trojaniello et al., 2014c]. In brief, the main movement direction was determined by the direction of the velocity during the swing phase within the horizontal plane. Then, the 3D velocity data for each stride is integrated a second time to obtain the 3D sensor trajectory for each stride. Finally, the stride length, width, and height are calculated as defined in Section 2.3.3.

Gait Parameters from Gait Laboratory

The true initial and final foot contact events have been derived from the data measured by the force plates of the split-belt treadmill. The ground reaction forces of the vertical direction were filtered with a low-pass fir filter with a cut-off frequency of 30 Hz. Sequences of a vertical ground reaction force smaller than 30 N and shorter than 0.2 s were equally set to zero. Every sequence with non-zero values was treated as a stance phase. The beginning and end of each stance phase were identified as the IC and FC, respectively. For each stride, its duration, the swing phase, the double support phase, and the step duration have been computed as defined previously. Whenever a participant stepped in the middle of the dual-belt treadmill, a signal was generated on both the left and right force plate, leading to an indistinguishable swing phase from the stance phase. As this contaminated the ground truth measurement, these strides had to be excluded. Trials with fewer than ten valid strides in total were excluded from the analysis. The spatial gait parameters were derived from the data of the reflective markers attached to the sensors. The 3D displacement of the markers was segmented into stride sequences from the ground-truth IC to the following IC of the same side. The stride length was calculated as the difference between the anterior–posterior positions of the marker in the direction of the treadmill at the beginning and end of each cycle, plus the distance the treadmill belt moved during that time span. The stride height was computed as the maximum displacement in the vertical direction during the swing phase compared to MST. The stride width was defined as the maximum lateral derivation of the foot from the straight line.

2.3.4 Statistical Analysis

To characterize the walking pattern of the SCI patients and healthy controls, the means and standard deviations of the spatio-temporal gait parameters were computed for the different speed conditions. In addition, the intra-subject variability was obtained as the average of the within-subject standard deviations. The differences between the sensor-derived gait parameters and the ground truth values from the gait laboratory were computed for each gait cycle to investigate the performance of the algorithm. This difference is referred to as the error in the following. For each participant the average error over all gait cycles was computed for the left and right side. As some of the patients had an asymmetric gait pattern, all participants' left and right sides were treated separately to not average out the effect of the more affected side. Furthermore, the mean relative error was obtained as the mean error divided by the corresponding ground truth gait parameter. For the initial and final contact detection no mean relative error can be computed, because the error was derived as the difference in timing and not as the difference to an actual gait parameter. In addition, no mean relative error was reported for the stride width and stride height, because the ground truth values were in comparison to the errors rather small leading to inflated values when the error was divided by values close to zero.

As summary metrics, mean and standard deviation values were reported for the different speed conditions and cohorts. A Bland–Altman analysis was performed on the trials of all speed conditions and cohorts to investigate whether the algorithm is affected by any measurement bias [Bland and Altman, 1999]. For this, the mean error and the 95% limits of agreement between the sensor-derived gait parameters and the ground-truth values from the gait laboratory were computed. Due to the non-normality of the data, an unpaired two-sample Wilcoxon test was applied to reveal the difference between the algorithm's performance on the two different cohorts of this study. Furthermore, a Friedman rank-sum test was performed to investigate the effect of speed on the performance of the algorithm. The Wilcoxon test and the Friedman rank-sum test used the median and the interquartile ranges of the errors and a significance level of 0.05.

2.4 Results

2.4.1 Subjects

The data of 26 participants of this study (50% female) were included in the analysis. For one patient, there was no trial with more than ten valid strides. Therefore, this patient was excluded from the further analysis. For all the remaining nine SCI patients and 17 healthy controls all trials had a sufficient number of strides and thus were all included. The average age of the control group was younger (27.6 ± 2.9 years) than the age of the patient group (59.6 ± 7.4 years). However, the SCI patients and the healthy participants had a similar height of 172.8 ± 7.5 cm and 170.6 ± 9.5 cm, respectively, and similar BMI of 22.7 ± 4.4 kg/m² and 22.0 ± 2.8 kg/m², respectively. The lesion completeness on the AIS score was ranked as D (sensory and motor incomplete) for all SCI patients, with a NLI range of C7 to L3. More specifically, the patients had an average lower extremity motor score (LEMS) of 47.6 ± 4.9 out of 50, indicating moderate motor deficits. In terms of sensory deficits, the patients achieved an average pin prick score of 40.6 ± 14.6 and an average light touch score of 45.4 ± 9.5 out of a maximum score of 56. All patients suffered from sensory or motor deficits of different degrees, except for patient SCI06. Even though this patient achieved a full score in the LEMS, light touch, and pin prick assessment, he reported difficulties in postural control and thus balancing during walking. An average score of 37.2 ± 4.2 out of 40 was assessed for the mobility domain of the Spinal Cord Independence Measure (SCIM)

Chapter 2. Towards a Mobile Gait Analysis for Patients with a Spinal Cord Injury: A Robust Algorithm Validated for Slow Walking Speeds

Table 2.1: Demographics (age, sex, height, and BMI) and clinical scores are listed of the spinal cord injury (SCI) patients who participated in the study. Within clinical scores, the completeness of injury (AIS), neurological level of injury (NLI), lower extremity motor score (LEMS), light touch, pin prick, and the mobility sub-score of the spinal cord independence measure (SCIM) are reported. The preferred walking speed as determined during the measurement is given for each patient.

ID	Age	Sex	Height	BMI	AIS	NLI	LEMS	Light Touch	Pin Prick	SCIM	Speed
	(yrs)	(m/f)	(cm)	($\frac{kg}{m^2}$)				L/R	L/R		
SCI01	69	f	167	16.1	D	C7	23/23	53/52	53/50	38	0.6
SCI02	48	m	184	24.8	D	L5	24/24	40/50	40/50	40	0.9
SCI03	58	f	163	24.5	D	T4	25/25	39/39	27/41	29	0.8
SCI04	58	f	170	19	D	T7	25/25	42/56	33/56	40	1
SCI05	55	m	169	19.3	D	C6	10/25	56/56	30/56	39	0.4
SCI06	70	m	170	23.2	D	T4-6	25/25	56/56	56/56	40	0.8
SCI07	66	m	170	25.6	D	T3	25/25	38/38	26/38	40	0.8
SCI08	54	m	184	31	D	T12	25/25	45/45	45/45	38	0.7
SCI09	58	m	178	20.8	D	C1	25/24	28/28	1/28	31	0.8

score. Details of the demographics and clinical scores of the SCI patients are reported in Table 2.1.

2.4.2 Walking Characteristics

The walking pattern of healthy controls and SCI patients was characterized using the ground-truth spatio-temporal parameters derived from the gait laboratory. In total, 5590 gait cycles of the SCI patients and 2924 gait cycles of the healthy controls were included in the analysis, and the results are reported in Table 2.2. Strides had to be excluded when the participants stepped in the middle of the dual-belt treadmill.

Table 2.2: Typical spatio-temporal parameters derived from the 3D motion capture and force plates are summarized for the SCI participants and healthy controls (HC). Values are given as mean±standard deviation (intra-subject variability) for the different walking speeds.

Group	SCI	HC
Walking Speed [m/s]	0.3	0.5
Number of included Gait Cycles	1493	1843
Number of excluded Gait Cycles	50	123
Stride Duration [s]	2.14±0.47 (0.12)	1.69±0.26 (0.08)
Step Duration [s]	1.07±0.25 (0.08)	0.84±0.14 (0.05)
Swing Phase [%]	28.7±5.9 (3.1)	33±4.2 (2.7)
Double Support Phase [%]	21.2±5.1 (2.9)	16.9±2.5 (1.9)
Stride Length [cm]	64.3±14.3 (4.3)	84.3±12.8 (4.4)
Stride Width [cm]	2.1±1.3 (1.1)	2.1±1.1 (1.2)
Stride Height [cm]	9±2.2 (0.9)	10.1±2.2 (0.6)
	0.76 ±0.17	0.5
	2254	2924
	269	50
	1.38±0.26 (0.04)	1.60±0.18 (0.05)
	0.69±0.14 (0.03)	0.80±0.09 (0.03)
	35.5±4.1 (2.0)	34.2±1.9 (1.9)
	14.5±2.8 (1.2)	15.8±1.9 (1.4)
	101.4±16.2 (3.5)	80.2±8.9 (3.1)
	1.9±1.0 (1.2)	1.9±0.9 (0.6)
	11.1±2.5 (0.5)	10±1.3 (0.5)

Chapter 2. Towards a Mobile Gait Analysis for Patients with a Spinal Cord Injury: A Robust Algorithm Validated for Slow Walking Speeds

As the majority of these spatio-temporal parameters are speed-dependent, only the gait parameters of the 0.5 m/s speed condition were compared between the two cohorts. Both participant groups walked with a similar stride length, resulting in a similar stride duration driven by the fixed speed of the treadmill. Similarly, comparable results have been obtained for the remaining gait parameters. However, the standard deviation of all gait parameters of the SCI patients exceeded the standard deviation of the control group indicating a higher inter-subject variability. Similarly, a higher intra-subject variability was obtained for all gait parameters in the SCI cohort compared to healthy controls. For SCI patients, this intra-subject variability was lower than the inter-subject variability for all gait parameters, except for the stride width.

The SCI patients had a preferred walking speed of 0.76 ± 0.17 m/s. By comparing the gait parameters of the 0.5 m/s and 0.3 m/s speed condition to the preferred speed, a longer stride duration, shorter stride lengths, and decreased stride heights were obtained. In addition, the percentage of the swing phase decreased with a decreased walking speed, whereas the relative stance phase and thereby the double support phase increased. Furthermore, the intra-subject variability and the inter-subject variability were with few exceptions lower or equal in the preferred walking speed condition compared to the 0.3 m/s and 0.5 m/s walking speed for all gait parameters.

The patients showed a range of different walking deficits, which were qualitatively described by a physiotherapist. Patients SCI01, SCI02, SCI04, and SCI05 were walking with a drop foot on either one or both sides. An ataxic walking pattern was observed for patients SCI01, SCI03, and SCI09. Patients SCI01, SCI03, SCI06, and SCI09 suffered from spasticity or an increased muscle tone during walking. Moreover, patients SCI03 and SCI08 had a decreased stability and balancing issues. Patient SCI05 had an asymmetric walking pattern due to a left sided tetraparesis. This induced a circumduction of the left leg and toe walking of the left side as a compensatory strategy. Only patient SCI07 showed a normal walking pattern with no obvious walking deficits.

2.4.3 Validation of Sensor-Derived Gait Parameters

The error of the typical spatio-temporal parameters was calculated between the GRAIL-estimated ground truth and the results of the proposed algorithm. Neither missed nor extra gait cycles generated by the proposed algorithm were observed.

Comparison of Errors Between Cohorts at 0.5 m/s

The algorithm's performance was analyzed using the same speed condition of 0.5 m/s for both the SCI patients and healthy controls. The mean error between the gait parameters derived from the gold standard and the inertial sensors attached to the ankles has been found to be similar for most of the parameters for the two cohorts, as shown in Figure 2.4. The values of the average and standard deviation for the different conditions can be found in Tables A.1 and A.2 of the Appendix. A significant difference in the performance of the algorithm was obtained for the determination of the initial contact and swing phase. According to the results, the initial contact was detected more accurately for the SCI patients (5 ± 12 ms) than for the healthy controls (10 ± 9 ms). However, these results should be treated with caution because they are close to the resolution of the measurement method defined by the sampling rate of 200Hz. The average and standard deviation of the error of the final foot contact detection (24 ± 39 ms) for the SCI participants are larger than in healthy controls, which resulted in larger errors and standard deviations for the estimation of the swing phase (-19 ± 48 ms) and the

double support phase (17 ± 44 ms). However, only the swing phase was statistically significantly different between the two cohorts. Some of the SCI patients that participated in this study suffered from a so-called drop foot and thereby a pathological toe-off, which is typical, for example, for patients with a weak Tibialis Anterior [Beekman et al., 2000] and explains the larger standard deviation for these parameters. For all the other gait parameters, no significant difference has been found between the two cohorts.

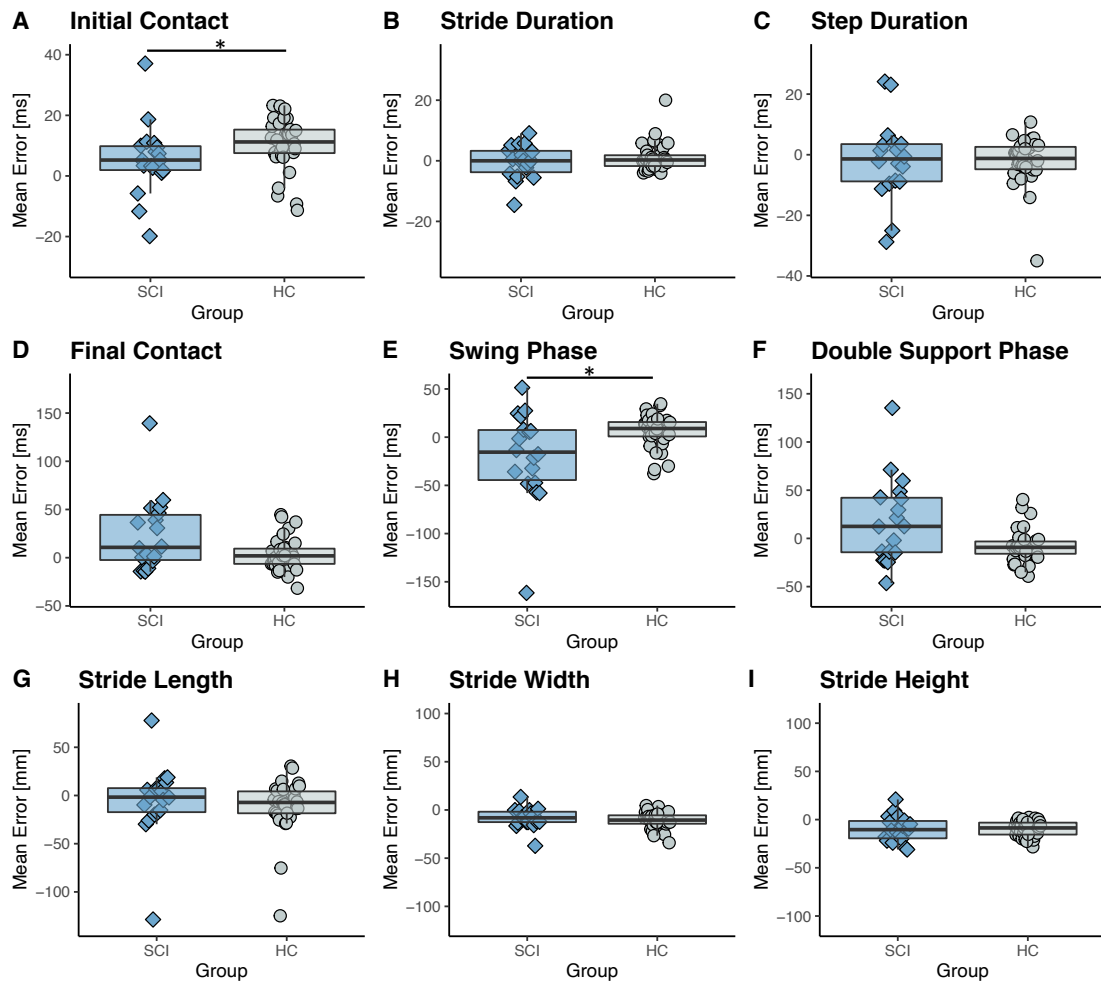


Figure 2.4: Mean error between the ground truth and sensor-derived gait parameters (initial contact (A), stride duration (B), step duration (C), final contact (D), swing phase (E), double support phase (F), stride length (G), stride width (H), stride height (I)) for the SCI patients and healthy controls (HC) walking on a treadmill at 0.5 m/s are shown. Boxes indicate 1st to 3rd quartile and the whiskers extend from the hinges to the largest/smallest value within 1.5 interquartile range. The black bar in the boxes displays the median. Significant differences between the two cohorts are indicated by * ($p < 0.05$).

Chapter 2. Towards a Mobile Gait Analysis for Patients with a Spinal Cord Injury: A Robust Algorithm Validated for Slow Walking Speeds

Comparison of Errors Between Slower and Preferred Walking Speed

Speed had no effect on the algorithm performance in pathological gait for the majority of calculated parameters. The relative mean errors of the gait parameters are summarized in Figure 2.5 for the different walking speeds. Mean errors in [mm] are reported for parameters with small values, as a normalization would result in inflated values. This includes stride width and height. Moreover, mean errors in [ms] are reported for the initial and final foot contact detection, where normalization is not feasible. No statistically significant effect of speed was observed, except for the initial foot contact detection and the estimation of the stride width. Specifically, the initial contact was detected earlier than the ground truth for slower walking speeds. However, this had no significant effect on the estimation of any of the other temporal parameters. The stride width was more underestimated for slower walking speeds than for preferred walking speed. This can be explained by the drift in the double integration, which is larger for a longer stride duration due to the less frequent velocity updates and thus drift corrections. The values of the average and standard deviation for the different speed conditions can be found in Tables A.1 and A.2 of the Appendix.

Overall Performance of the Algorithm

The Bland–Altman plots of the gait phases and spatial parameters of all speed conditions and cohorts are shown in Figure 2.6A–G. A maximum measurement bias of 9 ms was observed for the temporal parameters (stride duration, step duration, swing phase, and double support phase) and of –9.5 mm for the spatial parameters (stride length, width, and height). Therefore, there was a negligible small measurement bias for all the parameters. Moreover, there were negligible levels of dependency of the errors on parameter magnitude.

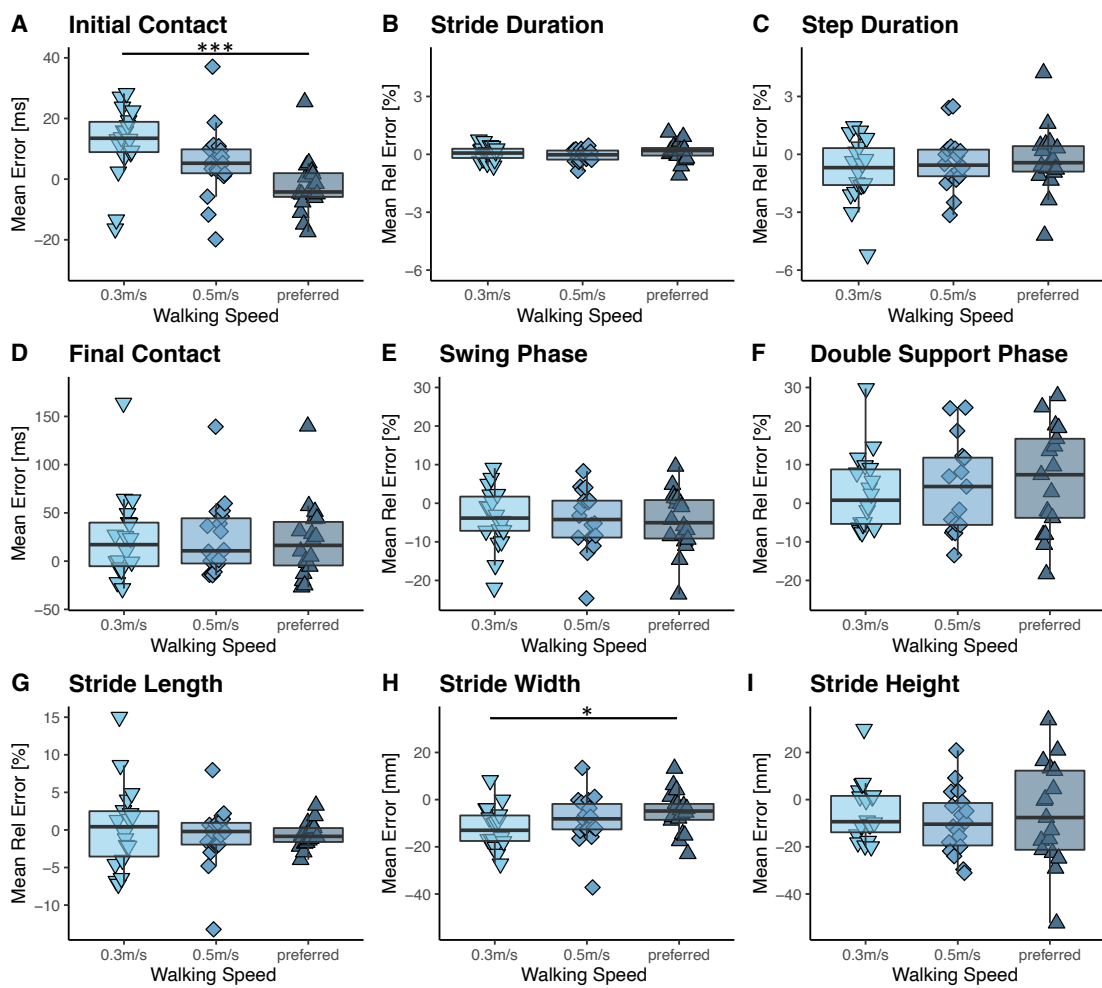


Figure 2.5: Mean error and mean relative error between ground truth and sensor-derived gait parameters (initial contact (A), stride duration (B), step duration (C), final contact (D), swing phase (E), double support phase (F), stride length (G), stride width (H), stride height (I)) for SCI patients walking on a treadmill at 0.3 m/s, 0.5 m/s, and their preferred speed. Boxes show 1st to 3rd quartile and the whiskers extend from the hinges to the largest/smallest value within 1.5 interquartile range. The black bar in the boxes displays the median. Significant differences between the different speed levels are indicated by * ($p < 0.05$) and *** ($p < 0.001$).

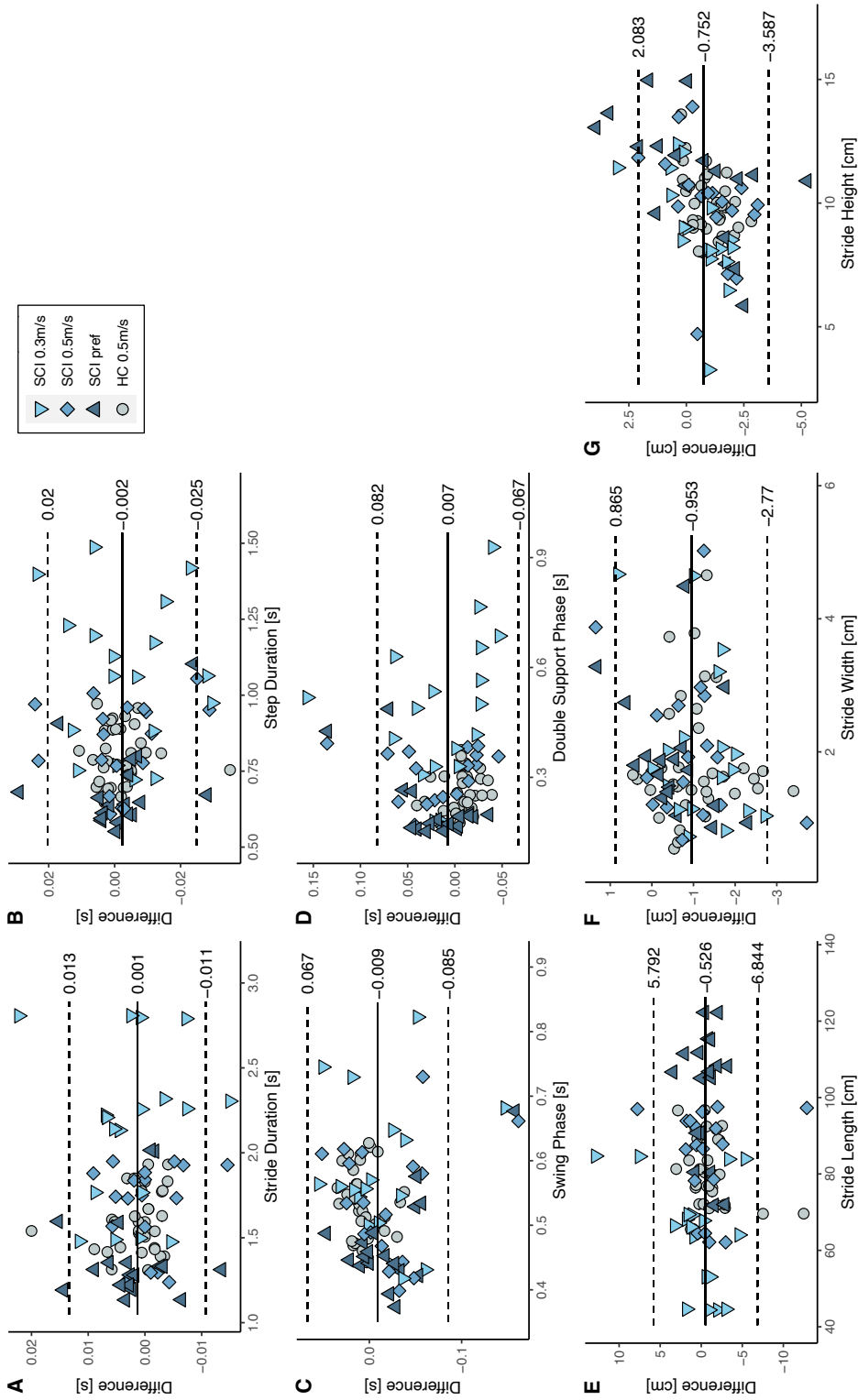


Figure 2.6: Bland-Altman analysis of the differences between the sensor-derived gait parameters and the ground truth gait parameters for HC walking at 0.5m/s and SCI walking at 0.3m/s, 0.5m/s, and at their preferred speed. Differences are shown for the stride duration (A), step duration (B), swing phase (C), double support phase (D), stride length (E), stride width (F), and stride height (G). The black line indicates the mean difference between the two setups and the dashed lines represent the upper and lower limits of agreement.

2.5 Discussion

This study proposes a method to extract spatio-temporal parameters from inertial sensors attached laterally above each ankle. In contrast to other algorithms, the proposed algorithm automatically uses personalized thresholds to detect each subject's gait cycles and gait events.

The sensor-derived spatio-temporal parameters were validated for SCI patients walking at a steady state on an instrumented treadmill at 0.3 m/s, 0.5 m/s, and their preferred walking speed (0.76 ± 0.17 m/s). The preferred walking speed of patients included in this study is similar to the average walking speed of 0.88 ± 0.06 m/s found by Barbeau et al. [Barbeau et al., 2007] for chronic SCI patients performing the six-minute walking test. Therefore, our study population is representative for this cohort. The algorithm's performance for SCI patients was compared to that of healthy controls walking at 0.5 m/s to have an equivalent condition for the two groups. No extra or missing steps, and thus gait events, were detected in these two groups, which demonstrated the robustness of the proposed algorithm. Similarly, no missed or extra gait cycles were obtained for the different speed conditions in the SCI cohort. The results for the SCI patients walking at their preferred walking speed were compared to the performance of other algorithms from literature using shank-mounted inertial sensors for patients with a neurological disorder.

With the proposed algorithm, a mean error of -2 ± 9 ms and 20 ± 40 ms for detecting the initial (IC) and final (FC) foot contact have been obtained, respectively. Comparing these results to Jasiewicz et al. [Jasiewicz et al., 2006], our algorithm slightly outperforms their algorithm even for their cohort of SCI patients with regular footfall both for the IC (-15 ± 17 ms) and FC (28 ± 32 ms). However, the accuracy of the correct timing of the gait event detection is strongly dependent on how accurately the optical motion capture system and the sensor system are synchronized. Thus, comparing these results to literature is of less importance.

The mean errors of the stride (2 ± 7 ms) and step (-1 ± 13 ms) duration, which depend on the correct detection of the initial contact, were found to be similar to the results of Trojaniello et al. [Trojaniello et al., 2014b]. On average, their proposed algorithm resulted in a mean error of 0 ± 15 ms for the stride duration and 0 ± 18 ms for the step duration for the four cohorts investigated: elderly, hemiparetic, Parkinsonian, and choreic participants walking at different walking speeds. The lowest walking speed investigated was 0.61 ± 0.24 m/s with hemiparetic patients and the fastest walking speed was 1.49 ± 0.22 m/s with elderly participants. Thus, the range of speeds differs to the walking speeds evaluated in this study.

The results for the swing phase (-23 ± 44 ms) were slightly less accurate than the results of Salarian et al. for patients with Parkinson's disease (5.9 ± 29.6 ms) [Salarian et al., 2004]. This can be explained by the fact that SCI patients often suffer from abnormal footfalls, making the detection of the final foot contact difficult [Jasiewicz et al., 2006].

The stride length has been estimated with an error of -6 ± 17 mm, which corresponds to a mean relative error of -0.6% , vastly outperforming the results of Hundza et al. for Parkinson's patients (110 ± 76.2 mm) [Hundza et al., 2014]. The high achieved accuracy was surprising, especially considering the slow walking speeds investigated in this study. Slower walking speeds and the corresponding slower strides result in larger drifts, and thereby often larger errors. It seems that introducing an additional high-pass filter for abnormally long steps appropriately addresses this issue and significantly improves estimation accuracy.

Chapter 2. Towards a Mobile Gait Analysis for Patients with a Spinal Cord Injury: A Robust Algorithm Validated for Slow Walking Speeds

To the best of our knowledge, the research articles available in the literature investigating the performance of sensor-based algorithms for slow walking speeds are very limited. This is especially important for the rehabilitation of SCI patients who are about to regain their walking function since they typically start to walk with speeds in the range of 0.34 m/s [Hedel, 2009]. Forrest et al. demonstrated that a minimum of 0.44 m/s is necessary for limited community ambulation after an incomplete SCI [Forrest et al., 2014]. Clinical application of sensor-based gait analysis aims to chart the recovery trajectory. Therefore, it is of paramount importance that algorithm performance is independent of walking speed and that the algorithm is validated for this range of low speeds. We here demonstrate that our algorithm meets these criteria for all typical spatio-temporal gait parameters, except initial foot contact detection and stride width estimation. However, the speed-dependent properties of these parameters did not carry over to other parameter estimations.

2.5.1 Limitations and Future Work

The limitation of our validation method is that it was performed in a controlled setting, including steady-state straight walking on a treadmill only. There is an accumulation of evidence in healthy that treadmill walking can act as a rhythmic generator and reduce the variability of movement patterns [Hollman et al., 2016]. Nevertheless, the basic kinematics are expected to remain similar [Song and Hidler, 2008]. As our algorithm was designed to perform well with high inter- and intra-subject variability, it seems plausible that it would function similarly well for steady-state over-ground walking. However, any application of the algorithm to walking including turns, uneven ground, or overcoming obstacles must be done with caution. In addition, our algorithm has been validated in nine SCI patients only due to the limited availability of SCI patients fulfilling the inclusion criteria. Nevertheless, these nine patients had varied sensory and motor impairments to cover a wide range of walking phenotypes, as demonstrated in the significant spread of ground-truth-derived gait parameters.

Future work of our group will focus on applying this algorithm to long-term data of SCI patients in daily life settings. Little is known on how walking during therapy time of SCI patients and the progress assessed by the clinical walking tests translate to daily life [Hedel et al., 2009]. The benefit of monitoring daily life walking over clinical gait assessments was demonstrated already for healthy participants of different age groups [Czech et al., 2020], and patients with Parkinson's disease [Atrsaei et al., 2021]. Long-term measurements in a non-laboratory setting provide the possibility to assess the walking performance of SCI patients outside the therapy sessions. Furthermore, the walking performance can be compared to that during therapy time to objectively measure the progress and effect of therapeutic interventions on the daily life of the patients. This would be helpful not only as a research tool to measure the effect of novel therapeutic interventions and medications applied for SCI patients but could also be integrated into the daily clinical routine to track and motivate patients to translate their progress in therapy to leisure time. In addition, we believe that this algorithm could be applicable to other populations with atypical gait patterns. Therefore, we recently established a collaboration with a children's hospital to investigate whether this algorithm can be generalized for use in children with neurological conditions. Similarly to SCI, this patient population suffers from diverse gait deficits depending on the neurological condition.

2.6 Conclusion

In this work, a novel algorithm that extracts typical spatio-temporal parameters from shank-mounted inertial sensors is proposed for the population of SCI patients. The spatio-temporal parameters were validated with 3D motion capture and force plates, a setup widely accepted as gold standard for gait analysis. For most of these parameters, the algorithm performed similarly well for both SCI patients and healthy controls, and the performance of the algorithm has been found to be robust for a wide range of walking speeds, including slow walking with a speed of 0.3 m/s. The results obtained are similar to those reported in literature for other patient populations with a neurological disorder. Due to the robustness over various walking speeds and the accuracy compared to gold standard measurements, we believe that the proposed algorithm is suitable for monitoring daily clinical routine and assessing the walking performance of SCI patients. This provides two clinically relevant perspectives: An extension of current clinical walking assessments to include markers of walking quality, and a high-density measurement of locomotor activity within and outside of clinical therapy. Both of these are necessary building blocks to achieve the leap to next-generation precision locomotor therapy.

3 Data-Driven Characterization of Walking after a Spinal Cord Injury using Inertial Sensors

Charlotte Werner*, Meltem Gönel*, Irina Lerch, Armin Curt, and László Demkó
under evaluation

* both authors share first authorship

Charlotte Werner was leading the study design, data analysis, and writing of the manuscript, and was partially involved in the data collection.

3.1 Abstract

Background An incomplete spinal cord injury (SCI) refers to remaining sensorimotor function below the injury with the possibility for the patient to regain walking abilities. However, these patients often suffer from diverse gait deficits, which are not objectively assessed in the current clinical routine. Wearable inertial sensors are a promising tool to capture gait patterns objectively and started to gain ground for other neurological disorders such as stroke, multiple sclerosis, and Parkinson's disease. In this work, we present a data-driven approach to assess walking for SCI patients based on sensor-derived outcome measures. We aimed to (i) characterize their walking pattern in more depth by identifying groups with similar walking characteristics and (ii) use sensor-derived gait parameters as predictors for future walking capacity.

Methods The dataset analyzed consisted of 66 SCI patients and 20 healthy controls performing a standardized gait test, namely the six-minute walking test (6MWT), while wearing a sparse sensor setup of one sensor attached to each ankle. A data-driven approach has been followed using statistical methods and machine learning models to identify relevant and non-redundant gait parameters.

Results Clustering resulted in 4 groups of patients that were compared to each other and to the healthy controls. The clusters did differ in terms of their average walking speed but also in terms of more qualitative gait parameters such as variability or parameters indicating compensatory movements. Further, using longitudinal data from a subset of patients that performed the 6MWT several times during their rehabilitation, a prediction model has been trained to estimate whether the patient's walking speed will improve significantly in the future. Including sensor-derived gait parameters as inputs for the prediction model resulted in an accuracy of 80%, which is a considerable improvement of 10% compared to using only the days since injury, the present 6MWT distance, and the days until the next 6MWT as predictors.

Conclusion In summary, the work presented proves that sensor-derived gait parameters provide additional information on walking characteristics and thus are beneficial to complement clinical walking assessments of SCI patients. This work is a step towards a more deficit-oriented therapy and paves the way for better rehabilitation outcome predictions.

3.2 Introduction

Depending on the severity and location of the lesion, spinal cord injury (SCI) causes heterogeneous deficits [Hillen et al., 2013]. The most consistently appearing consequence is a change in the sensorimotor function [Wirz and van Hedel, 2018], leading to impairments in the function of the legs, arms, or whole body. Due to recent advances in the acute management and prevention of secondary injuries, an increasing number of SCI present as incomplete [Shin et al., 2013, Wyndaele and Wyndaele, 2006], meaning that there is spared function below the level of injury. This incomplete injury allows for a significant change in neuroplasticity, with a partial or full locomotor recovery [Barbeau et al., 1999]. Indeed, approximately 70% of the incomplete SCI patients will regain some ambulatory walking function [Wirz et al., 2006]. However, most of the patients who regain mobility walk with deficits. An SCI gait is typically described with a reduced speed, changes in gait phase durations, and impairments in gait quality and balance [Hillen et al., 2013].

Measurement tools with good clinimetric properties are essential to assess gait deficits comprehensively and to track the impact of interventions during rehabilitation on locomotion recovery [Hillen et al., 2013, Deyo et al., 1991]. In the current clinical routine, walking capacity is mainly assessed using standardized gait tests, such as the six-minute walking test (6MWT), where the distance is measured that the patient is able to walk within six minutes. And indeed, walking speed has been described as the most responsive to improvement in walking capacity [Hedel et al., 2006]. However, this quantitative test does not give any insights into the patient's underlying impairments [Awai et al., 2016] and compensatory mechanisms [Levin et al., 2009]. To assess these, gait laboratories using marker-based motion capture are currently considered as the gold standard. They provide a detailed gait analysis with both spatiotemporal and kinematic parameters. However, their main drawback is that the assessments are restricted to the necessary laboratory environment, and the related expenses, time, and expertise required.

Wearable sensors such as inertial measurement units (IMUs) could become a compromise between clinical walking tests and gait laboratories. With advances in sensor technology and accessibility of these devices, they are becoming increasingly popular and have the potential to revolutionize clinical research as well as established clinical assessments [Chen et al., 2016]. The sensor units are affordable, easy to use, and do not add any burden to the patient [Lambercy et al., 2016]. For SCI patients, data derived from IMUs could provide additional information during a quantitative walking test by describing the gait pattern and thus capturing the gait deficits objectively. Given the relatively long duration of the 6MWT, typical spatiotemporal parameters as well as metrics related to fatigability and quality of the gait can be gathered for analysis. To this date, most of the research using wearable inertial sensors during the 6MWT were pilot, proof-of-concept, validation and feasibility studies in mostly multiple sclerosis, stroke, Parkinson's disease, and chronic obstructive pulmonary disease populations as summarized in the recent review of Storm et al. [Storm et al., 2020].

One of the challenges of using technology-aided assessments is the plethora of generated outcome measures which often have a high covariance [Kanzler et al., 2022] and are usually difficult to interpret for clinicians [Shirota et al., 2019]. To avoid redundancy and facilitate interpretation, approaches such as principal component or factor analysis can be used to identify and group relevant outcome metrics into domains, e.g. rhythm and symmetry of gait. This approach has been applied to elderly, and Parkinson's disease populations, as well as in idiopathic fallers using gait metrics generated from an electronic walkway [Lord et al., 2013]. Up to this date, no study has identified relevant gait parameters from IMU data to characterize walking in patients with a SCI.

Current clinical assessments have mainly two purposes: to track the patient's current status objectively

Chapter 3. Data-Driven Characterization of Walking after a Spinal Cord Injury using Inertial Sensors

but also to serve as a foundation for rehabilitation outcome predictions by clinicians. Technology-aided assessments could further enhance such rehabilitation outcome estimations. As an example, Kanzler et al. [Kanzler et al., 2022] have shown that including digital health metrics for the prediction of upper limb rehabilitation outcomes in multiple sclerosis remarkably increased the accuracy of the model by 10%. Whether sensor-derived gait parameters could similarly help to predict if a patient will improve his or her walking capacity has not yet been investigated for SCI patients. Especially in this heterogeneous patient cohort, better prediction models of recovery profiles are needed to manage the patient's expectations better and to improve personalized and targeted treatment plans further.

The project aimed to identify sensor-derived gait parameters that complement a standardized walking test. A dataset of patients with a SCI and healthy controls performing a 6MWT while wearing a sparse sensor setup of one IMU attached to each ankle has been acquired. Further, demographics and clinical scores were collected to bring the sensor-derived gait parameters into context with established clinical characteristics. A subset of the participants with SCI was performing the instrumented 6MWT several times during their course of rehabilitation. This longitudinal dataset allowed the training of a prediction model to estimate whether a patient will improve the walking capacity or not. The hypotheses of this project were that (i) sensor-derived gait parameters can identify gait deficits not captured by the walking speed, such as compensatory movements, and (ii) including sensor-derived parameters as predictors will improve the classification accuracy of whether a patient will improve the walking capacity in the future. A data-driven approach using signal processing and machine learning techniques to extract and select the relevant sensor parameters was used to address these two research hypothesis.

3.3 Methods

3.3.1 Subjects

The participants of this study were individuals with an incomplete SCI, undergoing either a stationary or ambulatory rehabilitation program. Patients with all neurological levels of injury were included if they were older than 18 years and were able to walk for at least 10m without physical assistance. Participants had to be excluded if comorbidities affecting their gait, such as orthopedic problems, were present. In addition, data from neurologically unimpaired participants was collected as reference data of healthy controls. Similarly, these participants had to be older than 18 years and without any orthopedic problems. The measurements were approved by the ethics committee of the Canton Zurich (BASEC No. 2022-00730) and merged with a previously recorded dataset, including data from healthy controls (KEK- ZH No. 2013-0202). All measurements were performed at the University Hospital Balgrist in accordance with the standards of the Declaration of Helsinki and Good Clinical Practice guidelines.

3.3.2 Protocol and data collection

Clinical scores were collected (if available) from the electronic medical record system for the participants with SCI. From the American Spinal Injury Association impairment scale (AIS), the lower extremity motor score (LEMS), the neurological level of injury (NLI) and the completeness of the injury were retrieved. Further, the Spinal Cord Independence Measure (SCIM) [Itzkovich et al., 2007], the Mobility domain of the SCIM, the Walking Index for Spinal Cord Injury (WISCI) [Morganti et al., 2005], and the days since injury were compiled. A patient was assumed to be in a chronic stage if the

injury happened more than 365 days ago. Demographic information has also been gathered for all participants, such as age, weight, height, and sex.

All participants performed a 6MWT at their self-selected walking speed. The subjects were asked to walk safely but as quickly as possible along a hallway. Rest was allowed, and patients could also use walking aids if needed. The type of walking aid used and whether the participant needed an ankle orthosis were recorded. An experienced physiotherapist administered the test as part of the rehabilitation program. A subset of the participants with SCI performed the 6MWT several times during their rehabilitation, leaving at least two weeks between two consecutive assessment sessions to track their improvement.

During the walking test, the participants had one inertial sensor unit (ZurichMOVE, Switzerland) attached with flexible straps lateral above each ankle. The IMU modules (35x35x12mm, 18g), which included a tri-axial accelerometer, a tri-axial gyroscope, and a tri-axial magnetometer, recorded at a sampling frequency of 200Hz. Magnetometer data was not included in the analysis because the magnetic field is often distorted indoors. The two inertial sensor units were time synchronized via Bluetooth Low Energy.

3.3.3 Data postprocessing

IMUs require appropriate post-processing to extract metrics of interest from the raw sensor data. Here, an algorithm was used that was previously developed in our group and validated specifically for the population of SCI [Werner et al., 2021]. In brief, the algorithm uses adaptive thresholds to detect individual steps and gait events based on the frequency spectrum of the data, which makes this algorithm robust across a wide range of walking speeds. The cadence and typical gait phases, such as the swing, stance, and double support phases can be derived from the gait events, e.g. the initial and final foot contact. Further, the 3D sensor trajectory for each stride is reconstructed using a typical double integration approach. The underlying concept is to integrate the acceleration data twice to obtain displacement trajectories. However, accelerometers measure not only movement acceleration, but also gravity, which needs to be subtracted prior to integration. In addition, the sensor data suffers from thermo-mechanical noise, which results in a second-order drift when being integrated twice. Smartly chosen boundary conditions address this issue, such as the “zero-velocity-update” during mid-stance modified for the ankle sensor placement. Spatial parameters like the stride length, height (maximum vertical displacement), and width (maximum sideways displacement) can then be extracted from the sensor trajectory. Further, the walking speed is derived from the stride duration and length.

All gait parameters X (stride duration, step duration, swing phase, double support phase, stride length, stride width, stride height) were extracted for both legs and all strides. Statistical features were computed for these, such as the mean, coefficient of variation, the asymmetry and difference to reference. The coefficient of variation (cov) is defined as the standard deviation σ divided by the mean \bar{X} of all strides during the 6MWT.

$$cov = \frac{\sigma}{\bar{X}} * 100\% \quad (3.1)$$

Further, the asymmetry (asym) between both sides was computed with the symmetry index [Blazkiewicz

Chapter 3. Data-Driven Characterization of Walking after a Spinal Cord Injury using Inertial Sensors

et al., 2014]:

$$asym = \frac{|\bar{X}_{left} - \bar{X}_{right}|}{0.5 * (\bar{X}_{left} + \bar{X}_{right})} * 100\% \quad (3.2)$$

And the difference to reference (d2r) was computed as the difference to the gait parameter of healthy controls \bar{X}_{ref} interpolated to the same walking speed.

$$d2r = \frac{\bar{X} - \bar{X}_{ref}}{\bar{X}_{ref}} * 100\% \quad (3.3)$$

In addition to the spatiotemporal gait parameters, ankle cyclograms have been derived from the 3D sensor trajectory by subtracting the endpoint's displacement with reference to each stride's starting point. This processing step results in 3D enclosed shapes, as shown for one example patient in Figure 3.1. After scaling and centering these top view and side view cyclograms, the shape can be compared to a physiological reference shape with the sum of squared differences (SSD) as described by Awai et al. [Awai and Curt, 2014]. The advantage of this method is that it is independent of the stride length. An SSD of 0 would indicate no difference between the cyclogram of the participant and the physiological reference. Furthermore, the within-subject cycle-to-cycle consistency of these cyclograms was quantified by the angular component of coefficient of correspondence (ACC) as described by Field-Fote et al. [Field-Fote and Tepavac, 2002]. The range of ACC goes from 0% (no consistency) to 100% (perfect consistency). In addition, the area enclosed in these cycles was derived. The SSD, ACC, and the area were computed for the side and top view cyclograms.

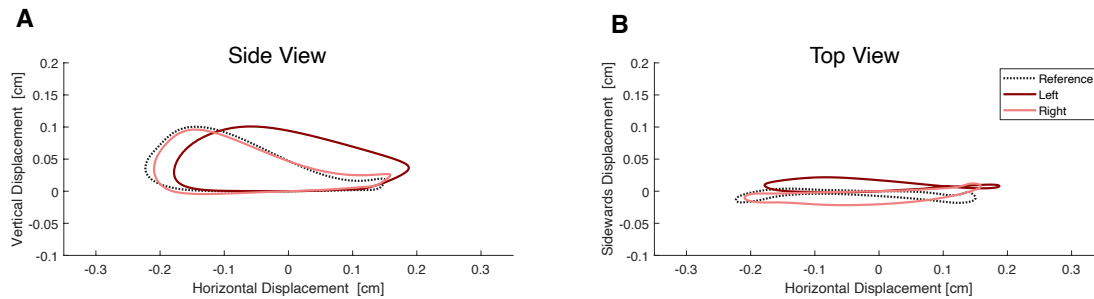


Figure 3.1: Side view and top view cyclograms of the ankle endpoint trajectory. Curves are shown for both the left and right sides of an exemplary SCI patient (with a clear more and less physiological side), together with the averaged reference data of healthy controls.

The movement smoothness was quantified by the frequency spectrum of the sagittal angular velocity. More specifically, the modified spectral arc length was calculated according to Balasubramanian et al. [Balasubramanian et al., 2012], because this method is less prone to differences in the duration of the movement and can be applied for cyclic movements like gait [Balasubramanian et al., 2015].

Further, the change in speed, stride length, and cadence over the 6 minutes was computed as a measure of fatigue. The change was defined as the slope of a linear fit of the speed, stride length, and cadence divided by the intercept of this linear fit. In addition, the speed inconsistency was computed as the absolute value of the change in speed.

To reduce redundant information, gait parameters were only used for the analysis from the more impaired side (if available for both sides), which was defined as the side with the lower LEMS. The right side was taken for the healthy controls, and if both sides had the same LEMS score. The collection of the extracted gait parameters can be found in the Appendix in Table A.3.

3.3.4 Statistical analysis

Identifying gait clusters

A cluster analysis was performed on the gait parameters of the first 6MWT of all participants with SCI to identify patients with similar gait characteristics. First, a principal component analysis was executed on the scaled and centered gait parameters to reduce the high-dimensional dataset. The number of principal components (PCs) for the clustering was selected based on the cumulative explained variance. To identify the optimal number of clusters a hierarchical clustering using Ward's criterion was performed. A k-means clustering on the PCs assembled the SCI participants into distinct groups. A variance analysis of demographic data and clinical scores identified significant differences in the cluster composition. In particular, a Kruskal-Wallis test was chosen for the continuous variables (e.g., SCIM) and a Fisher test for the categorical variables (e.g., percentage of acute patients) due to the non-normality of the data. Further, the most discriminating gait parameters between the clusters were identified to characterize the walking pattern of the different clusters. More specifically, the first five gait parameters that contributed the most to each PC were selected. This set of parameters was further reduced to a core set of gait metrics, by only keeping parameters that showed a significant difference between the clusters (Kruskal-Wallis, $\alpha = 0.05$) and by eliminating parameters that highly correlated with another parameter (Pearson correlation coefficient > 0.9) to reduce redundant information. A post-hoc test (Dunn test, $\alpha = 0.05$) identified significant differences between the clusters in this core set of gait parameters and allowed the comparison of the clusters to healthy controls.

Prediction of improvement in walking capacity

To predict whether a patient will improve the walking capacity significantly in the future, a machine learning model has been trained on the data of participants that performed the 6MWT at least twice. The dependent variable of the model was whether the participant improved in the 6MWT from the "present" to "future" assessment more than the standard error of measurement (SEM), which was reported to be 16.5m for SCI [Lam et al., 2008]. Any increase above this SEM was assumed to be an actual change in walking capacity rather than measurement noise. In other words, a binary random forest classifier was trained to predict whether a patient will improve above the SEM or not until the following 6MWT assessment.

Two different feature sets were used to identify whether the sensor-derived gait parameters can improve this prediction when using them as additional predictors. The first feature set only included the "present" 6MWT distance, at what time point after injury this "present" 6MWT was performed, and the number of days until the "future" 6MWT was performed. If the time point of the first 6MWT was more than 365 days after injury, all trials of this patient were shifted such that the first 6MWT was set to 365 days, because it is assumed that after this time point, the patient is in a chronic state. The second feature set additionally included all sensor-derived gait parameters from the "present" 6MWT as predictors. All features were scaled to have unit variance and centered around their respective mean. Further, redundant features (Pearson correlation coefficient > 0.9) were removed and only the first 10

Chapter 3. Data-Driven Characterization of Walking after a Spinal Cord Injury using Inertial Sensors

most contributing features were included to avoid overfitting of the model to the training data.

The classifier was trained and evaluated in a leave-one-subject-out cross-validation procedure, which means that the classifier was trained on all trials except for the trials of one participant, and then tested on the trials of this excluded participant. This procedure was repeated until the classifier was trained and tested on all data to evaluate the model's generalizability to unseen data. Sensitivity, specificity, and accuracy were chosen as evaluation metrics to compare the predictive power of the two different feature sets. Difference in features between improvers and non-improvers were analysed with the Kruskal-Wallis test ($\alpha = 0.05$).

3.4 Results

3.4.1 Participants

The demographics and clinical characteristics of the 66 participants with SCI and 20 healthy controls are summarized in Table 3.1. Both cohorts were similar in age, sex distribution, and BMI. However, the healthy controls achieved overall longer distances in the 6MWT compared to those achieved by the participants with SCI ($644 \pm 93\text{m}$ vs. $362 \pm 195\text{m}$). The cohort of participants with SCI was quite heterogeneous. The first measurement was conducted in the chronic phase (> 365 days after injury) for around 65% of the SCI participants. Around half of the participants had a traumatic injury. The majority had an injury that was both sensory and motor incomplete (AIS D score), whereas the NLI ranged from cervical to sacral. On average, the participants with SCI had a LEMS of 41.9 ± 9.5 out of a maximum achievable score of 50 and a SCIM of 76.2 ± 21.1 out of 100. Focusing only on the mobility domain of the SCIM, the participants had a score of 30.2 ± 10.6 out of 40. In terms of walking aids, 47% used some type of walking aid and 15.2% used an orthosis, which resulted in an overall WISCI score of 13.1 ± 5.4 out of 20.

A subset of 23 out of the 66 participants with SCI performed the 6MWT more than once at different time points during their rehabilitation: 10 were measured twice, 9 were measured three times, and 4 were measured four times. The days since injury and the 6MWT outcome for this subset of participants are shown in Figure 3.2. The median time between the two measurements was 35.5 days (Inter-quartile range: 30 to 79).

3.4.2 Characterization of the gait clusters

To identify groups of patients with similar gait characteristics, the patients were clustered on the PCs derived from the sensor gait parameters. The first four PCs of the gait parameters explained 69.4% of the variance in the data and were selected for the clustering. Four distinct clusters were obtained. Their composition in terms of demographics and clinical scores is presented in Table 3.2. The clusters neither differed in demographics (age, sex, BMI) nor in the diagnosis (traumatic/non-traumatic) or the chronicity of the injury. However, the clusters differed significantly in their performance in the 6MWT, which determined the cluster number ordering and is presented in Figure 3.3. It was found that both the first cluster and the healthy cohort differed significantly from every other. Further, the clusters varied in the clinical scores, such as the LEMS, SCIM, SCIM Mobility, use of walking aid or orthosis, and WISCI. With a few exceptions, the motor capacity and independence measures were decreasing, and the use of walking aids or orthosis was increasing with increasing cluster number.

Table 3.1: Demographics and clinical characteristics of the participants. Values are presented as mean \pm standard deviation. Abbreviations: BMI: Body Mass Index, AIS: ASIA Impairment scale, NA: Not Assessed, NLI: Neurological Level of Injury, LEMS: Lower Extremity Motor score, SCIM: Spinal Cord Independence Measure, WISCI: Walking Index for Spinal Cord Injury

Cohort	SCI	Healthy
Number	66	20
Age	55.6 \pm 15.1 years	58.6 \pm 11.4 years
Sex	28.8% female	20% female
BMI	24.9 \pm 4.9 kg/m ²	24.0 \pm 3.86 kg/m ²
6MWT	362 \pm 195m	644 \pm 93m
Chronicity	34.8% acute	
Diagnosis	48.5% traumatic	
AIS	B: 3 C: 2 D: 50 NA: 11	
NLI	Cervical: 25 Thoracic: 22 Lumbar: 12 Sacral: 2 NA: 5	
LEMS	41.9 \pm 9.5	
SCIM	76.2 \pm 21.1	
SCIM Mobility	30.2 \pm 10.6	
Walking Aid	47.0% with	
Orthosis	15.2% with	
WISCI	13.1 \pm 5.4	

Further, the clusters were compared in terms of the most relevant gait parameters, which were obtained with a feature selection procedure. More specifically, the five most important features of each PC were picked and then checked for redundancy. This procedure resulted in eight gait parameters shown in Figure 3.4, where the results are displayed for each cluster and the healthy controls. Comparing the clusters to the healthy controls with respect to these eight features, it was found that cluster 1 and healthy controls did only differ in terms of their performance in the 6MWT. Cluster 2 showed a significantly higher stride width, stride duration, and an abbreviated double support phase (negative d2r). Cluster 3 had a higher stride duration, a lower top view area, and a higher variability in the double support phase. Furthermore, the speed was less consistent than in healthy controls. Cluster 4 had a longer stride duration and higher stride width than healthy controls.

When comparing the individual clusters to each other, it was found that the stride duration of cluster 1 differed significantly from those of the other 3 clusters, but no substantial discrepancy has been found between these 3 clusters. The stride widths of clusters 2 and 4 were significantly higher compared to the other two clusters. Further, the top view area of cluster 2 was significantly higher than in the other three clusters. The stride length was more extended (positive d2r) in cluster 2 than in cluster 1. The variability (cov) of the double support phase was lower in cluster 1 than in cluster 2 and 3 and the d2r of

Chapter 3. Data-Driven Characterization of Walking after a Spinal Cord Injury using Inertial Sensors

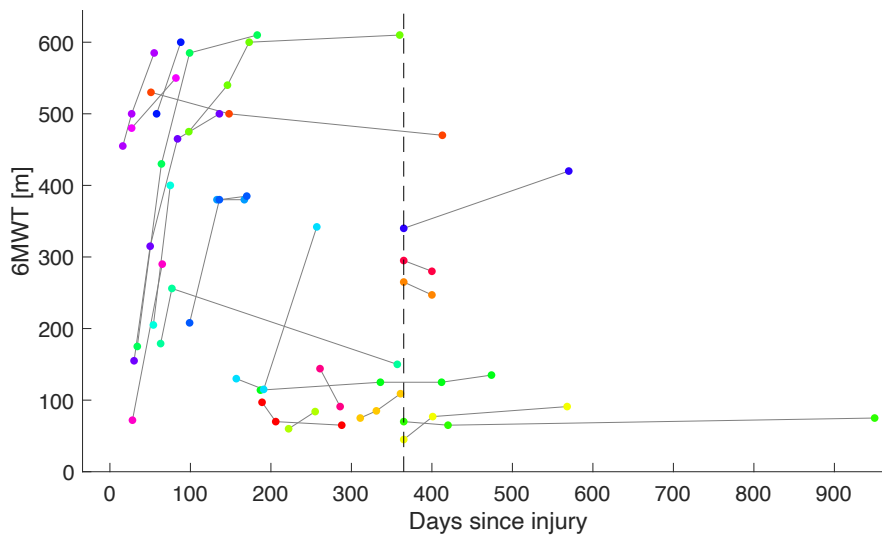


Figure 3.2: 6MWT outcome of the subset of 23 patients with SCI that performed the assessment at least twice during rehabilitation. Data points corresponding to the same patient are connected and displayed with respect to their time since injury. The dotted line indicates the beginning of the chronic phase.

Table 3.2: Cluster composition. Demographics and clinical characterization of the clusters with the corresponding p-values of the Kruskal-Wallis test. Values are presented as mean \pm standard deviation. Abbreviations: BMI: Body Mass Index, AIS: ASIA Impairment scale, NLI: Neurological Level of Injury, LEMS: Lower Extremity Motor Score, SCIM: Spinal Cord Independence Measure, WISCI: Walking Index for Spinal Cord Injury

	Cluster 1	Cluster 2	Cluster 3	Cluster 4	p-value
Number	37	14	8	7	
Age	54.8 \pm 15.3	60.2 \pm 15.4	52.2 \pm 14.3	55 \pm 15.7	0.619
Sex	24.3% female	21.4% female	62.5% female	28.6% female	0.193
BMI	25.3 \pm 4.6 kg/m ²	24.9 \pm 5.1 kg/m ²	22.1 \pm 8.2 kg/m ²	24.1 \pm 5.1 kg/m ²	0.752
6MWT	489 \pm 123m	306 \pm 135m	121 \pm 64m	80 \pm 42m	<0.001
Chronicity	29.7% acute	35.7% acute	62.5% acute	57.1% acute	0.232
Diagnosis	48.6% traumatic	42.9% traumatic	37.5% traumatic	71.4% traumatic	0.601
LEMS	45.8 \pm 7.6	37.3 \pm 9.3	41.1 \pm 10.3	34.7 \pm 10.1	0.005
SCIM	85.2 \pm 18.5	69.0 \pm 16.9	60.6 \pm 21.6	59.6 \pm 17.6	<0.001
SCIM Mob.	36.3 \pm 7.0	27.4 \pm 9.6	19.8 \pm 6.6	15.6 \pm 4.9	<0.001
Walking Aid	24.3% with	57.1% with	100% with	85.7% with	<0.001
Orthosis	10.8% with	0% with	25.0% with	57.1% with	0.006
WISCI	16.8 \pm 4.2	12.6 \pm 5.4	11.0 \pm 4.0	7.0 \pm 1.1	<0.001

the swing phase was different in cluster 2 compared to cluster 3. More specifically, the swing phase of cluster 2 was found to be prolonged, whereas that of cluster 3 shorter than in healthy controls walking at the same speed. Accordingly, the d2r of the double support phase differed significantly between clusters 2 and 3, as well as between clusters 2 and 4. The speed was less consistent in cluster 3 than in cluster 1.

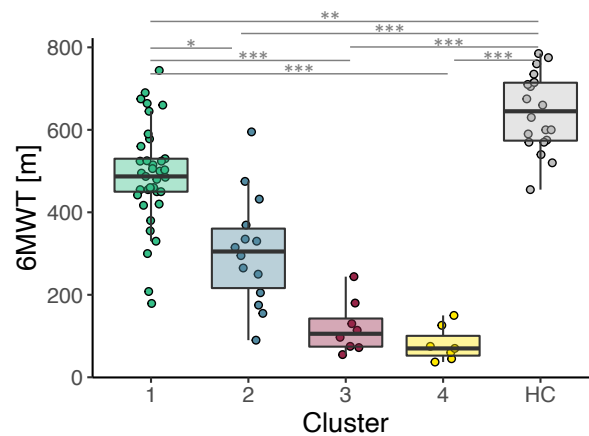


Figure 3.3: 6MWT performance of the 4 clusters and healthy controls (HC). Significant differences are indicated by *(<0.05), ** (<0.01) or ***(<0.001).

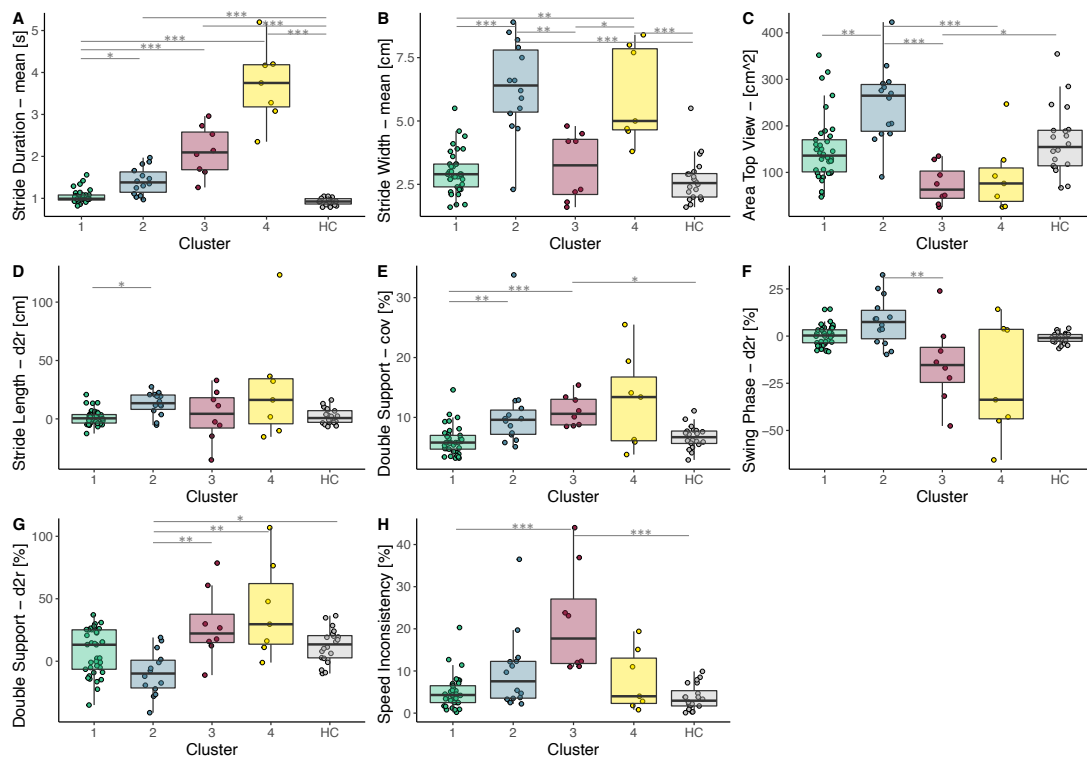


Figure 3.4: Selected gait parameters (A-H) shown for the 4 clusters and healthy controls (HC). Significant differences are indicated by *(<0.05), ** (<0.01) or ***(<0.001).

3.4.3 Prediction of improvement in walking capacity

A subset (23 patients) was measured either 2, 3, or 4 times during the course of their rehabilitation. When counting two consecutive 6MWTs as one observation for the prediction model, the dataset consisted of 40 observations. Twenty-one observations were “improvement” and 19 “no improvement”,

Chapter 3. Data-Driven Characterization of Walking after a Spinal Cord Injury using Inertial Sensors

depending on whether the improvement in the 6MWT distance was greater than the SEM of 16.5m or not, respectively.

The prediction model of whether a patient will perform better at the next 6MWT with an improvement more than the SEM was tested on two different feature sets and is presented in Table 3.3. The binary classification yielded an accuracy of 70% when the model was trained on the "present" 6MWT distance, the days since injury, and the days until the next 6MWT assessment only. Including sensor-derived gait parameters (feature set 2) improved the performance of the classifier by 10%. The 10 most important features selected by the model were (in the order of importance): the days since injury, the change in cadence, the side view ACC, the days until the next 6MWT, the asymmetry in the double support phase, the change in stride length, the asymmetry of the swing phase, the stride height, the change in speed, and the area of the side view. How the features of set 1 and the additional sensor-derived features differed between the improvers and non-improvers is shown in Figure 3.5 and Figure 3.6, respectively. Most improvers were in the acute phase. And on average, there were fewer days until the next 6MWT. Interestingly, the "present" 6MWT distance did not differ significantly between the improvers and non-improvers.

Table 3.3: Classification performance of the two different feature sets

Feature Set	Confusion Matrix		Sensitivity	Specificity	Accuracy
	No	Yes			
1	No	14	66.7%	73.7%	70%
	Yes	7			
2	No	14	85.7%	73.7%	80%
	Yes	3			

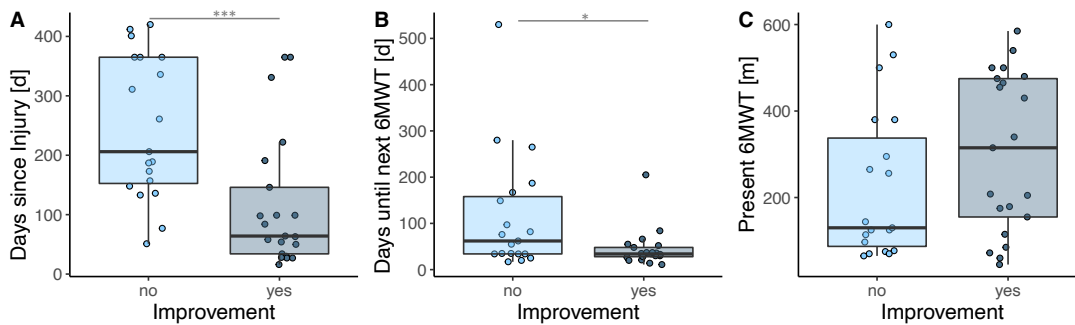


Figure 3.5: "Feature Set 1": Days since injury (A), days until next 6MWT (B) and present 6MWT (C) grouped by whether the patient will improve until the next 6MWT or not. Significant differences are indicated by *(<0.05), ** (<0.01) or ***(<0.001).

From the sensor-derived features, it was found that improvers tend to have a positive change in speed, stride length, and cadence. Further, the improvers showed a higher stride height and side view area. The improvers also showed on average a slightly better cyclogram consistency (ACC side view) and a slightly lower temporal asymmetry (asymmetry of the double support and swing phase), but these last findings were not found to be significant.

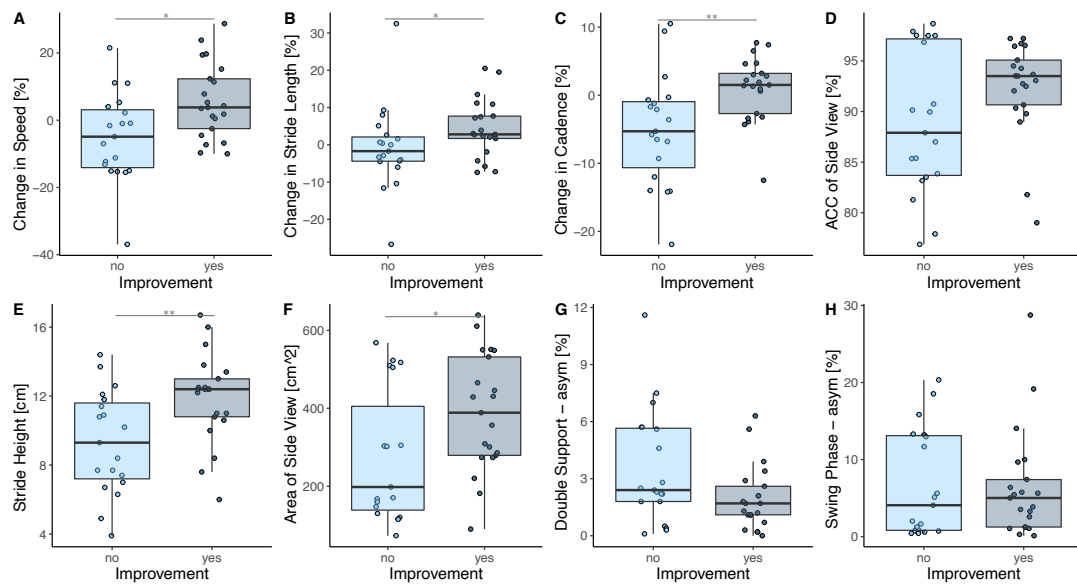


Figure 3.6: Gait parameters of “Feature Set 2” grouped by whether the patient will improve until the next 6MWT or not. Significant differences are indicated by * (<0.05), ** (<0.01) or *** (<0.001).

3.5 Discussion

In this work, we presented a data-driven characterization of the gait properties of patients with a SCI. The data of 66 participants with SCI and 20 healthy controls performing a 6MWT while wearing IMUs attached to their ankles was used. A subset of 23 SCI participants performed the 6MWT at least twice, with a minimum of two weeks between each assessment. Machine learning and statistical methods were used to select wearable sensor-derived outcome measures relevant (i) to identify and characterize groups of SCI patients with similar gait characteristics and (ii) to predict whether a patient will improve their walking capacity significantly in the future.

The patients with SCI included in this study represented this heterogeneous patient cohort. More specifically, patients with different levels (from cervical to sacral) and completeness (sensory and motor) of the spinal injury were measured, from both acute and chronic stages. The average performance in the 6MWT of the participants with SCI included in this study was slightly higher (362 ± 195 m) than values of chronic SCI patients (317 ± 22 m) found by Barbeau et al. [Barbeau et al., 2007]. The fact that around 35% of the participants with SCI in this study were in the acute phase and thus usually having a lower walking capacity explains the larger standard deviation.

3.5.1 Characterization of the gait clusters

A clustering procedure based on sensor-derived gait parameters separated the patients into four clusters. The cluster’s composition and gait characteristics were analyzed by identifying the most relevant and non-redundant gait parameters.

Chapter 3. Data-Driven Characterization of Walking after a Spinal Cord Injury using Inertial Sensors

Cluster 1 was the most prominent cluster, with 37 patients. The mainly chronic SCI patients in this cluster had a significantly lower performance in the 6MWT than the healthy controls but did not differ in any of the sensor-derived gait parameters. Hence, participants of this cluster walked slower but with a physiological walking pattern. Our recommendation for physiotherapy of patients in this cluster would be to improve their walking capacity by improving their intra- and inter-muscular regulation with strength training and coordination training. This should improve muscular control and overall fitness to foster speed improvement.

Participants of cluster 2 walked significantly slower than the participants of cluster 1. The most prominent walking characteristic of this cluster was the increased stride width and increased top view area, which are both indicators for a lateral circumduction and thus compensatory movements [Scivoletto et al., 2007]. Further, the double support phase is abbreviated (d2r) in cluster 2 in comparison to reference data presumably due to the compensatory movements mainly during the swing phase leading to redistribution in the relative gait phases. This indication is further confirmed when comparing the cluster composition of cluster 2 and 3: an overall lower LEMS and a higher percentage of chronic patients was found in cluster 2. Hence, we can assume that patients of cluster 2 learned compensatory strategies that enable this group to walk faster in comparison to acute patients with better muscle scores. This is in line with the literature, as several studies show that functional improvement can occur independently from neurologic recovery by using compensatory mechanisms [Curt et al., 2008, Wirz et al., 2006]. Our recommendation for patients in this cluster is to improve their movement quality by innervation training and strength training of the target muscles rather than focusing on improving speed.

The most prominent characteristic of cluster 3 was found to be the high variability of the double support phase and the speed inconsistency. This high variability in rhythm has been shown to be a risk factor for falling [Vienne et al., 2017]. We would recommend focusing on reducing mainly the temporal variability in these patients, e.g., by using robotic devices, such as the Locomat, or simple treadmill training. The predefined walking consistency and the many repetitions would foster a regular and periodic gait pattern towards safer walking.

Similar to cluster 2, an increased stride width was obtained in cluster 4, which again indicates a lateral circumduction and thus compensatory strategy [Scivoletto et al., 2007]. In addition, cluster 4 was the smallest cluster with only four patients and showed a high variance, especially in the gait parameters related to the gait phases. We assume these patients suffer from multiple gait deficits, resulting in a wide variance in the gait parameters. Especially for the 57% acute SCI patients included in this cluster, we recommend an individualized assessment of the foundations for walking, such as postural control and standing stability. Then, deficits with the possibility of improvement should be identified and addressed in a personalized deficit-oriented training manner.

The main findings of this clustering including a physiotherapy recommendation for each cluster are summarized in Figure 3.7.

3.5.2 Prediction of improvement in walking capacity

Using the longitudinal data of a subset of patients with SCI that performed the 6MWT at least twice, predictors of whether a patient will improve in the future more than the SEM were identified. When the present 6MWT distance, the time since injury, and the days until the next 6MWT were provided as inputs to the model a prediction accuracy of 70% was achieved. It was found that improvers were mainly

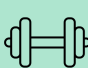



	Cluster 1 	Cluster 2 	Cluster 3 	Cluster 4 
Cluster composition	37 70.3% chronic LEMS: 46 ± 8	14 64.3% chronic LEMS: 37 ± 9	8 62.5% acute LEMS: 41 ± 10	7 57.1% acute LEMS: 35 ± 10
6MWT	489 ± 123m	306 ± 135m	121 ± 64m	80 ± 42m
Abnormal gait parameter	None	Increased stride width; increased top view area	Increased variability of double support; decreased speed consistency	General wide variance in gait parameter
Related gait deficit(s)	Physiological gait pattern; only slower than healthy controls	Lateral circumduction as a compensation strategy	Rhythm deficit	Combination of multiple gait deficits
Goal	Increase walking speed	Improve movement quality or more efficient compensation	Reduce temporal variability	Identify possibilities for improvement
Recommendations for physiotherapy	Strength and coordination training to improve muscular control and overall fitness	Innervation and strength training of target muscles and/or walking aid adjustment	Treadmill training to foster a regular and consistent walking pattern	Individualized assessments of foundations for walking; deficit-oriented training

Figure 3.7: Summary of the main findings on the cluster composition, gait characteristics and recommendations. Abbreviations: LEMS: Lower Extremity Motor Score

acute SCI patients that were measured again after a median of 34 days. Interestingly, the performance in the 6MWT of the improvers ranged from 45m to 585m and was not statistically different from the non-improvers, which means that both slow and fast walkers were able to improve their walking speed. This is in line with the literature where it was previously observed that the recovery of walking speed in SCI patients did not depend on the initial speed [Wirz et al., 2006]. Wirz et al. demonstrated that in SCI patients, it rather depended on an inherent capacity of functional improvement irrespective of initial impairment.

Adding sensor-derived gait parameters as predictors for the binary classification model could improve the prediction accuracy by 10%, to 80%. The sensor-derived features exhibited that improvers tend to have a higher change in speed, stride length, and cadence as predictors. Since the majority of improvers were in the acute phase, we assume that these patients improve their speed, stride length, and cadence consistency, both due to becoming more familiar with the test and also because they get better in estimating their abilities over the six minutes. Further, the non-improvers showed a lower stride height and lower side view area in the present 6MWT, which might indicate weak hip and knee flexors to lift the foot. Previous studies stated that hip flexors, hip extensors, and hip abductors are determinant for ambulatory function [Kim et al., 2004, Hussey and Stauffer, 1973]. In addition, improvers tend to have a lower asymmetry in the gait phases (double support and swing phase) and higher cyclogram consistency (higher ACC), even though these observations were not significant. In summary, patients that improved their performance in the 6MWT already had a more physiological walking pattern than the non-improvers, and thus it can be assumed that the improvers mainly improved their speed and thus performance in the 6MWT by improving their overall fitness and speed consistency. Accordingly, the gait deficits of the non-improvers presumably hinder this group from improving their speed considerably.

Chapter 3. Data-Driven Characterization of Walking after a Spinal Cord Injury using Inertial Sensors

3.5.3 Limitations

The main limitation of this work is that many of the gait parameters correlate with speed, such as for example the cadence, swing phase, and stride length, which is widely known [Kirtley et al., 1985]. Hence, it is difficult to disentangle walking quality and speed for participants walking at different speeds. Further, the slow walking patients are often the more severely affected part of the population. We tried to address this issue by providing parameters that are less related to walking speed, e.g., the measures related to variability and symmetry. Future work focusing on walking quality should consider collecting data of patients walking at similar speeds to get rid of this effect.

Since most of the data was collected as part of the clinical routine, the assessments were unequally spaced in time. 6MWT assessments were performed approximately every four weeks on average, but especially for chronic patients, the assessments were performed less often and only when the patient was in ambulatory rehabilitation. This unequal time spacing introduced additional noise in the data that we tried to address by providing the time until the following assessment as a predictor to the model.

3.5.4 Clinical implications and future work

The results underline the benefit of using wearable inertial sensors during the 6MWT. Based on the sensor-derived gait parameters, different groups of patients were identified that differed not only in terms of walking speed but also in terms of quality-related gait characteristics. Future work of our group will focus on translating these findings into the clinical routine by providing an easy-to-use tool for sensor-based gait assessments, including a tablet-based gait report. Part of this report will focus on the gait parameters identified in this work. Such a technical solution should foster more data collection, which is required to characterize this heterogeneous cohort even more precisely.

Further, predictors were identified that determine whether a patient will improve significantly in terms of walking speed. Interestingly, this was independent of current 6MWT performance and more related to the quality of walking, such as the actual gait pattern and speed consistency, characteristics that are not directly assessed by the 6MWT itself, but could be via the sensor-based measures. In addition, non-improvers, might still improve their walking pattern towards a more physiological gait, which again could be captured using inertial sensors.

3.6 Conclusion

This work presented a method to identify non-redundant and interpretable gait parameters to characterize walking after a SCI. Gait parameters were derived from a sparse inertial sensor setup, which opens up the possibility of being used within the clinical routine as a technology-aided gait assessment. The extracted gait metrics complemented the standard clinical assessment by providing information related to fatigue, compensatory mechanisms, and rhythm issues. Hence, the diverse gait deficits of this heterogeneous patient cohort could be described more objectively and comprehensively than in the current clinical practice. Further, sensor-derived gait parameters enhanced the prediction of whether a patient will improve his or her walking capacity in the future and exhibited predictors related to improvement in walking capacity. In conclusion, this work is a step towards using sensor-based gait analysis for rehabilitation assessment of patients with a SCI. Such sensor measures could not only foster a more deficit-oriented therapy by providing objective measures on gait deficits but also enhance

more targeted rehabilitation plans under consideration of better recovery profile prediction models when including sensor-derived parameters.

4 Estimating Wheeling Propulsion Patterns using a Sparse Inertial Sensor Setup

Charlotte Werner, Anita Linke, Wiebe de Vries, Armin Curt, and László Demkó
in preparation

Charlotte Werner was leading the study design, data analysis, and writing of the manuscript.

4.1 Abstract

Background The extensive reliance on hand and arm function for daily life activities and mobility by means of manual wheelchair use constitutes a main risk factor of upper limb pain and injuries in SCI patients. Hence, kinematic measurement of upper limb movements related to wheelchair propulsions provides important information associated with overuse injuries. Wearable inertial sensors offer the possibility to measure wheeling biomechanics in an objective, unobtrusive, and unconstrained way. However, so far only basic wheeling parameters, such as the number of strokes, distance or speed, are provided by commercial wearable devices.

Methods The aim of this work was to present a novel algorithm, which extracts actual wheeling propulsion patterns and more advanced wheeling metrics from a sparse inertial sensor setup with one sensor attached to the wrist and one sensor attached to the wheel of the wheelchair. The sensor-based algorithm was validated by comparing the results to an analysis based on data from an instrumented wheel and marker-based motion capture, widely accepted as a gold standard. After, validation, the algorithm was applied to an extensive dataset of 41 individuals with a spinal cord injury. Using time-series clustering, an unsupervised machine learning approach, on the sensor-derived wheeling patterns, dominating propulsion patterns within this cohort were identified.

Results Excellent results were obtained when comparing the performance of the sensor-based algorithm to the reference system: only 2% of the strokes were not detected by the algorithm. The average difference between the two measurement systems for detecting the initial and final pushrim contact was -6.1ms and 11.7ms, respectively, and wheeling propulsion pattern shapes could be reliably reconstructed. After applying the algorithm to a dataset of the target cohort and clustering the individuals based on their wheeling patterns, four dominant propulsion patterns were obtained. The wheeling pattern clusters did not only differ in quantitative wheeling metrics, such as speed, stroke frequency, and distance per stroke, but also in qualitative wheeling markers, such as the push angle, and propulsion pattern consistency. Further experienced wheelers dominated more efficient and less harmful wheeling pattern clusters.

Conclusion This work presents a novel method for an objective, unobtrusive and accessible measurement of wheeling metrics and propulsion techniques, which enables further research on the link between wheeling patterns and upper extremity injuries in a real-world setting and for a broader cohort. Hence, this work is a step towards providing personalized recommendations to optimize wheeling performance and thus reducing the risk of upper extremity injury for the individual.

4.2 Introduction

Wheelchairs enable mobility and thus independence for individuals with impairments in their lower extremities. For example, spinal cord injury (SCI) patients with a disability in their legs often rely on a wheelchair [Hosseini et al., 2012]. As wheelchair-bound individuals depend more on their upper extremities than able-bodied individuals for daily life activities including mobility, they use their arms more extensively. Pain and injury in the upper extremities occur more often than in the able-bodied population due to the extensive use [Arnet et al., 2021, Boninger et al., 2001, Boninger et al., 2003, Bossuyt et al., 2018, Eriks-Hoogland et al., 2012, Eriks-Hoogland et al., 2014, Gironde et al., 2004, Jahanian et al., 2022, Jensen et al., 2005]. Since wheelchair-dependent individuals are strongly dependent on the arms these overuse injuries have serious functional consequences. Consequences include a reduction of independence in daily life activities resulting in a decreased experience of quality of life and additional medical costs [Requejo et al., 2008, Jensen et al., 2005, Turner et al., 2001, Eriks-Hoogland et al., 2011, Gutierrez et al., 2007]. Many studies report that repetitive tasks, most prominently wheelchair propulsion, are associated with the development of upper extremity pain and injury [Dalyan et al., 1999, Davidoff et al., 1991, Curtis et al., 1999, Boninger et al., 1999]. Boninger et al. [Boninger et al., 1999] reported that this overuse injuries can, in addition to other factors, such as the BMI and age, to some extent be associated to the wheeling propulsion technique. As a consequence, a suboptimal wheeling technique is one significant risk factor for developing upper extremity injuries and pain.

The wheelchair propulsion patterns differ between manual wheelchair users. Mainly, four different wheeling patterns were identified in multiple studies [Kwarciak et al., 2012, Boninger et al., 2002]. These patterns differ in their trajectory during the recovery phase, when the hand is not in contact to the wheel. In the "arcing" pattern (ARC) the hand just follows the arc of the wheel back during the recovery phase. The "semicircular" pattern (SC) is an under-rim wheeling pattern, where the arm partially or fully extends and the hand falls below the push rim. If the hand follows a trajectory above the rim, it is called "single looping over propulsion" pattern (SLOP). In the "double looping over propulsion" pattern (DLOP), the hand first goes above the rim and then under the rim, such that the shape of the wrist trajectory looks similar to an infinity sign. It was found that the under-rim patterns tend to have a lower risk of developing upper extremity injuries, because it is in general more efficient [Boninger et al., 2002, Kwarciak et al., 2012]. However, most studies investigating wheeling propulsion patterns were conducted in laboratory setting using marker-based motion capture systems and/or treadmills [Groot et al., 2005, Richter et al., 2007, Groot et al., 2004] often together with instrumented wheels [Cooper et al., 1997], which measure forces and torques applied to the handrim. These setups provide a comprehensive kinematic and kinetic description of the upper limb biomechanics during wheeling. Consequently, these setups are rather cost intensive and bound to the laboratory setting.

Objectively, unobtrusive tools are needed to measure wheeling propulsion techniques not only in a laboratory setting for research purposes, but also as part of the clinical routine during the rehabilitation process of patients relying on a wheelchair. With technological improvements in the past decade, Internet of Things technologies became more and more available. For example, wearable sensors have the capacity to perform measurements in real life settings for prolonged periods of time (weeks/month) and are more accessible than biomechanical laboratories due to their costs and ease of use. More specifically, inertial measurement units (IMU), provide the possibility to assess movements in an unobtrusive way. In a recent review of MacDuff et al. [MacDuff et al., 2022] IMUs or simple accelerometers were identified as the most prominent devices to measure manual wheelchair propulsion metrics. Nevertheless, the field is still in its infancies: using wearables the physical activity could be quantified by the overall

Chapter 4. Estimating Wheeling Propulsion Patterns using a Sparse Inertial Sensor Setup

energy expenditure or simple activity counts [Ahmadi et al., 2018, Brogioli et al., 2017, Marco-Ahulló et al., 2021, Moreno et al., 2020, Nightingale et al., 2015, Popp et al., 2018] and wheeling metrics, e.g. the stroke count and the speed could be extracted [Kooijmans et al., 2014, Kressler et al., 2018, Lewis et al., 2018]. To the best of our knowledge, no one has demonstrated so far the possibility of deriving the actual wheeling propulsion patterns from IMU sensor data. However, given the link between these patterns and the risk of developing upper limb pain and injuries we see a great interest in assessing these propulsion techniques objectively and in an uncontrolled setting.

In this study, we present a novel algorithm to extract wheeling propulsion patterns and related wheeling metrics from a sparse sensor setup: one IMU attached to the wrist and one IMU attached to the wheel of the wheelchair. The algorithm's performance was validated with a setup widely accepted as a gold standard for biomechanical analysis. Further, the algorithm was applied to data of individuals with a spinal cord injury performing a wheeling trial. An unsupervised machine learning was applied to sensor-derived wheeling pattern, to identify the most dominant wheeling propulsion techniques of this cohort. Further, it was investigated how these clusters of patterns differed in terms of other quantitative wheeling metrics but also in clinical scores.

4.3 Methods

4.3.1 System Setup and Data Collection

The sensors used in this project were State-Of-The-Art IMUs, which comprise a tri-axial accelerometer, a tri-axial gyroscope and a tri-axial magnetometer. As the magnetic data is often distorted by electromagnetic fields indoors it was excluded from further analysis and a magnetometer-free approach was chosen [de Vries et al., 2009]. These sensors were attached with a flexible strap lateral above the wrist similar to a watch and with a custom-made solution parallel to the wheelchair spokes as shown in Figure 4.1. Data was collected from wheeling activities only.



Figure 4.1: Participant wearing sensor modules attached to the right wrist and the wheelchair wheel.

Two different datasets were collected. The first dataset was collected for validation purposes. The participants were wheeling on a treadmill at slow speed (2km/h), fast speed (4km/h) and with a slope (6% at 2km/h) for around 30s each. Participants were equipped with passive reflective markers attached to the upper body recorded by eight cameras at 100Hz (Qualisys). The right wheelchair wheel was replaced by an instrumented wheel (SmartWheel) measuring contact forces of the wheelchair rim at 240Hz. Further, participants had one IMU attached to the wrist and the wheelchair wheel (Shimmer), which were recording at 100Hz.

The second dataset was recorded to apply the algorithm to data of the target cohort. Wheelchair-bound patients were asked to wheel a distance of 160m, which included two 90° and two 180° turns. The participants were instructed to wheel at a comfortable speed: rapid while still feeling safe. The participants were equipped with IMUs (ZurichMOVE) as described above, which were recording at a sampling frequency of 50Hz. Participants were measured either once or several times with around 4 weeks in between each session, up to four times.

4.3.2 Participants

For the validation of the algorithm, the data of three able-bodied individuals with no pain in the upper extremities and wheelchair-experience was recorded. These measurements were approved by the responsible local ethics committee (EKNZ, Project-ID: 2020-01961).

The participants of the second part of this study were individuals with a SCI, undergoing either an in- or out-patient rehabilitation program. Patients with all neurological levels of injury were included if they were older than 18 years and were dependent on using a manual wheelchair. Both experienced (using the wheelchair for more than two years) and inexperienced wheelers were included. The measurements were approved by the ethics committee of the Canton Zurich (BASEC No. 2022-00730). All measurements were performed in accordance with the standards of the Declaration of Helsinki and Good Clinical Practice guidelines.

The data of 41 patients with SCI was collected. Clinical scores and demographics were retrieved (if available) from the electronic medical record of the participant. These participants had an average age of 55.3 ± 17.3 years, were 39% female and had an average BMI of 23.8 ± 3.9 kg/m². 22% of the participants were tetraplegic and 58.5% had a traumatic injury. At the time of the first measurement 65% were in the acute stage, having the SCI since less than one year. The upper extremity motor score (UEMS), a measure of muscle strength, was 46.5 ± 8.4 out of a maximum achievable score of 50. Further, the participants had on average a score of 55.1 ± 21.1 out of 100 in the spinal cord independence measurement (SCIM) scale. Focusing only on the mobility subdomain of this scale, the participants achieved 8.8 ± 5.4 out of 40. Around one third (31.7%) of the participants were considered "experienced" wheelers, using the wheelchair for more than two years.

4.3.3 Wheeling Pattern Estimation

The sensor data of the IMU attached to the wheel and the wrist is fused to extract wheeling metrics, such as the distance per stroke or the push phase duration, and the wrist trajectory, which is needed to reconstruct the wheeling propulsion pattern. The processing steps are explained in the following and are also displayed as a flowchart in Figure 4.2. First, the wheel IMU data is processed, which gives robust estimations of the velocity, displacement and path of the wheelchair. Further, individual strokes are identified by local peaks in the filtered angular velocity of the wheel. Then, a position strapdown integration approach is followed to get the wrist trajectories, similar to gait analysis algorithms developed for estimating the stride length from ankle-mounted sensors [Werner et al., 2021]. However, the uniqueness of this algorithm is that information from the wheelchair sensor is fused in the double integration procedure to improve the estimations.

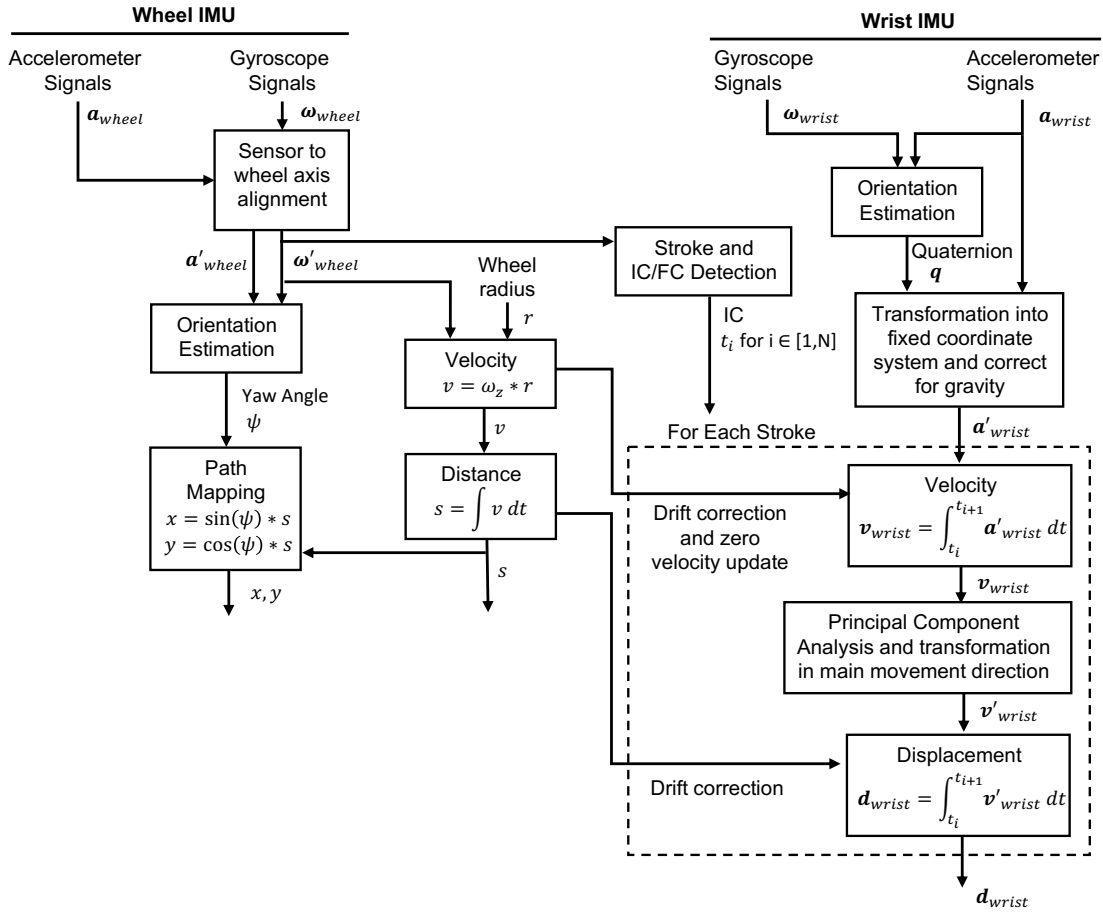


Figure 4.2: Flowchart of the algorithm.

Sensor to Wheel Alignment and Path Mapping

First, the data of the wheel sensor is transformed into a coordinate system that has one axis aligned with the wheeling axis. This is necessary because the sensor attached to the wheel is mounted to the spokes, which are usually not perpendicular to the wheel axis. Hence, any rotation of the wheel does not only induce an angular velocity around one but two axes. Here, this offset inclination angle is simply estimated by the average proportion of the gyroscope signal around these two axes.

After transforming the wheel sensor data into a coordinate system that is aligned with the wheel axis, the angular velocity around this wheel axis (ω_z) is multiplied by the known wheelchair radius to obtain the wheeling velocity. Further, this velocity is integrated to acquire the distanced travelled. The yaw angle is derived using the orientation estimation algorithm developed by Seel et al. [Seel and Ruppig, 2017], which fuses the gyroscope and accelerometer data using an analytical solution. Combining this yaw angle and the distance travelled, the path of the wheelchair can be mapped. Note that this yaw angle suffers with the magnetometer-free orientation estimation from drift, which is tolerable for short measurements (few minutes), but should be considered for longer measurements.

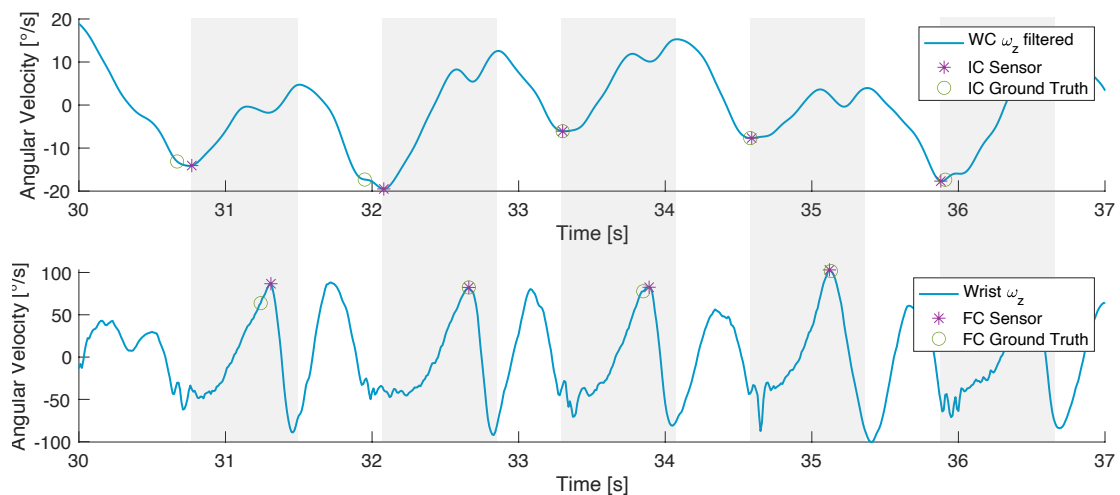


Figure 4.3: Example of the sensor-derived and ground truth initial (IC) and final (FC) contact events and the corresponding sensor data. Acceleration phase is highlighted in grey.

Detection of Stroke and Wheel Contact Events

Individual strokes are identified using the angular velocity data of the axis parallel to the wheel axis because each push induces an increase in this angular velocity. This angular velocity was bandpass filtered (Cut-off frequencies: 0.15-2Hz, 5th order) to only include the increasing and decreasing trends, which correspond to the push and recovery phases, respectively. Hence, individual strokes corresponded to local peaks in this data. To robustify the local peak detection, a frequency analysis revealed the main frequency components of this signal. The most prominent frequency within 0.5 to 2Hz, which equals a normal wheeling cadence range, was chosen as an estimate for the peak distance. More specifically, the peaks needed to have a minimum of half this average stroke duration in between each other to be considered a stroke and a minimum peak prominence of 10°/s. The initial contact (IC) of the pushrim was then identified as the local minimum before each accelerating phase. The end of the acceleration phase was marked by the following local maximum. The final contact (FC) was identified by a local peak in the angular velocity of the wrist sensor in between this acceleration phase. The sensor data including the ground truth and sensor derived initial and final contact events are displayed in Figure 4.3.

Stroke Trajectory Estimation

The wrist trajectories have been derived using a common double integration approach with the uniqueness of including information of the wheelchair sensor for drift correction. First, the accelerometer data needed to be transformed into a fixed coordinate system to remove the gravity component of the signal. This is necessary, because the accelerometer does not only measure movement acceleration, but also earth's gravity. With the quaternion derived from the orientation estimated by the wrist sensor data [Seel and Ruppel, 2017], the acceleration could be transformed in a fixed coordinate system and gravity could be subtracted from the vertical axis. Then this acceleration data has been segmented into individual strokes using the time stamps of the initial contacts derived previously from the wheelchair sensor data. The acceleration data was integrated once to obtain the wrist velocity. As any noise, e.g. thermo-mechanical noise, of the sensor data results in a first order drift when being integrated, this

Chapter 4. Estimating Wheeling Propulsion Patterns using a Sparse Inertial Sensor Setup

drift has been corrected using a zero-velocity update and the information of the velocity in the driving direction obtained from the wheelchair sensor data. Further, as the wrist sensor was most often not aligned with the main movement direction, this main movement direction was determined using a principal component analysis by an eigendecomposition of the covariance matrix of the estimated wrist velocity in the horizontal plane. Then this wrist velocity was rotated around the vertical direction, such that the forward direction was aligned with the main movement direction, which corresponds to the direction of the eigenvector with the largest eigenvalue. Subsequently, the wrist velocity was integrated to derive the wrist trajectory. Again, the drift resulting from also integrating sensor noise, was removed. It was assumed that the displacement along the forward direction corresponds to the distance travelled within that time span by the wheelchair. Further, as we were less interested in the actual sensor trajectory, but more in the wheeling pattern cyclograms the endpoint displacement was subtracted from this trajectory such that enclosed shapes with a start and endpoint at the origin have been obtained. Further, the trajectories have been interpolated to 100 datapoints and averaged over all strokes to obtain the mean wheeling pattern of this participant.

Extraction of Wheeling Metrics

Wheeling metrics could be extracted using the output of the algorithm. Temporal parameters, such as the stride duration could be computed as the time between two consecutive initial contacts. The push phase duration was derived as the time between the initial and following final contact. This push phase was normalized to the stride duration to obtain the relative push phase in relation to the recovery phase, when the hand is not in contact with the wheelchair rim. Further, spatial parameters such as the distance per stroke or the velocity per stroke (as the distance or velocity travelled during the duration of this stroke) could be derived. In addition, the push angle was computed by knowing that the distance travelled during the push phase corresponds to the arc length. The turning rate was obtained from the derivative of the wheelchair yaw angle. Further, the change in speed was quantified as the slope of the linear fit on the wheeling velocity over the whole trial, normalized by the intercept. The wheeling pattern consistency was determined by the angular component of coefficient of correspondence (ACC) as described by Field-Fote et al. [Field-Fote and Tepavac, 2002], which ranges from 0% to 100% and corresponds to no and perfect consistency, respectively. Further, the area enclosed in the wheeling pattern shapes was derived.

4.3.4 Postprocessing of the Validation Data

The tri-axial force data recorded by the smartwheel was processed to obtain the ground truth IC and FC time stamps for each stroke. The euclidian norm of the tri-axial force vector was computed, low-pass filtered (cut-off frequency: 20Hz, 5th order) and downsampled to 100Hz. Values below 10N were set to zero and determined the non-contact phase. The first resp. last value of such a non-contact phases corresponded to the final and initial contact, respectively. Unreasonably short non-contact or contact phases were removed, if they were less than 10% of the median stride duration long. The time difference between the ground truth events and the sensor-derived events were computed. The ground truth wrist trajectory was derived from the marker-based motion capture system. Here, the Processus Styloideus Radialis, a bony landmark at the wrist, was extracted. This 3D wrist trajectory was computed with reference to the wheelchair axis and segmented into individual strokes using the time stamps of the ICs obtained from the instrumented wheel as described above. To obtain the wheeling patterns, the data of each cycle was interpolated to 100 datapoints, the startpoint was set to the origin and enclosed shapes

were obtained by subtracting the endpoint displacement in correspondence to the processing of the sensor data. Further, the trajectories of all strokes of one participant were averaged to derive the mean wheeling pattern.

4.3.5 Clustering of Wheeling Patterns

An unsupervised machine learning approach was chosen to identify groups within the SCI patients with a similar wheeling pattern. The mean side view patterns of all measurements of all patients were included. First, this 2D time series data was centered to have 0 mean and scaled to have unit variance. This scaling prevented that the groups were not just grouped by the size of the shapes. Further, outlier shapes were identified and removed before clustering as they tend to distort the clusters. Outliers were detected by computing the distance matrix, which contains the pairwise distances between all observations. Soft dynamic time warping (dtw) was chosen as a measure for the distance between two time series [Cuturi and Blondel, 2017]. In comparison to the standard dtw this method is not invariant to time shifts as it provides a weighted average similarity score across all alignment paths instead of choosing just the single best path as done in a standard dtw. An observation was marked as an outlier, when the mean distance to all other observation was higher than 1.5 times the standard deviation of the mean distance of each shape to all other shapes. Then a k-means clustering was performed on the remaining observations choosing the best out of 15 initializations. The k-means method partitioned the observations into the cluster with the nearest distance to the cluster mean, using soft-dtw as a distance measure. The number of clusters was varied from 3 to 10 and the best cluster number was identified by the silhouette score, which ranges from -1 to 1 and describes how similar objects are to their own cluster compared to the other clusters. A value close to 1 means that clusters are well apart from each other and clearly distinguished. Further, typical wheeling metrics were compared between the different clusters and the cluster composition in terms of demographics and clinical scores was analyzed.

4.4 Results

4.4.1 Validation of IMU-derived Kinematics

The main parts of the presented algorithm were validated using force measurements and motions capture data, which is widely accepted as the gold standard for a biomechanical analysis. More specifically, the detection of individual stroke and contact events were validated using force measurements from an instrumented wheel. Force sensors precisely measure contact to the wheelchair rim, from which the actual time stamps of the IC and FC could be derived. Further, marker-based motion capture functioned as a reference for the validation of the wrist trajectories.

The algorithms performance to detect the individual strokes and wheel contact events was analyzed for three participants wheeling under three different conditions. The difference between the strokes and events derived from the sensors and from the gold standard is presented in Table 4.1. For the three participants 9,1, and 0 strokes out of 154, 140, and 75 were not identified by the algorithm. This corresponds to around 2% of missing strokes. The error for the sensor-based IC detection was -6.1ms, when averaged over the complete session of all three participants. The IC error of the slope condition was higher than for the slow and fast speed condition for all three participants. An average error of 11.7ms was obtained for the FC detection for the complete session, when being averaged over all three

Chapter 4. Estimating Wheeling Propulsion Patterns using a Sparse Inertial Sensor Setup

participants. Similar to the IC detection, the error was highest for the slope condition.

Table 4.1: The mean error \pm standard deviation of the sensor-derived initial (IC) and final (FC) contact to the wheel with respect to the events derived from an instrumented wheel. The values are reported for three participants wheeling at slow speed (2km/h), fast speed (4km/h), and with a slope (6% at 2km/h).

Condition	complete session	slow	fast	slope
IC [ms]				
Participant 1	-18.5 \pm 23.1	-9.0 \pm 22.9	-10.1 \pm 16.0	-37.5 \pm 19.1
Participant 2	4.4 \pm 13.3	13.5 \pm 7.9	10.1 \pm 6.5	-9.6 \pm 9.8
Participant 3	-4.3 \pm 14.5	7.2 \pm 16.6	0.4 \pm 12.8	-11.3 \pm 11.7
Mean	-6.1	3.9	0.1	-19.5
FC [ms]				
Participant 1	8.3 \pm 19.3	-5.7 \pm 9.9	-2.7 \pm 5.7	32.9 \pm 7.4
Participant 2	21.3 \pm 13.8	18.2 \pm 11.2	8.6 \pm 5.6	33.7 \pm 6.8
Participant 3	5.5 \pm 18.3	-6.1 \pm 18.1	-6.2 \pm 7.6	23.0 \pm 12.0
Mean	11.7	2.1	-0.1	29.9

Further, the wheeling patterns derived from the IMUs was compared to the motion capture ground truth data and are displayed in Figure 4.4. Three participants with different wheeling patterns were selected to test the ability of the algorithm to capture these different shapes. For both, the side view and top view, similar shapes were found when comparing the two different systems.

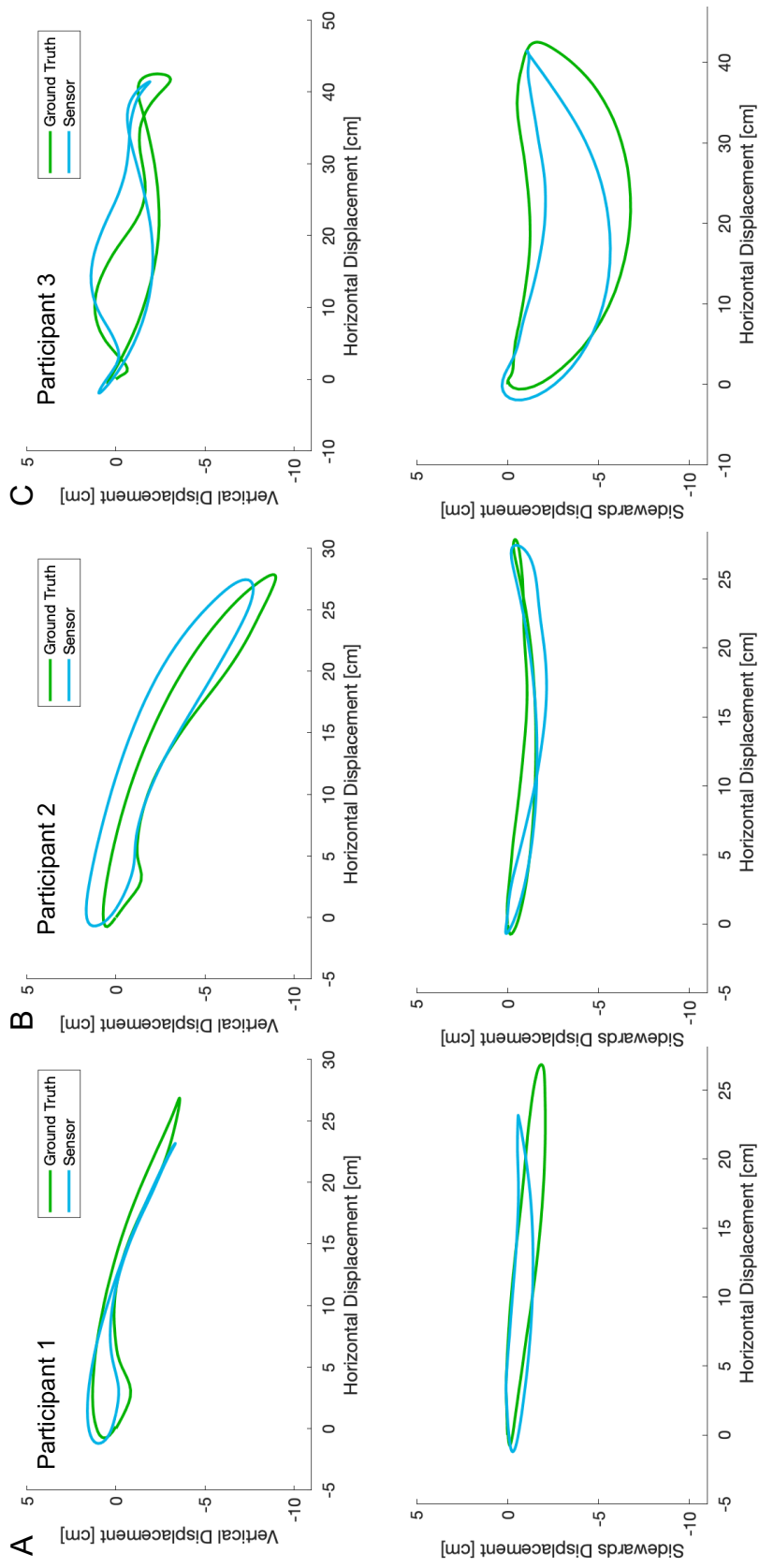


Figure 4.4: Extracted wheeling patterns from "ground truth" and sensor data for three participants (A-C). Both, side view (top row) and side view (bottom row), are shown.

Chapter 4. Estimating Wheeling Propulsion Patterns using a Sparse Inertial Sensor Setup

4.4.2 Application to Clinical Data

An unsupervised time series clustering of the wheeling patterns was performed on the dataset of all trials of the 41 participants with SCI. In total, this dataset included 73 observations as a subset of the participants was measured more than once. The time series clustering resulted in four distinct groups as shown in Figure 4.5. The number of clusters was chosen, because 4 clusters had the second best silhouette score of 0.36. 7 clusters gave a slightly better silhouette score of 0.37. Since for the 7 clusters we observed similar shapes that were just partitioned into subgroups and the silhouette score was only marginally better, we decided to choose 4 as the best cluster number. The complete list of silhouette scores for the corresponding number of clusters can be found in the Appendix in Table A.4. 13 observations were grouped to cluster 1 showing an overall over-rim wheeling pattern similar to a SLOP pattern. Cluster 2, showing an ARC wheeling pattern, was the largest cluster with 32 observations. Cluster 3 included 9 observations, which had a SC wheeling pattern and cluster 4 had 11 observations, showing a DLOP pattern. 8 observations were identified as outliers and their shapes are displayed in Figure A.1 in the Appendix. For the following analysis they were grouped together as cluster 0.

The cluster numbers (1 to 4) were selected based on the average wheeling speed of the cluster, which is displayed together with other wheeling parameters in Figure 4.6. It was found that there was a difference in average wheeling speed between the clusters ranging from around 1m/s for cluster 1 to around 1.7m/s for cluster 4. Interestingly, this difference in speed was less due to a difference in stroke duration (determines the cadence) but originated more from the difference in stroke distance. Further, for the ARC pattern (cluster 2) a wider range of wheeling velocity was found than in cluster 1, 3, and 4. The velocity range of the outlier cluster (cluster 0) was even larger and included the slowest and fastest wheelers. The push ration was around 35% for all clusters, only the SC pattern (cluster 3) showed a lower push ratio of around 30%. Cluster 1 to 4 showed a positive change of speed over the whole wheeling trial. Only a few observations in cluster 0 showed a negative change in speed. The ARC pattern (cluster 2) had the highest cyclogram consistency and together with the SLOP pattern (cluster 1) the lowest cyclogram area. The participants with the DLOP pattern (cluster 4) wheeled with a wide range in cyclogram consistency, but had together with the participants with a SC wheeling pattern the highest cyclogram area. The push angle varied between the different wheeling patterns the SLOP pattern and the ARC pattern had overall lower push angles of below 90° than the outliers and the other two patterns. The maximum turning rate was similar to the distribution of the velocity over the clusters.

A subset of 24 participants were measured more than once (19 two times, 3 three times, 2 four times). 17 out of the 24 participants (71%) were clustered always to the same group. Considering only the first trial of each participants the cluster composition is summarized in table 4.2. The percentage of tetraplegic participants was rather evenly distributed over the clusters. The cluster with the SC pattern (cluster 3) and the DLOP-like pattern (cluster 4) included both more than 80% of patients with a traumatic injury. The percentage of traumatic injuries in the clusters with the ARC pattern (cluster 1) and the SLOP-like pattern (cluster 1) was around 40%. Cluster 1 (SLOP) had the highest and cluster 4 (DLOP) the lowest percentage of acute patients. The UEMS was fairly similar between the 4 clusters, but the SCIM and the SCIM Mobility differed: the cluster with the DLOP-like pattern (cluster 4) had overall higher scores than the other clusters. This cluster also had together with the outlier cluster (cluster 0) the highest percentage of experienced wheelers of above 60%. Cluster 1 (SLOP) and 2 (ARC) only had around 15% of experienced wheelers.

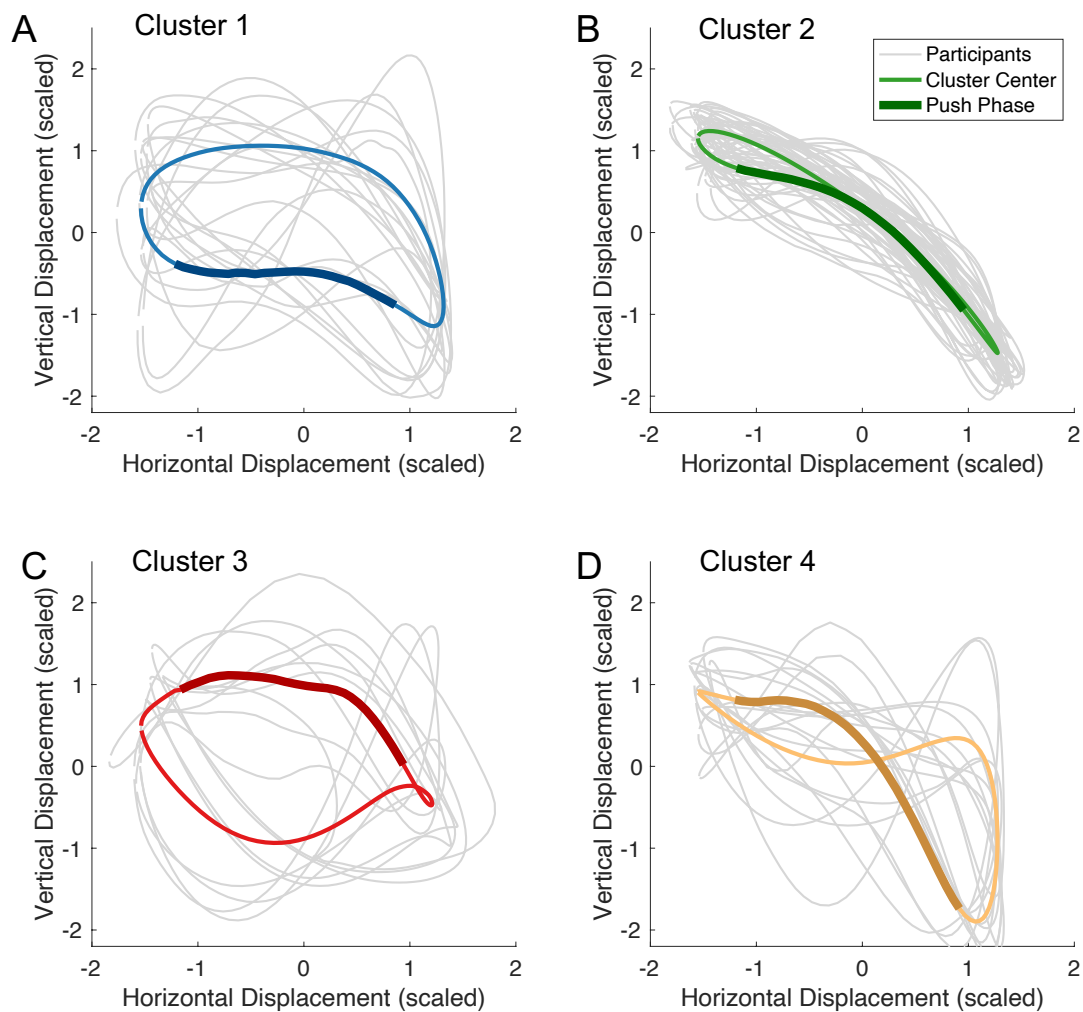


Figure 4.5: Side view wheeling patterns of the four clusters (A-D). Wheeling patterns of all participants belonging to that cluster and the cluster centroids (with highlighted push phase) are displayed.

4.5 Discussion

In this work, we presented an algorithm that is able to extract wheeling propulsion patterns besides other wheeling metrics from a sparse wearable inertial sensor setup. The performance of the algorithm was validated using an instrumented wheel and a marker-based motion capture system, which is widely accepted in the field as the gold standard for biomechanical analysis. Further, the algorithm was applied to data of the target population. More specifically, unsupervised machine learning was applied to the data of wheelchair-bound participants with a spinal cord injury, wheeling a distance of 160m at a comfortable speed. The clustering procedure resulted in 4 distinct wheeling patterns. How these wheeling pattern groups differ in other sensor-derived wheeling metrics was investigated and their composition in terms of clinical scores was studied.

The validation of the algorithm with a gold standard demonstrated overall good performance. Regarding

Chapter 4. Estimating Wheeling Propulsion Patterns using a Sparse Inertial Sensor Setup

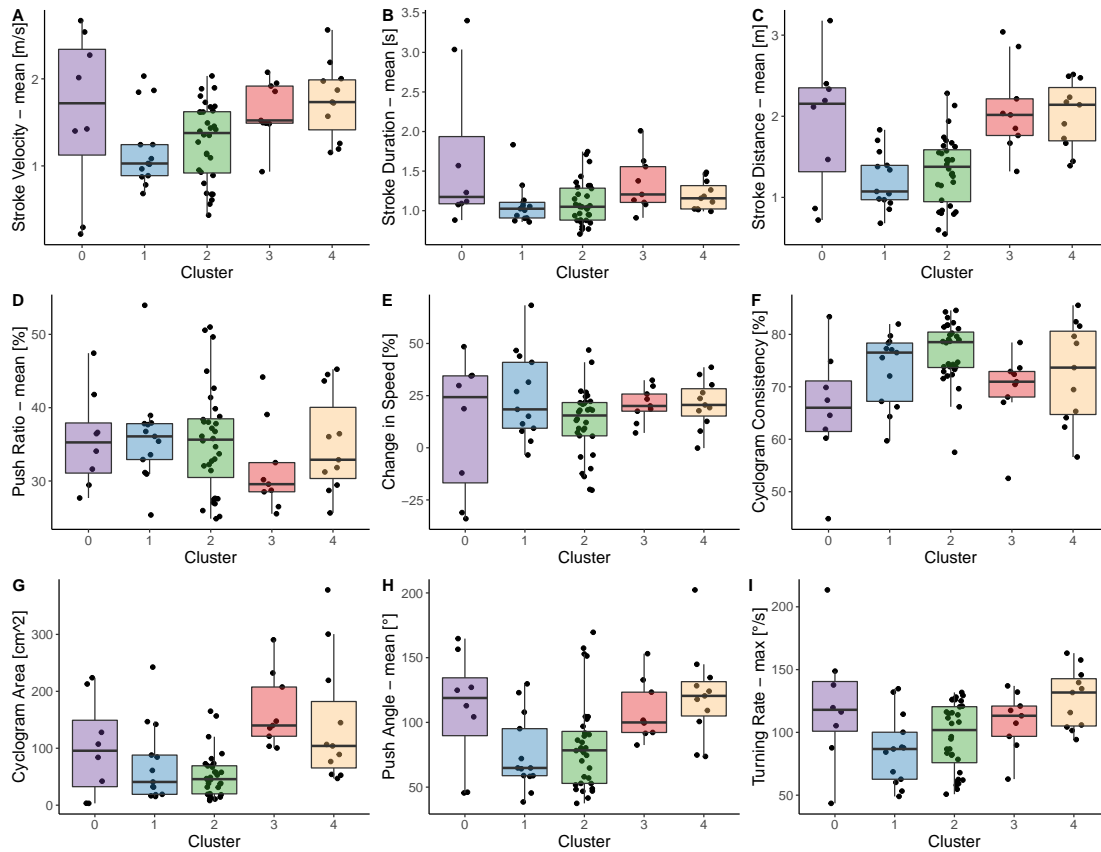


Figure 4.6: Boxplots of sensor-derived wheeling metrics (A-I) for the four clusters and the outlier cluster (cluster 0).

the validation of the IC and FC detection, a time difference of -6.1ms and 11.7ms, respectively, was found between the sensor derived events and the ground truth events derived from the instrumented wheel. Since this dataset was recorded at 100Hz, this means that the detection of the events was on average only 1 sample (10ms) apart. Lewis et al. [Lewis et al., 2018] obtained a mean absolute error of 13ms for estimating the stroke duration (from IC to IC) for their algorithm, which is comparable to the results presented in this study. However, with their IMU setup, one sensor attached to each wheel, and for their cohort of wheelchair athletes, they were unable to robustly capture the final contact. The presented algorithm detected 98% of all strokes. Comparing this to consumer-level activity monitors, Kressler et al. [Kressler et al., 2018] found on average a relative error 3-6% for counting strokes at higher wheeling frequencies, which were comparable to the dominating cadences in our dataset. The reconstructed wheeling propulsion patterns were of very similar shape to the pattern derived from motion capture data, even though the three participants had different wheeling propulsion techniques.

Applying the algorithm to an extensive dataset of wheelchair bound individuals with a SCI, four dominating wheeling propulsion patterns were identified when using unsupervised machine learning. These patterns are similar to what has been found previously in literature [Boninger et al., 2002, Kwarciak et al., 2012, Kwarciak et al., 2009]: the ARC, SC, SLOP, and DLOP patterns. The ARC pattern was the most dominant wheeling pattern in this dataset. The propulsion pattern clusters differed not only in the wheeling pattern, but also in other wheeling metrics, e.g. speed, cyclogram area, push

Table 4.2: Composition of the clusters considering only the first trial of each participant. Abbreviations: tetra.: tetraplegic; traum.: traumatic; UEMS: Upper Extremity Motor Score; SCIM: Spinal Cord Independence Measure; exp.: experienced

Cluster	n	tetra. [%]	traum. [%]	acute [%]	UEMS	SCIM	SCIM Mobility	exp. [%]
0	3	33.3	66.7	66.7	42 ± 13.9	47.3 ± 14.5	6.3 ± 2.3	66.7
1	7	14.3	42.9	85.7	46.7 ± 7.8	48.9 ± 22.5	8.7 ± 7.7	14.3
2	18	22.2	44.4	77.8	46.9 ± 7.8	53.8 ± 21.4	7.7 ± 4	16.7
3	5	20	80	60	43.6 ± 14.3	52.5 ± 24.3	6.2 ± 1.8	40
4	8	25	87.5	25	48.8 ± 2.4	74.4 ± 14.8	13.9 ± 5.8	62.5

angle, or stroke duration. Since a lower cadence [Lenton et al., 2008] and a higher push ratio [Groot et al., 2002] were found to be more efficient, this study further confirms that the propulsion technique is linked to wheeling efficiency. The highest percentage of experienced wheelers was found in the DLOP pattern cluster. Kwarciak et al. [Kwarciak et al., 2009] recommend the SC and DLOP pattern due to lower initial contact braking moments and power loss. Hence, the experienced wheelers in this study did chose a more efficient and less harmful wheeling pattern or were more trained to do so. The "weakest" wheelers showed the SLOP-like pattern. Moreover, 71% of the participants that were measured more than once were always clustered to the same cluster. This demonstrates that participants stick in general to their specific wheeling pattern over time.

The main limitation of this study is that the algorithm was only validated for a small sample size of three participants and not in the target population but in able-bodied individuals. However, the selection of participants showed three different wheeling patterns and the participants were wheeling with different speeds to test the algorithm for multiple conditions and different patterns. Hence, we believe that the results would be similar for the target cohort.

4.6 Conclusion

With the presented algorithm, extracting wheeling propulsion patterns and wheeling metrics from a sparse sensor setup becomes feasible with comparably reliable results to complex motion capture systems. The application of this algorithm to an extensive dataset of wheelchair-bound individuals exhibited distinct wheeling propulsion patterns and highlighted their differences in other wheeling metrics. In general, more experienced wheelers chose a more efficient wheeling pattern. The method enables future research on how wheelchair biomechanics is related to overuse injuries where the proposed setup could be used not only for short measurements, but also to analyze wheeling in real-world environments by providing insights into the actual wheeling behavior. Furthermore, this setup can be applied in a clinical setting to provide objective feedback on the wheeling performance. Therapists and clinicians could train more efficient wheeling propulsion techniques, test different wheeling positions or wheelchair products and assess the effect on the wheeling propulsion technique objectively. Hence, this study provides an objective, unobtrusive and cost-effective solution, which makes a wheeling biomechanical analysis broadly accessible and possible in various environments with the overall goal to improve wheeling efficiency and reduce overuse injuries for the individual.

5 Using Wearable Inertial Sensors to Estimate Clinical Scores of Upper Limb Movement Quality in Stroke

Charlotte Werner*, Josef G. Schönhammer*, Marianne K. Steitz, Olivier Lambercy, Andreas R. Luft, László Demkó, and Chris Awai Easthope
Frontiers in Physiology, 2022

* the authors share first authorship

In collaboration with Josef G. Schönhammer, Charlotte Werner was leading the data analysis and writing of the manuscript.

Chapter 5. Using Wearable Inertial Sensors to Estimate Clinical Scores of Upper Limb Movement Quality in Stroke

5.1 Abstract

Background Neurorehabilitation is progressively shifting from purely in-clinic treatment to therapy that is provided in both clinical and home-based settings. This transition generates a pressing need for assessments that can be performed across the entire continuum of care, a need that might be accommodated by application of wearable sensors. A first step toward ubiquitous assessments is to augment validated and well-understood standard clinical tests. This route has been pursued for the assessment of motor functioning, which in clinical research and practice is observation-based and requires specially trained personnel.

Methods In our study, 21 patients performed movement tasks of the Action Research Arm Test (ARAT), one of the most widely used clinical tests of upper limb motor functioning, while trained evaluators scored each task on pre-defined criteria. We collected data with just two wrist-worn inertial sensors to guarantee applicability across the continuum of care and used machine learning algorithms to estimate the ARAT task scores from sensor-derived features.

Results Tasks scores were classified with approximately 80% accuracy. Linear regression between summed clinical task scores (across all tasks per patient) and estimates of sum task scores yielded a good fit ($R^2 = 0.93$; range reported in previous studies: 0.61 to 0.97). Estimates of the sum scores showed a mean absolute error of 2.9 points, 5.1% of the total score, which is smaller than the minimally detectable change and minimally clinically important difference of the ARAT when rated by a trained evaluator.

Conclusion We conclude that it is feasible to obtain accurate estimates of ARAT scores with just two wrist worn sensors. The approach enables administration of the ARAT in an objective, minimally supervised or remote fashion and provides the basis for a widespread use of wearable sensors in neurorehabilitation.

5.2 Introduction

Neurological health conditions, such as stroke [Lindsay et al., 2019], traumatic brain injury [Dewan et al., 2019], multiple sclerosis, spinal cord injury, and Parkinson's disease [Feigin et al., 2017] are major causes of disability, often leading to limitations in motor functioning of the upper limbs [Hendricks et al., 2002, Katz et al., 1998, Kister et al., 2013, Broeks et al., 1999, Kwakkel et al., 2003]. In accordance with the International Classification of Functioning, Disability, and Health (ICF), motor functioning is typically analyzed at different levels of granularity, at the level of body joints and segments (ICF function level) and at the level of the execution of movement tasks (ICF activity level) [WHO, 2001]. The ICF further distinguishes motor functioning observed in controlled settings and in the person's natural/home environment (ICF capacity and performance). The measurement of motor functioning is a vital part of both research and practice in neurorehabilitation as it provides the basis for the evaluation of new rehabilitation programs [Brunner et al., 2017], new medications [Samuel et al., 2017], prediction of recovery [Wolf et al., 2021] as well as the design of patient-specific interventions.

The current gold standards for the measurement of motor functioning are mainly based on standardized clinical tests [Pohl et al., 2020, Prange-Lasonder et al., 2021, Kwakkel et al., 2017], in which patients perform a series of pre-defined movements in standardized conditions and experts score each movement on pre-defined criteria, such as task completion, task duration and kinematic and kinetic characteristics [Demers and Levin, 2017]. The tests must satisfy specific requirements in terms of both psychometric properties (validity, reliability, responsiveness) [Murphy et al., 2015] and clinical applicability (time and ease of training, administration, scoring, interpretation, cost) [Prange-Lasonder et al., 2021].

An emerging requirement regarding clinical applicability is that the tests should be suitable for the entire rehabilitation process from in-clinic to ambulant and home settings (further referred to as continuum of care). This is desirable since neurorehabilitation is expected to shift to patients' homes due to capacity limitations in healthcare and advances in home-based rehabilitation technologies [Lambercy et al., 2021]. However, the need for a trained evaluator to conduct a clinical test conflicts with the goal of ubiquitous measurement protocols.

Another requirement is that assessments should take into account movement quality [Kwakkel et al., 2017]. Movement quality refers to the degree to which patients' motor execution of a task resembles that of normal individuals [Kwakkel et al., 2019]. High movement quality is associated to the restitution of pre-morbid movement execution patterns, whereas low movement quality is linked to alternative (compensatory) movement patterns [Demers and Levin, 2017, Jones, 2017]. Specifically, task execution of patients with neurological disorders is typically characterized by slow and jerky movements of the arm end point, abnormal grasping, reduced elbow extension, and increased shoulder abduction compared to age-matched healthy individuals [Saes et al., 2022].

Ideally, movement quality should be quantified with kinematic measures [Saes et al., 2022]. However, the identification of kinematic measures of arm movement quality is challenging because many kinematic parameters exist [Schwarz et al., 2019], their relevance depends on the specific movement task [Schwarz et al., 2019], selected kinematic measures require extensive psychometric validation [Murphy et al., 2011, Murphy et al., 2012, Thrane et al., 2020, Frykberg et al., 2021], and the measurement systems are usually stationary, expensive, and require expert users [Murphy et al., 2018].

Due to the difficulties with establishing kinematic measures of movement quality studies started to explore an intermediate goal. Supervised machine learning algorithms and low-cost sensor data were

Chapter 5. Using Wearable Inertial Sensors to Estimate Clinical Scores of Upper Limb Movement Quality in Stroke

used to estimate clinical test scores (for reviews see [Simbaña et al., 2019, Kim et al., 2021, Boukhennoufa et al., 2022]). This approach has the advantages that the clinical tests have established psychometric properties [Kim et al., 2021], that clinical scores are easy to interpret [Kim et al., 2021] and that wearable movement sensors can be used which are low cost and enable data collection across the entire continuum of care [Simbaña et al., 2019, Kim et al., 2021, Boukhennoufa et al., 2022]. Tests of ICF activity capacity assess limitations in the accomplishment of tasks that are relevant for activities of daily living [Prange-Lasonder et al., 2021]. Importantly, clinical scores of ICF activity capacity often contain information about movement quality since evaluators visually examine movement quality to determine the test scores [Sapienza et al., 2017, Adans-Dester et al., 2020, Yozbatiran et al., 2008].

One of the most prominent clinical test of upper-limb ICF activity capacity is the ARAT [Lyle, 1981, Yozbatiran et al., 2008], which provides a combined score comprising the aspects of movement speed, successful task completion, and hand and arm movement quality [Yozbatiran et al., 2008]. In the ARAT, a patient performs several tasks that require combined reaching and grasping. Performance in each task is rated on an ordinal scale depending on task duration and observed movement quality characteristics (e.g., smoothness of the arm endpoint, abnormal grasp, compensatory movements) [Lyle, 1981, Yozbatiran et al., 2008]. Individual task scores are then summed up to a total score [Lyle, 1981, Yozbatiran et al., 2008]. The ARAT is the most frequently used assessment of upper-limb functioning in clinical studies [Murphy et al., 2015], as it is used in a broad range of neurological health conditions such as stroke, traumatic brain injury, multiple sclerosis [Prange-Lasonder et al., 2021] and Parkinson's Disease [Song, 2012], has excellent psychometric properties [Pike et al., 2018], is widely accepted and recommended by experts [Pohl et al., 2020, Prange-Lasonder et al., 2021, Kwakkel et al., 2017], and is a significant predictor of motor recovery in stroke [Wolf et al., 2021]. Despite the importance of the ARAT, however, wearable sensor data were never utilized to estimate the test outcome, to the best of our knowledge [Simbaña et al., 2019, Kim et al., 2021, Boukhennoufa et al., 2022].

In the current study, we collected data of stroke patients performing the ARAT while two inertial sensors were attached to their wrist. ARAT task and total scores were estimated using supervised machine learning. We hypothesize that with this approach it is feasible to estimate ARAT scores with an error that is similar or smaller than clinically relevant changes, namely, the minimally detectable change [Simpson and Eng, 2013] and the minimal clinically important difference of the ARAT task and total scores [Lee et al., 2001]. Such sensor-based estimates of clinical scores may pave the way for automated, expert-independent administration. In addition, the simple setup of using just two wearable sensors enables location independent measurements with the potential to be used across the whole continuum of care.

5.3 Methods

The current study was a secondary analysis of data collected under a randomized-controlled trial [[Steitz et al., 2022]; Kantonale Ethikkommission Zentralschweiz, approval number: BASEC:2017-00199] and during an evaluation of sensor types in clinical routine (Kantonale Ethikkommission Zentralschweiz, request number: Req-2020-00995). Both studies adhered to the Declaration of Helsinki. Participants were recruited at the University Hospital Zurich and the Center for Neurology and Rehabilitation cereneo, and gave informed consent prior to both studies.

5.3.1 Participants

Participants were included if they were (i) 18 years of age or older, (ii) in a sub-acute stage of stroke (3-90 days after symptom onset) with lateral ischemia (or hemorrhage) as confirmed by brain imaging and (iii) showed subsequent impairment of arm function with a Fugl-Meyer Assessment for the Upper Extremities (FMA-UE) score between 15 to 59 points. Participants were excluded in case of (i) other neurological disorders that might result in dementia, cognitive dysfunction or central motor symptoms, (ii) severe sensory aphasia, (iii) preexisting arm paresis, (iv) intake of sedatives or neuroleptics, or (v) relevant hearing.

Data of 21 participants who satisfied these criteria were acquired. The age of the participants was 68 +/- 10 years (mean +/- standard deviation), out of which 5 were female and 20 right-handed. All patients were in a subacute stroke stage at the time of the first assessment, with symptom onset 38 +/- 17 days before the assessment. All patients had lateralized ischemia or hemorrhage as confirmed by brain imaging, and suffered subsequent impairment of the arm function, i.e., the FMA-UE score was 33 +/- 15 points. The median of the total clinical ARAT score of the 21 patients was 35.5 (interquartile-range: 19.5-47.3) and 57 (interquartile-range: 45-57) for the more and less affected sides, respectively. The study population thus covered a broad range of patients with different upper extremity motor function.

5.3.2 Apparatus, Instruments, and Procedures

The ARAT was administered twice per participant, at baseline and 1-4 weeks later. The ARAT comprises of 19 movement tasks that are grouped into 4 domains (grasp, grip, pinch and gross movements). Each task is performed with the less impaired arm first and the more impaired arm second, and assigned an ordinal rating with a range from 0 to 3. The ARAT was conducted with standardized materials (Figure 5.1A) and procedure [Yozbatiran et al., 2008], with one exception: In the standard procedure, subjects make an attempt on the first, most difficult task in each domain, and, in case of normal functioning, skip the remaining, easier tasks of the domain. In this study, however, all task were administered to maximize the data obtained from each participant. The performance of each movement of each patient has been assessed by one of two experienced evaluators, resulting in a maximum achievable total score of 57 per arm and per test. Since the ARAT is highly standardized and has high inter-rater and test-retest reliabilities (ICC < 0.98)[Lee et al., 2001], we believe that the selection of the evaluators does not affect the rating results.

During the assessment, wearable inertial sensors (ZurichMOVE, Switzerland) were tightly attached to each wrist with custom-made flexible straps as shown in Figure 5.1B. The main components of the sensor modules are a tri-axis accelerometer, gyroscope and magnetometer, measuring at a sampling frequency of 50Hz, which is sufficient given that there was no aim to reconstruct the actual movement trajectories. The magnetometer data was excluded from the analysis, because magnetic fields are often distorted indoors, and thus the magnetometer data is considered to be unreliable. Furthermore, the timestamp of the beginning and end of each task was recorded.

5.3.3 Data Preprocessing and Analysis

Since accelerometers measure both the movement acceleration and gravity, the gravitational component has to be subtracted from the acceleration signal. For this, the orientation of the sensors in space was obtained by using the sensor fusion algorithm developed by Seel et al. [Seel and Ruppin, 2017].

Chapter 5. Using Wearable Inertial Sensors to Estimate Clinical Scores of Upper Limb Movement Quality in Stroke

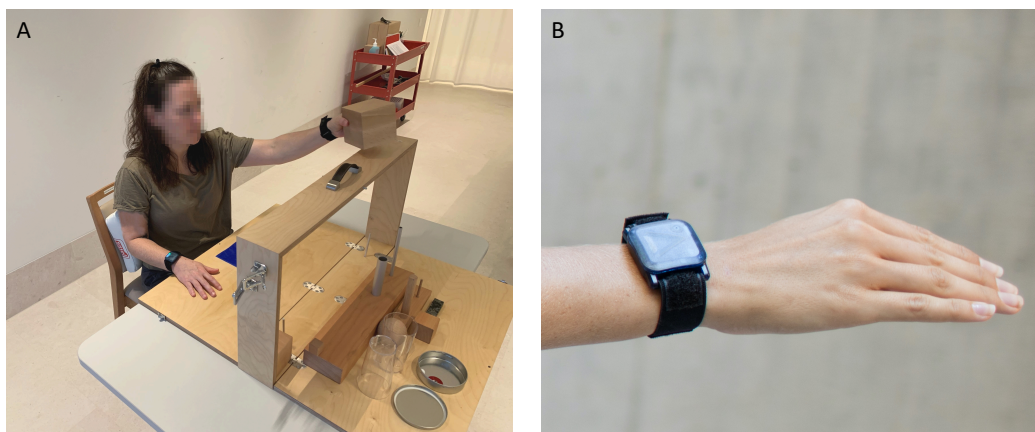


Figure 5.1: **(A)** A participant performing ARAT task 1, which is part of the grasp domain. The task is to grasp a wooden block (10 cm in size) at the start position (blue patch on the table) and to put it on the shelf in front of the subject. **(B)** Close-up of the inertial sensor attached to the wrist.

This algorithm is based on an analytical solution to remove the drift in the inclination angle with the information of the direction of gravity from the accelerometer. Based on the sensor orientation the acceleration data could be transformed from the moving coordinate system into a coordinate system fixed in space. In this fixed coordinate system, the gravitational component is pointing in the vertical direction and can thus be easily removed by subtracting g from this axis. This procedure resulted in the pure movement acceleration data.

The tri-axial acceleration and angular velocity data was then segmented according to the recorded start and stop times of each task. This resulted in 6D time series sequences of different lengths, depending on how long the patient needed to perform the given task. Short sequences lasted around 1-2s, while the maximum sequence length was limited to 60s (as per ARAT definition if the patient was unable to complete the task within this time). In rare cases (<6.7%), data were missing due to technical problems or because the patient did not attempt to perform the task. In such cases, the patient received a score of 0 for this task, and a sequence of non-moving data of 10s from this patient was used in order to have complete data sets.

5.3.4 Feature Extraction and Classification

The machine learning approach used in this study required features for the classification. Hence, descriptive features were extracted from each time series sequence. The selection of features was based on the recommendations of Suto et al. [Suto et al., 2017] for human activity recognition. In order to characterize the sequences of each task in the time domain, the following features were computed for each axis of the acceleration and angular velocity time series data: mean, standard deviation, minimum (defined as the 5th percentile), maximum (95th percentile), range (minimum to maximum), mean absolute deviation, interquartile range (25th to 75th percentile), upper quartile (75th percentile), zero-crossing rate, and kurtosis. To characterize the frequency spectrum of the data, a fast Fourier transform was applied to the vector-wise norm of acceleration and angular velocity time series data of

each task. The following features were extracted: maximum frequency component, spectral energy of different frequency ranges (0 to 5Hz, 5 to 10Hz, 10 to 15Hz, 15 to 20 Hz, and 20 to 25Hz), and spectral centroid. This resulted in altogether 74 features for each task: 60 features characterizing the movement in the time domain and 14 features characterizing the movement in the frequency domain.

The model received these sensor-derived features as an input to estimate the 4-point scale ARAT task scores. All features were standardized by centering them around the mean and scaling them to have unit variance in order to provide features of similar magnitude to the classifier. An ordinal classifier as described by Frank et al. [Frank and Hall, 2001] was chosen as a model to consider the ordinal ranking of the 4 ARAT task scores. A logistic regression was then selected as classifier, and regularization was used to prevent overfitting on the training data. This ordinal logistic regression classifier was trained individually for each of the 4 ARAT domains, because the movements within these domains differed significantly. The grasp and pinch domains consist of pick-and-place tasks that differ in terms of grasping type. Tasks of the grip domain on the other hand resembles daily life activities, e.g. pouring water from a bottle to a glass, while the gross domain includes shoulder and arm movements across a wide workspace. The separation into the four domains fostered each classifier to differentiate between different executions of the same movement task as opposed to training a single classifier on all tasks, which would have needed to handle the high variability introduced by the different nature of the movement tasks.

The less affected arm achieved the maximal score in many of the subtasks, which resulted in a highly unbalanced data set. To counteract this, the training data set has been balanced by upsampling the number of rare observations using the synthetic minority over-sampling technique (SMOTE) [Chawla et al., 2002]. Due to the small sample size leave-one-subject-out cross-validation procedure was used to test the classifiers on unknown data. More specifically, the upsampled data of all subjects and all sessions except for the data of one subject and both sessions (if available) was used to train the model, which was then tested on the original (non upsampled) data of the remaining subject. This process was repeated until the model was tested on the data of all subjects. A flowchart of the data processing and classification workflow is displayed in Figure 5.2.

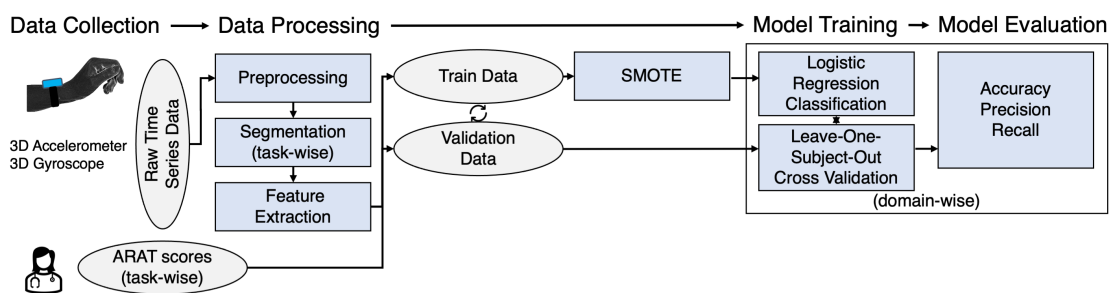


Figure 5.2: Flow chart of the framework to estimate task-wise ARAT scores from inertial sensors attached to the wrist.

5.3.5 Evaluation of the Model

The performance of the classifiers for each domain has been estimated based on accuracy, precision, and recall computed from the clinically assessed (further referred to as clinical) ARAT task scores and

Chapter 5. Using Wearable Inertial Sensors to Estimate Clinical Scores of Upper Limb Movement Quality in Stroke

the estimated ARAT task scores. These metrics were weighted by the distribution of the samples within the classes to account for class imbalances. For each arm, the estimated task-level ARAT scores were summed up to yield an estimate of the total ARAT score. Linear regression was used to study the relationship between the clinical and the estimated total ARAT scores. Furthermore, the mean error and the root mean squared error (RMSE) were computed as the average and the root mean squared of the differences between the estimated and the clinical ARAT scores, respectively.

5.4 Results

5.4.1 Estimation of the ARAT task scores

The measurement of the 21 patients resulted in 1366 observations altogether (2 observations had to be excluded) that were divided into the 4 domains to train the ordinal classifiers. No patient received a score 0 in any of the tasks of the gross domain. Hence, the gross classifier was only trained on 3 classes. For all domains, the classifiers identified the task scores of 3 well. However, the classifiers had difficulties discriminating score 1 from 0 and 2, which were also the cases with fewer number of observations in comparison to the other cases. The normalized confusion metrics and number of observations per class are shown in Figure 5.3.

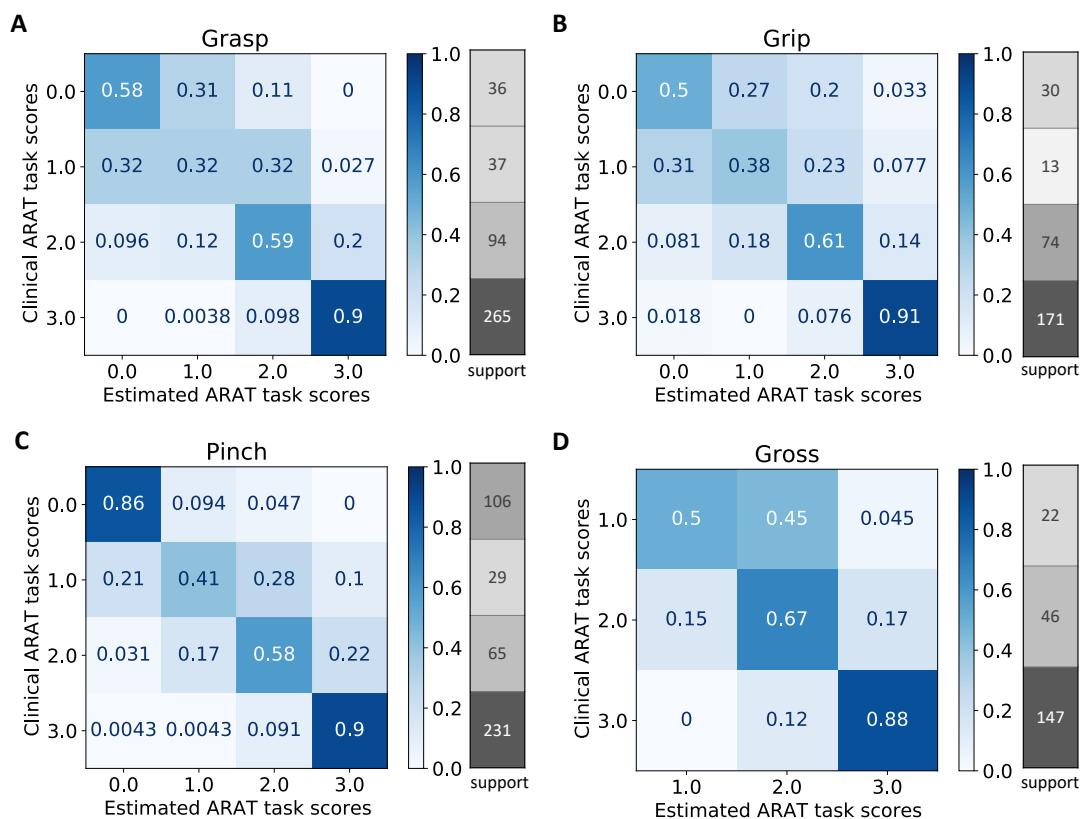


Figure 5.3: Normalized confusion matrices and number of observations per class (support) for the four domains: grasp (A), grip (B), pinch (C), and gross (D).

The 4 ordinal classifiers estimated the ARAT task scores from the sensor-based features with a weighted accuracy ranging from 76% (grasp) to 81% (pinch) as evaluated by the leave-one-subject-out cross-validation and summarized in Table 5.1. For the pinch and gross domains, weighted accuracy, precision, and recall values of above 0.8 were obtained. The classifiers performed slightly worse for the grasp and grip domains, where values below 0.8 were obtained for accuracy, precision, and recall. Note that the unbalanced nature of the data affects the weighted accuracies. More specifically, score 3, which was classified with high accuracy, has a strong influence on the overall accuracy as it was the most frequent observation, while the other, more infrequent scores, which were classified with low accuracy, have less impact.

Table 5.1: Overview of performance of the model predicting the ARAT task scores in the four domains: weighted accuracy, precision, and recall

Domain	Accuracy	Precision	Recall
Grasp	0.75	0.76	0.75
Grip	0.76	0.79	0.76
Pinch	0.81	0.82	0.81
Gross	0.80	0.81	0.80

5.4.2 Estimation of the total ARAT score

The total ARAT score, obtained by a summation of the estimated ARAT tasks scores, showed a mean error of 0.5, a mean absolute error of 2.9 points with a maximal error of 12 points. A RMSE of 4.7 was obtained. Relative to the maximum achievable total score of 57, this is a relative error of 8.2%. Higher estimation errors were obtained for the more affected side in comparison to the less affected side as depicted in Figure 5.4A. A linear regression between the clinical and estimated total ARAT scores resulted in a good fit ($R^2 = 0.93$) as plotted in Figure 5.4B, close to the ideal curve ($y=x$).

5.5 Discussion

The objective of this work was to determine whether a simple and fast setup of wearable sensors is sufficient to estimate clinical ARAT scores given by a trained evaluator. Successful estimation of ARAT is a first step toward evaluator-free measurement of ICF activity capacity and upper limb movement quality. For this purpose, data of 21 patients performing the standardized ARAT assessment while wearing two wrist-worn inertial sensors was recorded. By applying machine learning techniques to the time series sensor data, ARAT scores could be estimated at the task level. More specifically, ordinal classifiers were trained on the balanced observations of each domain, and the performance of the classifiers was evaluated by cross-validation using typical machine learning metrics. In addition, the estimated total score, which was obtained by the summation of all the task scores, was compared to the clinical total score.

Overall, the weighted averages of the classification accuracies of the task scores were around 80% for all ARAT domains, ranging from 32 to 91% for the individual classes within a domain. Differences in performance of the classifiers might have several reasons. First, the domains differ in the homogeneity

Chapter 5. Using Wearable Inertial Sensors to Estimate Clinical Scores of Upper Limb Movement Quality in Stroke

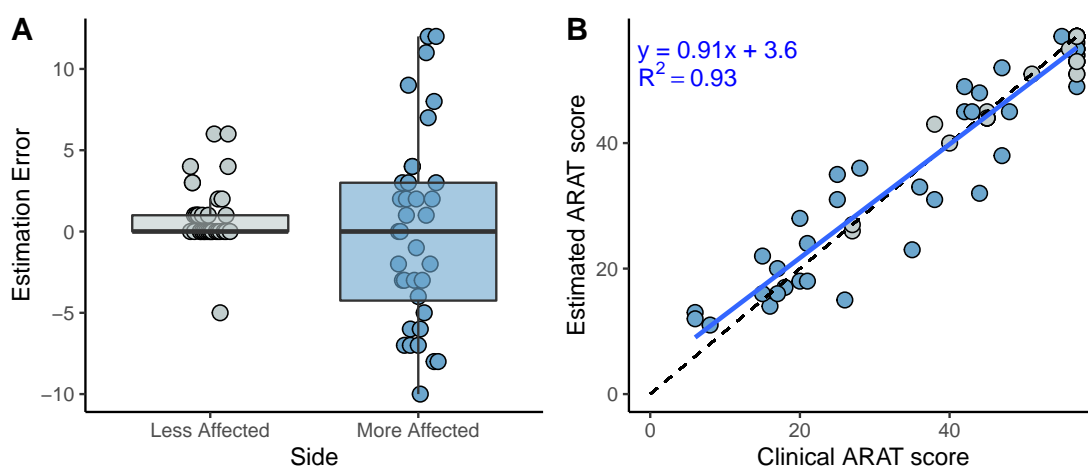


Figure 5.4: **(A)** Box plots showing the estimation error of the total ARAT scores for the more and less affected sides. **(B)** Linear regression (blue line) between the clinical and estimated total ARAT scores. The dashed line depicts the ideal case of $y=x$.

of the movements within the respective sets of tasks. In particular, the tasks in the grip domain require relatively dissimilar movements and, hence, the classifier had more difficulties to distinguish between different movement qualities. For example, one task is to pour water from one glass to another, whereas another task is to grasp a washer, to transfer it forward and to put it over a bolt. In contrast, the tasks in the pinch domain afford relatively similar movements, as all tasks consist of pick-and-place actions, where the main difference only lies in the tested fingers. Consequently, better classification performance was observed for the pinch domain. Second, the distributions of observations across the classes (i.e., the test scores) showed different degrees of imbalance between the domains. For example, the distribution of observations in the pinch domain was relatively well balanced and, accordingly, relatively high classification performance was observed. Conversely, in the remaining domains the distribution of observations was skewed even more toward higher test scores. This issue was addressed with the SMOTE oversampling technique. But certainly synthetically generated observations cannot substitute actual observations and, consequently, we observed lower classification performance in these domains. Third, in the gross movement domain we did not obtain any observation of score 0. Hence, for this domain the classifier only needed to be trained on 3 classes, which explains the rather good performance of this classifier compared to the classifiers of the other domains. Furthermore, classification accuracies differed between the task score levels. Specifically, for the grasp, grip, and pinch domain, the classifiers had difficulties to discriminate failure to complete the task even partially (score 0) from a partial completion (score 1), and a partial completion (score 1) from a completion of the task with great difficulty (score 2). An explanation might be that the extracted features captured this information only partially. The results suggest that the differences in wrist movements for these scores are minimal, and additional sensors, e.g. attached to the hand, could be beneficial to better identify the completeness of the task. In addition, high inter-subject variability in execution of the tasks (probably due to the different sensorimotor impairments of this patient population) and few observations of score 1 might have prevented more accurate identification of this score.

Estimates of the total ARAT score showed a mean absolute error of 2.9 points of the estimated total ARAT score as compared to the clinical total score. This error is below the minimally detectable change

(MDC: 3.5 points; [Simpson and Eng, 2013]) achieved by trained observers and our maximal error of 12 points is also below the minimal clinically important difference of ARAT found in the literature (MCID: 12-17 points; [Lee et al., 2001]). The good fit of the linear regression between the estimated and clinical ARAT total scores ($R^2 = 0.93$) suggests that our approach is suitable to generate accurate estimates of the ARAT total scores. Consequently, our method has an accuracy of clinical relevance and is precise enough to detect clinically important changes in the ARAT. These good results at the sum score level suggest that errors on the tasks level might have averaged out.

Using only wrist worn sensors, one might expect inferior results, as wrist worn sensors neither directly measure movements of the elbow joint or trunk which are highly correlated with the ARAT scores [Murphy et al., 2012], nor do they capture finger and hand movements which are visually examined by experts when rating the ARAT performance. However, wrist worn sensors directly capture wrist motion which is linked to movement quality aspects such as the speed and smoothness of arm movements [Kwakkel et al., 2019]. These kinematic variables are known to be correlated with the ARAT scores [Carpinella et al., 2014, Replik et al., 2018], which explains the fact that we nevertheless achieved good classification results. Additionally, it is possible that wrist-worn sensors indirectly capture motion of other joints and segments as well and that this information is represented in the selected features we used to estimate the ARAT scores. However, this statement remains speculative and further research would be required to systematically investigate how the number and placement of the sensor units, as well as the direct and indirect measurement of movements, contribute to the accuracy of clinical scores estimations. This question has never been addressed so far, neither in studies that estimated different clinical scores with larger numbers of sensors [Adans-Dester et al., 2020, Patel et al., 2010], nor in reviews of clinical assessments with wearable sensors [Simbaña et al., 2019, Kim et al., 2021, Boukhennoufa et al., 2022].

Since no previous study estimated ARAT scores from wearable sensors we compare our results to studies that either used different motion sensing techniques to estimate ARAT scores, or studies that used wearable sensors and estimated scores of different clinical tests of ICF activity capacity. For these studies, we inspected coefficients of determination for the relationship between clinical and estimated total scores and (when reported) the estimation error for the difference between clinical and estimated total scores. The results of our study fall in the range of previously achieved results. Alt Murphy et al. [Murphy et al., 2012] predicted total ARAT scores using kinematic data from marker-based motion capture and observed moderately strong association between clinical and estimated total scores ($R^2 = 0.67$). Patients performed a single 3D reaching task and a pre-selected set of movement features were calculated. Kinematic features included: smoothness of the arm endpoint, total movement time, trunk displacement and peak angular velocity of the elbow. The ARAT scores of the patients were obtained in a separate session, then a regression model predicted the total ARAT scores from the kinematic metrics. Olesh et al. [Olesh et al., 2014] estimated scores of the FMA-UE using kinematic data from a low-cost depth sensing camera. Clinical and estimated total FMA-UE scores showed strong association and small estimation errors ($R^2 = 0.86$, RMSE = 7.7%). The FMA-UE is a clinical test of ICF function capacity and is intended to assesses more fine-grained movements than the ARAT, but the scale was applied to a subset of movement tasks of the FMA-UE and the ARAT gross movement domain, which makes these results comparable to ours.

Other studies used wearable sensors but estimated different clinical test scales at the ICF activity capacity level. Previous studies estimated the Functional Ability Scale (FAS, which is a subscale of the Wolf Motor Function Test) based on data collected during the execution of a subset of the FAS tasks [Patel et al., 2010, Sapienza et al., 2017, Adans-Dester et al., 2020], using two (on wrist and sternum)

Chapter 5. Using Wearable Inertial Sensors to Estimate Clinical Scores of Upper Limb Movement Quality in Stroke

or six sensors (distributed over fingers, forearm, upper arm and sternum). R^2 ranged from 0.79 to 0.97 and RMSE from 2.9% to 7.6%. Other studies estimated the Chedoke Arm and Hand Activity Inventory (CAHAI) based on data collected in free-living settings with two wrist worn sensors [Chen et al., 2020, Tang et al., 2020], with R^2 ranging from 0.61 to 0.92, and RMSE from 3.1% to 12.0%. Compared to these results, our approach falls in the same range with the advantage of using just two wrist worn sensors.

One strength of this study is the minimalistic sensor setup, which minimizes costs, setup time and device obtrusion, all of which are barriers to the wide spread use of kinematic assessments of motor functioning [Saes et al., 2022]. The hardware costs of commercially available inertial sensors, approximately \$50 per sensor unit, are relatively low as compared to those of optoelectrical camera systems, approximately \$10'000 per system, which are the current gold-standard for clinical motion analysis. Additionally, the same set up is frequently used to measure other aspects of motor functioning [Simbaña et al., 2019, Kim et al., 2021, Boukhennoufa et al., 2022]. For example, many studies collected data during activities of daily living or free-living settings and aimed to develop new measures of ICF activity performance, such as quantifications of impaired arm use (e.g., [Lee et al., 2019, Bailey et al., 2015]). Hence, this setup and our analysis have great potential to be applied across the entire continuum of care. It is also worth pointing out that we only used statistical features of acceleration and angular velocity data, in time and frequency domain. These features are easy to obtain from most wearable inertial movement sensors. Hence, the approach is easier to apply and is less biased than solutions that require pre-selection and computation of kinematic features, such as the smoothness of arm endpoint movements or specific joint angles (e.g., [Kim et al., 2016, Olesh et al., 2014]).

The current study has several limitations. A first limitation is the small sample size. A larger and more diverse sample might increase the prediction accuracy and robustness of the model. In addition, we only included persons with stroke, and it could be interesting to include patients with other neurological disorders as well to further explore the applicability of the sensor-based ARAT estimations. Second, since only one evaluator per participant conducted the ratings we can only assume that the variability between evaluators had only a minor effect on the rating results. Third, other drawbacks are inherent to the use of clinical scores as reference information for training a machine learning model, and the fact that such a model only reproduces the information represented in the clinical scores. Hence, the information contained in the estimated scores depends on that contained in the clinical scores. We assume that the ARAT contains information about movement quality, similar to clinical studies about the ARAT [Yozbatiran et al., 2008], and similar to previous studies which used the FAS to capture information about movement quality [Sapienza et al., 2017, Adans-Dester et al., 2020]. These scales, however, assign a task score based on a combination of criteria, some of which might be associated with movement quality only indirectly [Demers and Levin, 2017].

Finally, even though estimated ARAT scores provide an objective and easily interpretable quantification of movement quality, they share the same discrete scale as the underlying, subjective clinical score. Clinical scores are embedded in the field so much that every new method that can estimate previously established clinical scores starts with a clear advantage. Still, scientific research should not stop here. It is worth to reiterate that the estimation of clinical scores is just one way to quantify movement quality using wearable sensors, and that this effort should be complemented with kinematic measures, since these provide quantification of movement quality on a continuous scale (e.g., [Formstone et al., 2021, Schwarz et al., 2019]). However, while wearable inertial sensor data were already used to explore kinematic measures of movement quality [Repnik et al., 2018], the selection and clinical validation of useful measures is still outstanding.

5.6 Conclusion

The present study demonstrates that it is possible to estimate ARAT task and sum scores with sufficient accuracy for clinical applications using wearable inertial sensors. More specifically, estimation errors smaller than the detectable and important changes of the observation-based ARAT were obtained. The proposed method uses a minimal sensor setup of only one sensor per evaluated arm, which offers a simple, objective, fast and inexpensive way to assess the quality of upper extremity motor functioning across clinical and remote settings. Hence, the current study is opening the doors to more objective and potentially unsupervised assessments of arm and hand motor functioning, in particular at the ICF activity capacity level.

6 General Discussion

The main goal of this thesis was to provide inertial sensor-based solutions to assess activities of daily living for patients with neurological disorders. The complete workflow, from identifying a sparse sensor setup for assessing three key activities of daily living to developing and validating algorithms to extract digital metrics, and the clinical understanding of such metrics, was investigated.

Chapter 2 presents a robust algorithm for a sensor-based gait analysis. Using shank-mounted inertial sensors, spatio-temporal gait parameters were robustly derived for patients with a SCI walking at slow and preferred walking speeds. In chapter 3, this algorithm was applied to an extensive dataset of SCI patients and healthy controls performing a 6MWT while wearing sensors. Using a data-driven approach, non-redundant and relevant sensor-derived gait metrics could be identified to characterize the clusters with similar gait phenotypes. Further, including sensor-derived metrics improved the prediction model, estimating whether a patient will increase his or her walking capacity. Chapter 4 presents a novel algorithm to extract wheeling propulsion patterns from inertial sensor data. Groups of individuals who use wheelchairs with similar wheeling patterns were identified and compared in terms of clinical characteristics and other sensor-derived wheeling metrics. Chapter 5 presents a method to replace therapist ratings by estimating the clinical scores from sensor-derived features. A widely used assessment of reaching and grasping function was chosen to demonstrate the feasibility of using inertial sensors for a minimally-supervised assessment.

In the following, the findings presented in the previous chapters will be discussed with respect to the objectives of this thesis, their contribution to the field and their clinical impact will be highlighted, and recommendations for future research possibilities will be given.

6.1 Synthesis of results with respect to objectives

On the quest to promote technology-aided assessments using wearable inertial sensors, the importance to consider the whole scheme from a selection of a suitable sensor setup, to the algorithm development and the evaluation of sensor-derived metrics for the target cohort has been identified and set the objectives of this thesis. Given this approach, this thesis extends most work in the field which is usually only focusing on proposing algorithms to derive metrics from the raw sensor data. However, these metrics are rarely validated in the target population and thus their clinical meaningfulness often remains unclear.

Chapter 6. General Discussion

Objective 1: Identify a modular, sparse sensor setup to assess key activities of daily living

Three key activities of daily living were identified, and a modular but sparse sensor setup was selected suitable for each application. The most important requirement for selecting the activities was the activity's relevance for the individual in terms of mobility and independence. This implies that functional movements were chosen that frequently occur during daily life. The frequent nature of these movements further ensured that enough data would be available to characterize those movements comprehensively. In addition, activities involving either the upper or lower limbs were selected. Based on these requirements, walking, wheeling, and grasping movements were selected as three key activities of daily living. Walking and wheeling were chosen from the mobility domain of physical activities, and grasping was selected as a movement relevant for many daily life activities, such as getting dressed, eating, and many more.

A suitable sensor setup was selected to assess each activity. A trade-off was made between capturing full-body kinematics with an extensive body sensor network and reduced information from fewer sensors attached to specific body positions. The number of sensors and body attachment sites was chosen to potentially allow long-term measurements of several days in a real-world setting in the future with the same setup. Since this is the key benefit of using wearable sensors in contrast to both motion capture systems and conventional assessments related to activity limitation [Jalloul, 2018]. The main requirements for the sensor positions were that the attachments had to be comfortable and unobtrusive for the patient while still being located close to the main moving body parts.

Similar to the favored attachment location of commercial devices, the wrist was identified as a comfortable and suitable position for the assessment of grasping movements. On the one hand, sensors attached to the wrist are watch-like and thus familiar to the individual; on the other hand, as being attached distally, the sensors carry favored information of combined shoulder and elbow movements. An additional sensor attached to the wheel was chosen to assess wheeling. This improved the algorithm's performance while not adding more sensors to the person itself. One sensor was attached to each ankle to assess walking. Ankles were preferred over foot-mounted sensors because ankle-mounted sensors can simply be attached with flexible straps like the sensors attached to the wrist, while the attachment of foot-mounted sensors depends on whether and what kind of shoes are worn. Furthermore, the superiority of shank-mounted sensors compared to trunk- or wrist-mounted sensors in terms of accuracy of the derived metrics has been widely shown [Mansour et al., 2015, Yang and Li, 2012].

Objective 2: Development and validation of novel algorithms to assess these activities

Algorithms to extract digital health metrics from the raw inertial sensor data are necessary to quantify and qualify the activities. As altered movement patterns of individuals with a CNS can be challenging for data processing, algorithms should be validated in the target cohort [Rast and Labrüyère, 2020].

The sensor-based gait analysis, presented in chapter 2, was based on existing algorithms found in the literature [Yang and Li, 2012]. The gait event detection procedure identifies peaks similar to algorithms presented previously [Trojaniello et al., 2014a, Sabatini et al., 2005]. Moreover, spatial parameters were derived using a double integration approach, including a zero-velocity update of the acceleration data, a method that is also widely used for sensor-based gait analysis [Li et al., 2010, Wahlstrom and Skog, 2021]. The main contribution of the proposed algorithm is the automatic adaptation of thresholds necessary to identify individual strides and gait events to the walking sequence of each patient. These

6.1 Synthesis of results with respect to objectives

adaptive thresholds make this algorithm more robust across different gait profiles and speeds than algorithms dependent on fixed thresholds, e.g., the algorithm presented by Trojaniello et al. [Trojaniello et al., 2014a]. This robustness was confirmed by comparing the algorithm's performance to ground truth data of healthy controls and individuals with a SCI. Furthermore, besides typical spatio-temporal parameters, a method was presented in chapter 3 on deriving ankle endpoint trajectory cyclograms. The benefit of such cyclograms is that metrics such as the cycle-to-cycle consistency and the difference to a reference shape with the ACC and SSD can be derived, respectively. Both metrics are independent of the stride length or walking speed and related to the walking quality. To the best of our knowledge, this is the first work deriving and analyzing these ankle cyclograms from shank-mounted inertial sensors.

A novel algorithm for estimating wheeling propulsion patterns was presented in chapter 4. Since wheeling shares the periodicity of the movement as a key characteristic with walking, core parts of the gait algorithm could be adapted to the wheeling movement. By fusing data from a sensor attached to the wheel and the wrist, wheeling propulsion patterns and other wheeling-related metrics were derived. The presented method showed promising results compared to the propulsion patterns and push events obtained from a gold standard. This algorithm largely extends the work presented in the literature, where mainly algorithms were developed to identify individual strokes or to estimate the energy expenditure during wheeling [MacDuff et al., 2022].

A machine-learning-based methodology to estimate clinical scores for reaching and grasping tasks from sensor data was presented in chapter 5. In contrast to the algorithms developed to assess wheeling and walking movements, this method uses metrics derived directly from the raw sensor data as inputs for a classifier. Compared to the minimal detectable change of the assessment adequate results were obtained for both estimating the task scores and the total score of the assessment.

Comparing the developed algorithms to extract metrics related to the three activities with each other, differences in their reliability and sophistication should be mentioned. Since walking is a well-defined and thoroughly investigated movement, the work presented in this thesis could build up on previously developed algorithms for sensor-based gait analysis and knowledge of gait metrics from biomechanical laboratories relevant to patients with neurological disorders. Wheeling motions are more diverse as different wheeling propulsion patterns exist, which makes the development of algorithms more challenging and might be the main reason very little work on sensor-based wheeling analysis exists. Nevertheless, using knowledge and experience from the gait projects, a novel algorithm could be developed benchmarking sensor-based wheeling analysis. Contrary to walking and wheeling, grasping is a non-cyclic movement, which makes it more challenging to estimate motion trajectories from sensor data and to extract metrics accurately with fewer movements available. Hence, a trade-off between the reliability of the sensor-derived metrics and their richness had to be made.

Objective 3: Bring extracted metrics in context with clinical characterization of patients

The wheeling and the walking algorithm were developed to derive interpretable metrics related to both activities. These interpretable metrics are easier to comprehend for clinicians than statistical features derived directly from the raw sensor data. Hence, interpretable metrics are generally more clinically meaningful and thus directly address the issue reported by Shirota et al. [Shirota et al., 2019], which identified the poor understanding and lack of interpretability as one of the main reasons why technology-aided assessments are rarely implemented in the clinical routine.

We performed clustering, an unsupervised machine learning method, purely on sensor-derived metrics for both the wheeling and walking project to identify groups of SCI patients with similar wheeling or walking characteristics, as presented in chapters 3 and 4. In both cases, sensor-derived metrics were identified that differed between the groups and that highlighted certain aspects of their wheeling or walking patterns. Further, the main differences between the clusters regarding their clinical characteristics were emphasized. Even though the clusters differed in specific clinical characteristics, such as the SCIM or motor scores, the added value of using sensor-derived measures to objectively assess wheeling and walking activities became apparent: complementary information was provided by the sensor-derived metrics.

Nevertheless, approaches based on metrics derived directly from the raw sensor data have the benefit that they can be easily implemented even by users unfamiliar with IMU-processing methods. Hence, we chose these simple metrics for training an ordinal classifier to estimate clinical scores of an established assessment of upper limb function, as presented in chapter 5. Since a promising accuracy of the classifier was obtained, the feasibility of estimating clinical scores with easily implementable methods could be demonstrated.

6.2 Contributions to the field, outlook, and clinical impact

Overall, this thesis contributes toward establishing technology-aided assessments using simple and affordable measurement tools. We developed novel algorithms with the focus on extracting clinically meaningful metrics related to key activities of daily living. The overarching goal was to provide more sensitive and comprehensive measures than conventional clinical assessments.

The generalizability of the sensor-based gait analysis, which we primarily developed and validated in patients with SCI, has been explored for another patient cohort in a side project [Rast et al., 2022]. In collaboration with Fabian Rast from the Children's Hospital in Zurich, the algorithm was tested for children with a neurological disorder, suffering from diverse gait deficits similarly to individuals with a SCI. We compared the sensor-derived walking speed in both a standardized and in a daily life-like condition to the walking speed derived from reference systems. Only minor differences of 0.01 ± 0.07 m/s and 0.05 ± 0.06 m/s were obtained between the measurement systems for the two conditions, respectively. This project confirmed that the algorithm could also be applied to data of other cohorts with diverse gait deficits. Further, the algorithm's validity in a less controlled setting was demonstrated, which opens up opportunities for the usage of this algorithm for long-term measurements in real-world environments. Moreover, this study showed that most children did not use the same speed in the standardized and the daily life-like condition, which raised the interest of assessing activities also in a real-world environment.

Future work should focus on applying the developed algorithms, especially the wheeling and walking algorithms, to daily life recordings by combining the proposed methods with a human activity recognition algorithm. The sparse sensor setup selected for this project would be applicable for such measurements. Further, the robustness of both algorithm across different speeds and wheeling or walking patterns should allow accurate measurements even under more unconstrained conditions. However, these presumptions need to be further validated. Since the wearable sensors' key advantage are long-term measurements in real-world settings, analyzing the activities in the patient's habitual environment instead of in a standardized setting would provide many new insights [Rast and Labruyère, 2020]. Such measurements would provide objective metrics on the impact of novel therapies or treat-

ment methods on the daily life of the patient in terms of activity limitation and participation restriction. Furthermore, the knowledge gap between capacity (what a patient can do) and performance (what the patient does) could be closed.

In addition, a clinical application of the wheeling and walking algorithms was found. Reports summarizing wheeling and walking characteristics were developed together with clinicians and therapists in an iterative process. Two exemplary reports of patients are attached in the appendix. The key concept of these reports is that the sensor-derived metrics were selected and displayed in a clinically meaningful way such that both therapists and patients themselves obtain an objective description of their wheeling and walking, similar to summaries provided by commercial activity trackers. In future projects, the usability of the sensor software, including generating the reports fully automatically, should be improved to realize a widespread use.

Further, technology-induced compensation strategies during grasping movements were investigated in another side project [Meyer et al., 2022]. More specifically, the effect of a wrist-constrained robotic hand orthosis on the grasping kinematic was assessed. Similar to the setup presented in chapter 5, the data of an inertial sensor attached to the wrist while performing a subset of the ARAT tasks with and without a robotic hand orthosis was analyzed. Schneider et al. [Schneider et al., 2019] derived a simple feature, the central range of the pitch angle, and showed that this metric is a marker for compensatory movements during grasping tasks. Indeed, using a robotic hand orthosis led to a higher central range indicating compensatory movements compared to not using the orthosis in non-disabled individuals. This demonstrated the issue of usability-related design trade-offs between compact and lightweight solutions, and more complex multi-degree of freedom devices. In the context of this thesis, this contribution confirmed that sensor-derived measures could complement a standard clinical assessment by providing measures, here compensation, otherwise not directly captured by the assessment. This implies that these measures can help to evaluate rehabilitation robotics more sensitive and comprehensive using simple and cost-effective solutions.

6.3 Overall conclusion

On the quest for establishing technological-aided assessments for patients with a neurological disorder, this doctoral thesis provides sensor-based methodologies to assess activities of daily living. These methodologies contribute toward implementing more sensitive and comprehensive assessment methodologies using unobtrusive and affordable measurement devices. Since thorough assessments are the foundation for clinical decision-making, this thesis is a step towards patient-specific treatment plans and precise evaluation of novel therapeutic interventions. The unique feature of portability that wearable inertial sensors possess enables remote and long-term monitoring. Therefore, the contributions in this thesis pave the way of translating assessments to the patient's habitual environment, endorsing an optimal continuum of care.

A Appendix

A.1 Supplementary Material

A.1.1 Supplementary Material to "Towards a Mobile Gait Analysis for Patients with a Spinal Cord Injury: A Robust Algorithm Validated for Slow Walking Speeds"

Appendix A. Appendix

Table A.1: Mean error (me), its standard deviation (std) and the mean relative error (mre) between the temporal gait parameters derived from the GRAIL and the inertial sensors. The values are reported for SCI patients and healthy controls (HC) and the speed levels of 0.3m/s, 0.5m/s and preferred (pref) walking speed.

Gait Parameter	Group	Speed	me [ms]	std [ms]	mre [%]
Initial Contact	SCI	0.3	12	12	0.6
		0.5	5	12	
		pref	-2	9	
Final Contact	SCI	0.3	24	45	
		0.5	24	39	
		pref	20	40	
Stride Duration	SCI	0.3	2	8	0.1
		0.5	0	6	-0.1
		pref	2	7	0.1
Step Duration	SCI	0.3	-4	15	-0.8
		0.5	-2	13	-0.4
		pref	-1	13	-0.3
Swing Phase	SCI	0.3	-14	47	-3.8
		0.5	-19	48	-4.3
		pref	-23	44	-4.7
Double Support Phase	SCI	0.3	12	50	2.7
		0.5	17	44	5.8
		pref	22	41	7.5
	HC	0.5	-8	17	-3.5

Table A.2: Mean error (me), its standard deviation (std) and the mean relative error (mre) between the spatial gait parameters derived from the GRAIL and the inertial sensors. The values are reported for SCI patients and healthy controls (HC) and the speed levels of 0.3m/s, 0.5m/s and preferred (pref) walking speed.

Gait Parameter	Group	Speed	me [mm]	std [mm]	mre [%]	
Stride Length	SCI	0.3	6	43	0.4	
		0.5	-6	39	-0.7	
		pref	-6	17	-0.6	
Stride Height	HC	0.5	-11	28	-1.5	
		SCI	0.3	-5	13	
			0.5	-10	14	
pref	-4		24			
Stride Width	HC	0.5	-10	8		
		SCI	0.3	-12	9	
			0.5	-8	10	
	pref		-5	9		
	HC	0.5	-11	9		

A.1.2 Supplementary Material to "Data-Driven Characterization of Walking after a Spinal Cord Injury using Inertial Sensors"

Table A.3: Description of gait parameters

Gait Parameter (Statistical Features)	Description
Stride duration (mean, cov, asym, d2r)	Time between two consecutive heel strikes of the same side
Step duration (mean, cov, asym, d2r)	Time between the heel strike of one side until the following heel strike of the opposite side
Swing phase (mean, cov, asym, d2r)	Relative time of the time between toe off and heel strike of the same side w.r.t. the stride duration
Double support phase (mean, cov, asym, d2r)	Relative time of the time when both feet are on the ground w.r.t. the stride duration
Stride length (mean, cov, d2r)	Distance in-between two heel strikes of the same side
Stride width (mean, cov, asym, d2r)	Maximum lateral displacement during a stride
Stride height (mean, cov, asym, d2r)	Maximum vertical displacement during a stride
Cyclogram top view (ACC, SSD, area)	Top view of the ankle endpoint trajectory
Cyclogram side view (ACC, SSD, area)	Side view of the ankle endpoint trajectory
Smoothness	Modified spectral arc length of the angular velocity of the sagittal plane
Change in speed, stride length, cadence	Slope divided by the intercept of the linear fit of the parameters over the 6 minutes
Speed inconsistency	Absolute value of the change in speed

A.1.3 Supplementary Material to "Estimating Wheeling Propulsion Patterns using a Sparse Inertial Sensor Setup"

Table A.4: Silhouette scores of the corresponding number of clusters.

Number of Clusters	3	4	5	6	7	8	9	10
Silhouette Score	0.32	0.36	0.35	0.28	0.37	0.22	0.19	0.17

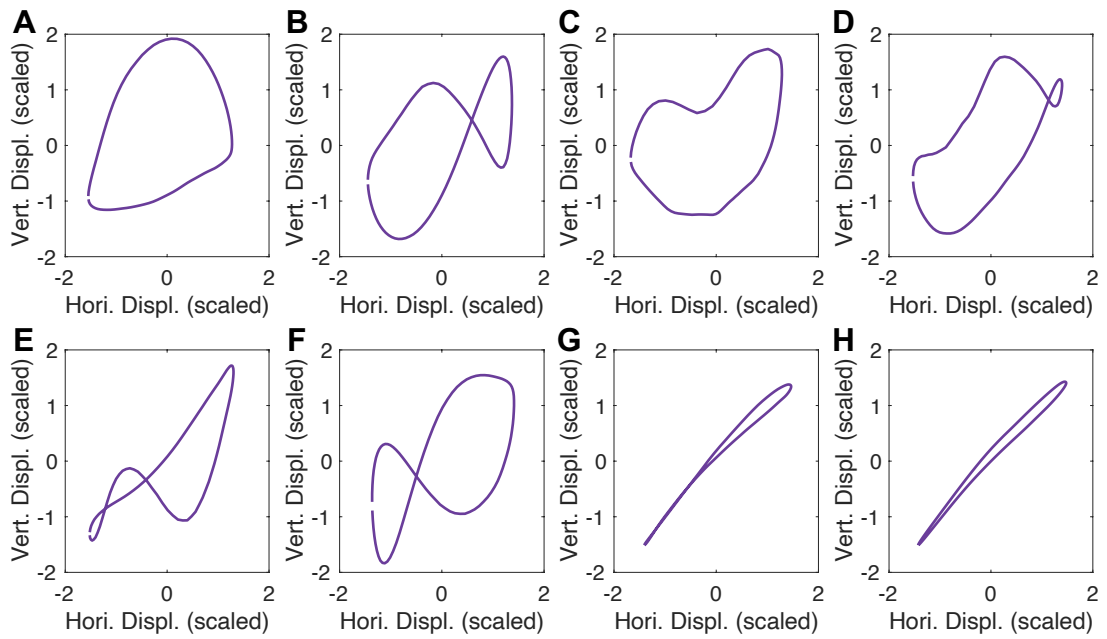


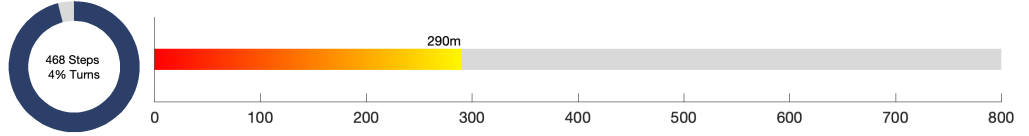
Figure A.1: Side view of the scaled wheeling patterns of the eight outliers combined to cluster 0.

A.2 Walking Report

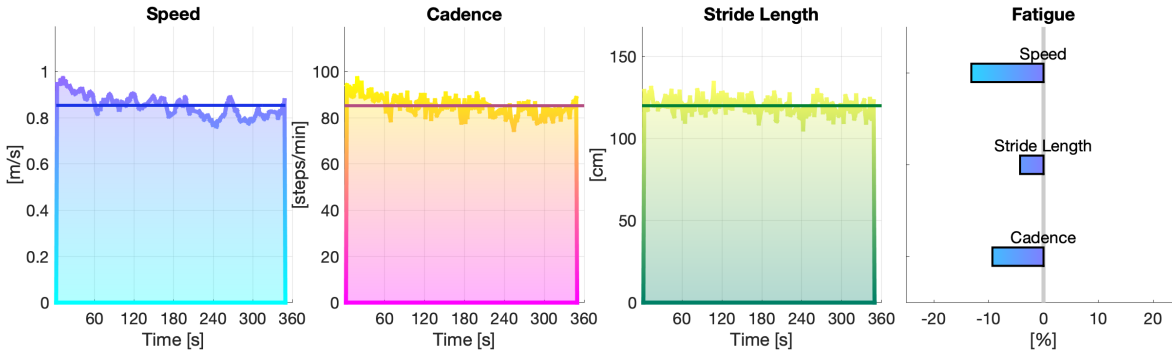
Gait Quality Report - patient 001

OVERVIEW

Start: 2021/07/02 11:18:07
Duration: 6m 4s
Distance: 290m
Steps: 468



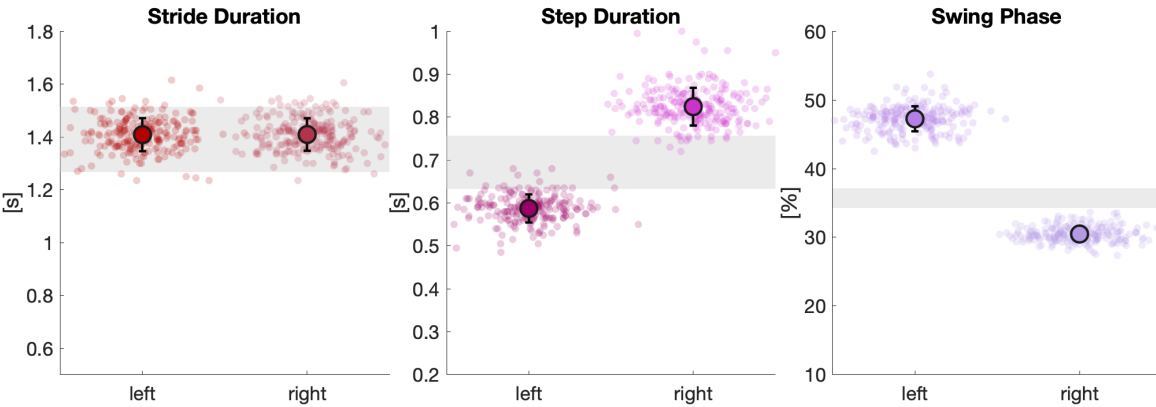
WALKING SPEED



Speed:
 mean: 0.85 m/s
 min: 0.77 m/s
 max: 0.94 m/s

Cadence:
 mean: 84.53 steps/min
 min: 78.83 steps/min
 max: 91.76 steps/min

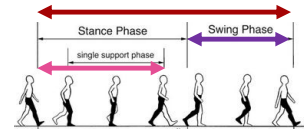
TEMPORAL PARAMETERS



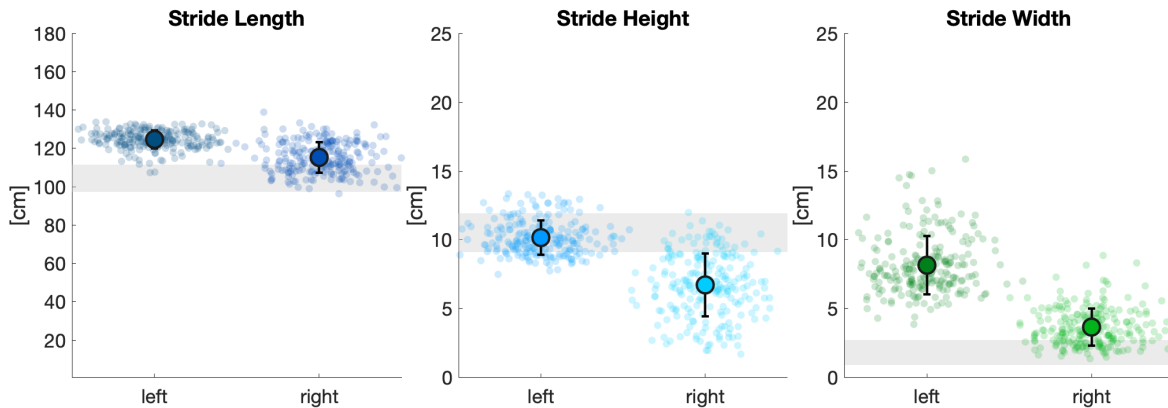
Stride Duration:
 1.41s (L) / 1.41s (R)

Step Duration:
 0.59s (L) / 0.82s (R)

Swing Phase:
 47.26% (L) / 30.48% (R)



SPATIAL PARAMETERS



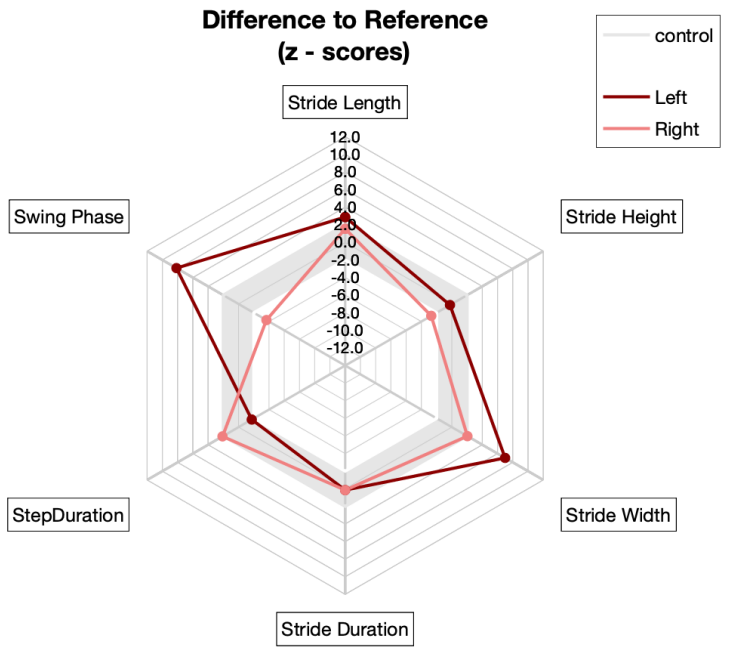
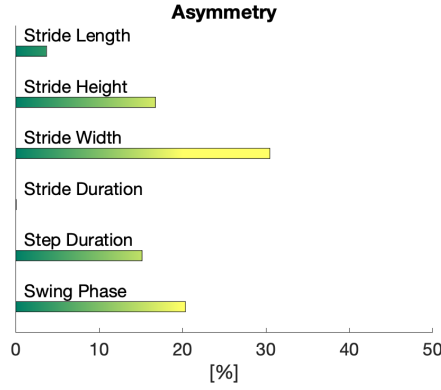
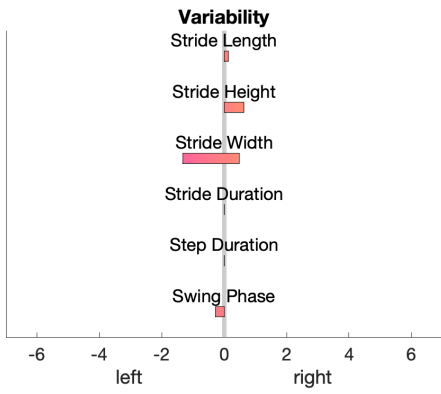
Stride Length:
 125cm (L) / 115cm (R)

Stride Height:
 10.2cm (L) / 6.7cm (R)

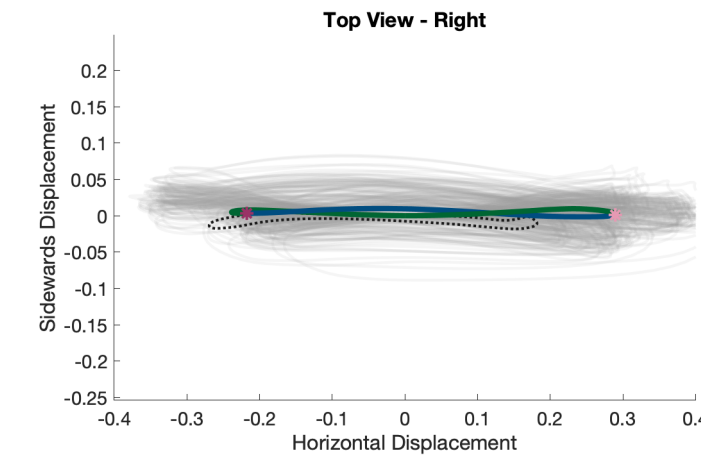
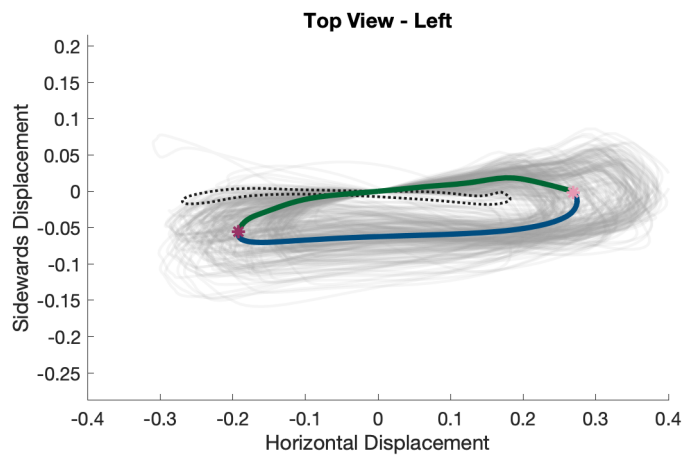
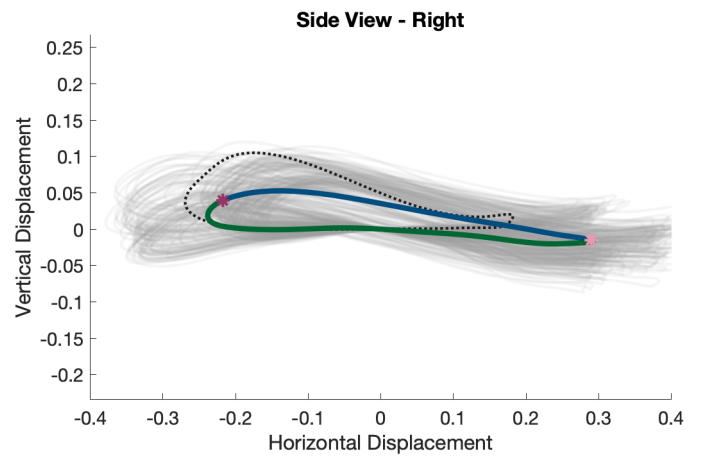
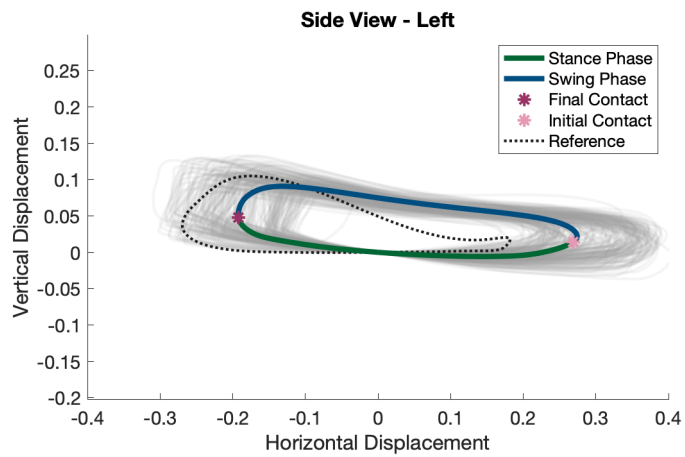
Stride Width:
 8.2cm (L) / 3.7cm (R)



VARIABILITY, SYMMETRY, DIFFERENCE TO REFERENCE



CYCLOGRAMS



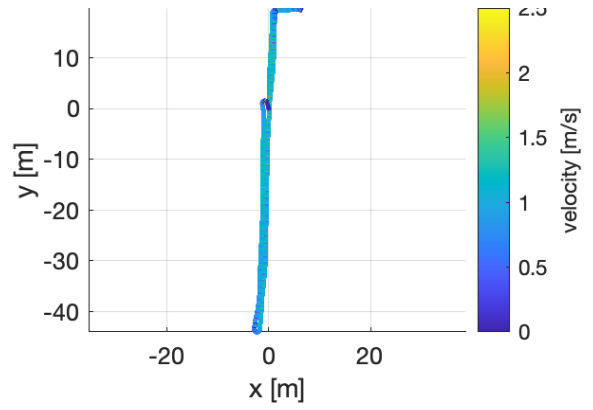
A.3 Wheeling Report

Wheeling Report

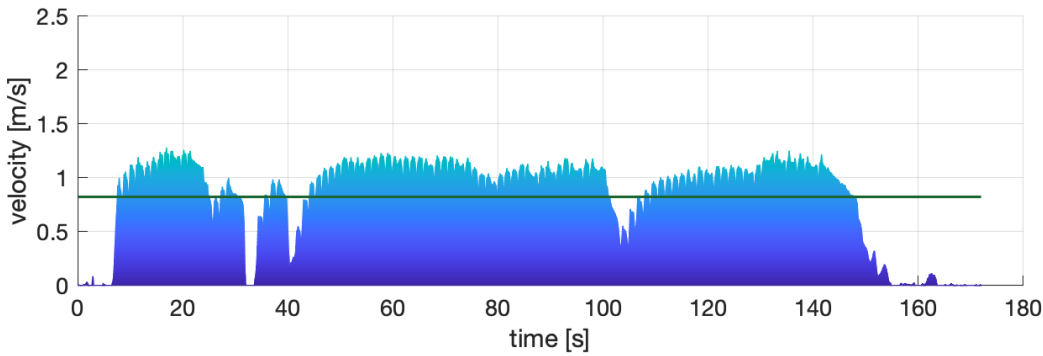
Wheeling_001

OVERVIEW

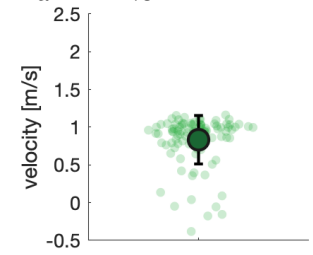
jumpID 2298
Start 2021/03/11 13:14:46
Duration 2m 52s
Distance 141.4 m
Strokes 97
Diameter 24



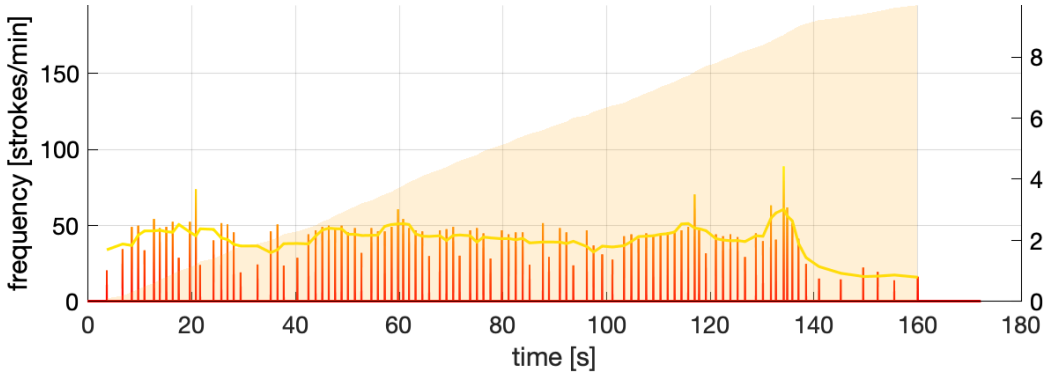
WHEELING SPEED



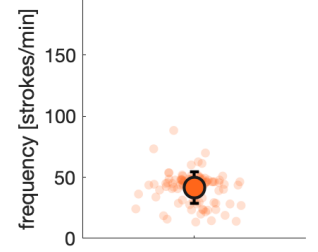
Mean velocity: 0.8 m/s
Max.: 1.2 m/s



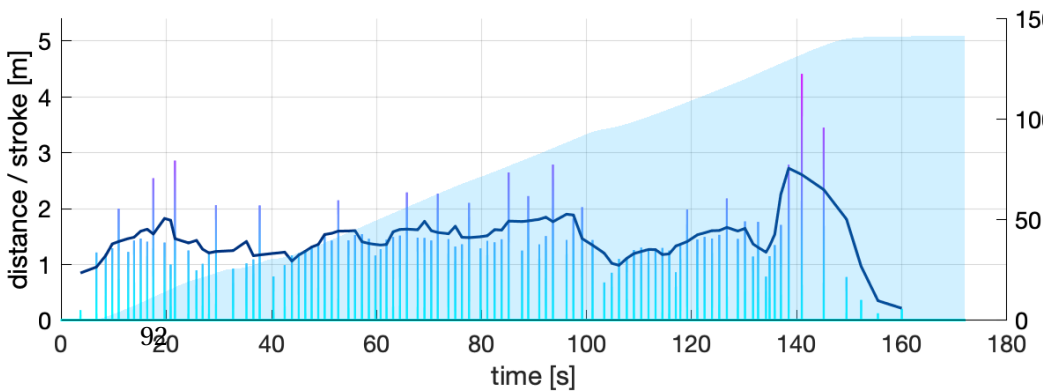
STROKE FREQUENCY



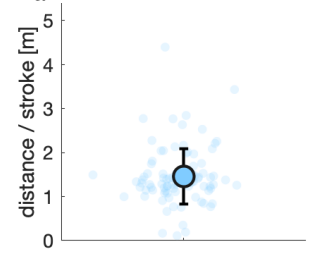
Mean freq.: 41.4 strokes/min
Min.: 18.5 strokes/min
Max.: 60.8 strokes/min



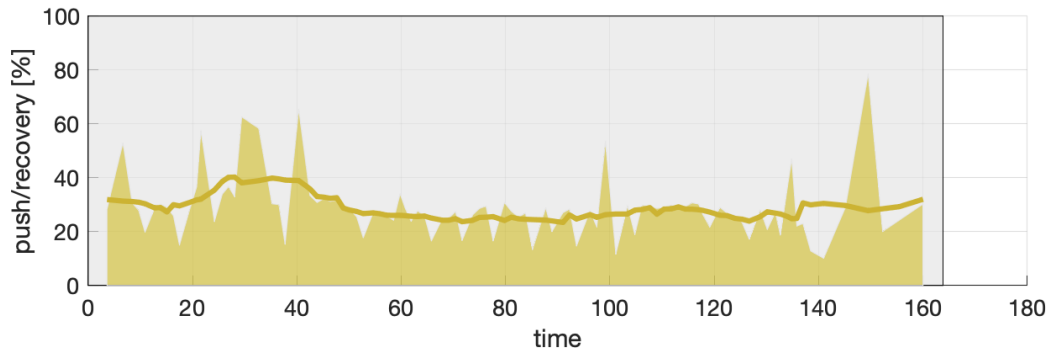
DISTANCE PER STROKE



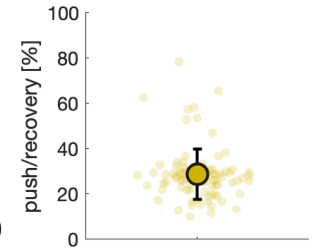
Mean distance/stroke: 1.5 m
Min.: 0.7 m
Max.: 2.7 m



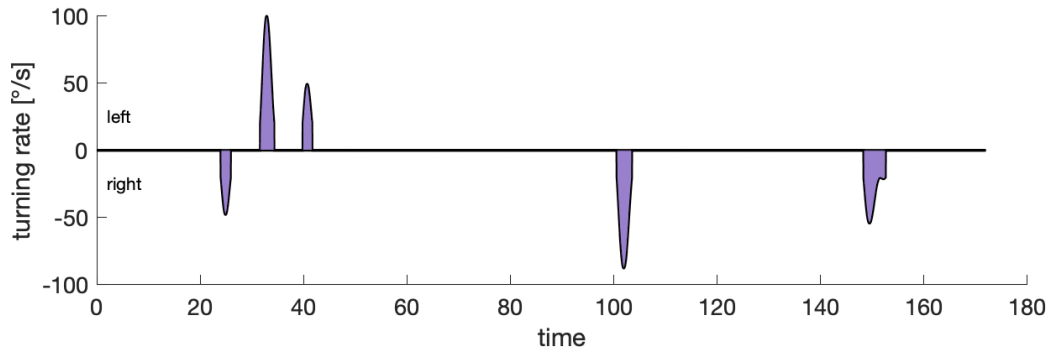
PROPULSION SHARE



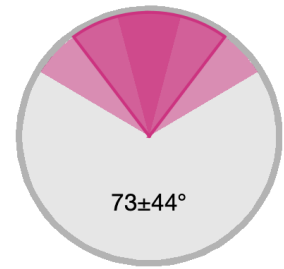
Mean stroke duration: 1.65 s
Mean propulsion: 0.47 s (28.7 %)
Mean recovery: 1.18 s (71.3 %)



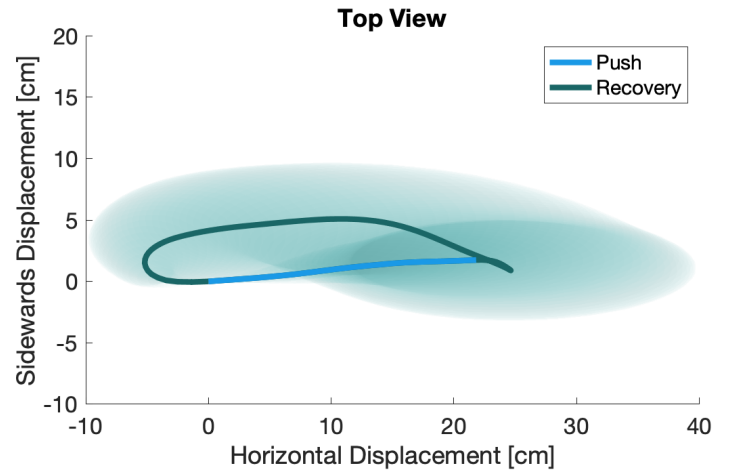
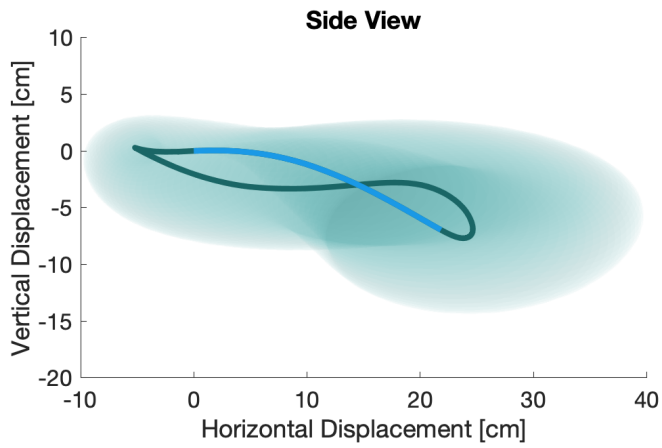
TURNING RATE AND PUSH ANGLE



Push Angle:



WHEELING PROPULSION PATTERN



Bibliography

- [Adans-Dester et al., 2020] Adans-Dester, C., Hankov, N., O'Brien, A., Vergara-Diaz, G., Black-Schaffer, R., Zafonte, R., Dy, J., Lee, S. I., and Bonato, P. (2020). Enabling precision rehabilitation interventions using wearable sensors and machine learning to track motor recovery. *npj Digital Medicine*.
- [Ahmadi et al., 2018] Ahmadi, M. N., Karinharju, K., Gomersall, S., Clancy, K., Tweedy, S., and Trost, S. G. (2018). Automated detection of wheelchair propulsion using a single wrist accelerometer. *Medicine & Science in Sports & Exercise*.
- [Albert and Kesselring, 2012] Albert, S. J. and Kesselring, J. (2012). Neurorehabilitation of stroke. *Journal of Neurology*.
- [Arnet et al., 2021] Arnet, U., de Vries, W. H., Eriks-Hoogland, I., Wisianowsky, C., van der Woude, L. H., Veeger, D. J. H., and Berger, M. (2021). Mri evaluation of shoulder pathologies in wheelchair users with spinal cord injury and the relation to shoulder pain. *Journal of Spinal Cord Medicine*.
- [Arnould et al., 2007] Arnould, C., Penta, M., and Thonnard, J. L. (2007). Hand impairments and their relationship with manual ability in children with cerebral palsy. *Journal of Rehabilitation Medicine*.
- [Atrsaei et al., 2021] Atrsaei, A., Corrà, M. F., Dadashi, F., Vila-Chã, N., Maia, L., Mariani, B., Maetzler, W., and Aminian, K. (2021). Gait speed in clinical and daily living assessments in parkinson's disease patients: performance versus capacity. *npj Parkinson's Disease*.
- [Awai et al., 2016] Awai, L., Bolliger, M., Ferguson, A. R., Courtine, G., and Curt, A. (2016). Influence of spinal cord integrity on gait control in human spinal cord injury. *Neurorehabilitation and Neural Repair*.
- [Awai and Curt, 2014] Awai, L. and Curt, A. (2014). Intralimb coordination as a sensitive indicator of motor-control impairment after spinal cord injury. *Frontiers in Human Neuroscience*.
- [Bailey et al., 2015] Bailey, R. R., Klaesner, J. W., and Lang, C. E. (2015). Quantifying real-world upper-limb activity in nondisabled adults and adults with chronic stroke. *Neurorehabilitation and Neural Repair*.
- [Balasubramanian et al., 2012] Balasubramanian, S., Melendez-Calderon, A., and Burdet, E. (2012). A robust and sensitive metric for quantifying movement smoothness. *IEEE Transactions on Biomedical Engineering*.
- [Balasubramanian et al., 2015] Balasubramanian, S., Melendez-Calderon, A., Roby-Brami, A., and Burdet, E. (2015). On the analysis of movement smoothness. *Journal of NeuroEngineering and Rehabilitation*.

Bibliography

- [Barbeau et al., 2007] Barbeau, H., Elashoff, R., Deforge, D., Ditunno, J., Saulino, M., and Dobkin, B. H. (2007). Comparison of speeds used for the 15.2-meter and 6-minute walks over the year after an incomplete spinal cord injury: The scilt trial. *Neurorehabilitation and Neural Repair*.
- [Barbeau et al., 1999] Barbeau, H., Ladouceur, M., Norman, K. E., Pépin, A., and Leroux, A. (1999). Walking after spinal cord injury: Evaluation, treatment, and functional recovery. *Archives of Physical Medicine and Rehabilitation*.
- [Beekman et al., 2000] Beekman, C., Perry, J., Boyd, L. A., Newsam, C. J., and Mulroy, S. J. (2000). The effects of a dorsiflexion-stopped ankle-foot orthosis on walking in individuals with incomplete spinal cord injury. *Topics in Spinal Cord Injury Rehabilitation*.
- [Bernhardt and Hill, 2005] Bernhardt, J. and Hill, K. (2005). We only treat what it occurs to us to assess: The importance of knowledge-based assessment. *Science-Based Rehabilitation*.
- [Bland and Altman, 1999] Bland, J. M. and Altman, D. G. (1999). Measuring agreement in method comparison studies. *Statistical Methods in Medical Research*.
- [Blazkiewicz et al., 2014] Blazkiewicz, M., Wiszomirska, I., and Wit, A. (2014). Comparison of four methods of calculating the symmetry of spatial-temporal parameters of gait. *Acta of Bioengineering and Biomechanics*.
- [Boninger et al., 1999] Boninger, M. L., Cooper, R. A., Baldwin, M. A., Shimada, S. D., and Koontz, A. (1999). Wheelchair pushrim kinetics: Body weight and median nerve function. *Archives of Physical Medicine and Rehabilitation*.
- [Boninger et al., 2003] Boninger, M. L., Dicianno, B. E., Cooper, R. A., Towers, J. D., Koontz, A. M., and Souza, A. L. (2003). Shoulder magnetic resonance imaging abnormalities, wheelchair propulsion, and gender. *Archives of Physical Medicine and Rehabilitation*.
- [Boninger et al., 2002] Boninger, M. L., Souza, A. L., Cooper, R. A., Fitzgerald, S. G., Koontz, A. M., and Fay, B. T. (2002). Propulsion patterns and pushrim biomechanics in manual wheelchair propulsion. *Archives of Physical Medicine and Rehabilitation*.
- [Boninger et al., 2001] Boninger, M. L., Towers, J. D., Cooper, R. A., Dicianno, B. E., and Munin, M. C. (2001). Shoulder imaging abnormalities in individuals with paraplegia. *Journal of Rehabilitation Research and Development*.
- [Bossuyt et al., 2018] Bossuyt, F. M., Arnet, U., Brinkhof, M. W., Eriks-Hoogland, I., Lay, V., Müller, R., Sunnåker, M., and Hinrichs, T. (2018). Shoulder pain in the swiss spinal cord injury community: prevalence and associated factors. *Disability and Rehabilitation*.
- [Boukhenoufa et al., 2022] Boukhenoufa, I., Zhai, X., Utti, V., Jackson, J., and McDonald-Maier, K. D. (2022). Wearable sensors and machine learning in post-stroke rehabilitation assessment: A systematic review. *Biomedical Signal Processing and Control*.
- [Bourguignon et al., 2022] Bourguignon, L., Tong, B., Geisler, F., Schubert, M., Röhrich, F., Saur, M., Weidner, N., Rupp, R., Kalke, Y.-B. B., Abel, R., Maier, D., Grassner, L., Chhabra, H. S., Liebscher, T., Cragg, J. J., Kramer, J., Curt, A., and Jutzeler, C. R. (2022). International surveillance study in acute spinal cord injury confirms viability of multinational clinical trials. *BMC Medicine*.
- [Brodie et al., 2016] Brodie, M. A., Psarakis, M., and Hoang, P. (2016). Gyroscopic corrections improve wearable sensor data prior to measuring dynamic sway in the gait of people with multiple sclerosis. *Computer Methods in Biomechanics and Biomedical Engineering*.

- [Broeks et al., 1999] Broeks, J. G., Lankhorst, G. J., Rumping, K., and Prevo, A. J. (1999). The long-term outcome of arm function after stroke: Results of a follow-up study. *Disability and Rehabilitation*.
- [Brogioli et al., 2017] Brogioli, M., Popp, W. L., Schneider, S., Albisser, U., Brust, A. K., Frotzler, A., Gassert, R., Curt, A., and Starkey, M. L. (2017). Multi-day recordings of wearable sensors are valid and sensitive measures of function and independence in human spinal cord injury. *Journal of Neurotrauma*.
- [Brunner et al., 2017] Brunner, I., Skouen, J. S., Hofstad, H., Aßmus, J., Becker, F., Sanders, A. M., Pallesen, H., Kristensen, L. Q., Michielsen, M., Thijs, L., and Verheyden, G. (2017). Virtual reality training for upper extremity in subacute stroke (virtues): A multicenter rct. *Neurology*.
- [Burrige et al., 2019] Burrige, J., Murphy, M. A., Buurke, J., Feys, P., Keller, T., Klamroth-Marganska, V., Lamers, I., McNicholas, L., Prange, G., Tarkka, I., Timmermans, A., and Hughes, A. M. (2019). A systematic review of international clinical guidelines for rehabilitation of people with neurological conditions: What recommendations are made for upperlimb assessment? *Frontiers in Neurology*.
- [Burrige et al., 2009] Burrige, J. H., Turk, R., Notley, S. V., Pickering, R. M., and Simpson, D. M. (2009). The relationship between upper limb activity and impairment in post-stroke hemiplegia. *Disability and Rehabilitation*.
- [Carpinella et al., 2014] Carpinella, I., Cattaneo, D., and Ferrarin, M. (2014). Quantitative assessment of upper limb motor function in multiple sclerosis using an instrumented action research arm test. *Journal of NeuroEngineering and Rehabilitation*.
- [Cervantes and Porretta, 2010] Cervantes, C. M. and Porretta, D. L. (2010). Physical activity measurement among individuals with disabilities: A literature review. *Adapted Physical Activity Quarterly*.
- [Chawla et al., 2002] Chawla, N. V., Bowyer, K. W., Hall, L. O., and Kegelmeyer, W. P. (2002). Smote: Synthetic minority over-sampling technique. *Journal of Artificial Intelligence Research*.
- [Chen et al., 2016] Chen, S., Lach, J., Lo, B., and Yang, G. Z. (2016). Toward pervasive gait analysis with wearable sensors: A systematic review. *IEEE Journal of Biomedical and Health Informatics*.
- [Chen et al., 2020] Chen, X., Guan, Y., Shi, J.-Q., Du, X.-L., and Eyre, J. (2020). Automated stroke rehabilitation assessment using wearable accelerometers in free-living environments. *arXiv*.
- [Cooper et al., 1997] Cooper, R. A., Robertson, R. N., VanSickle, D. P., Boninger, M. L., and Shimada, S. D. (1997). Methods for determining three-dimensional wheelchair pushrim forces and moments: A technical note. *Journal of Rehabilitation Research and Development*.
- [Coravos et al., 2019] Coravos, A., Khozin, S., and Mandl, K. D. (2019). Developing and adopting safe and effective digital biomarkers to improve patient outcomes. *npj Digital Medicine*.
- [Curt et al., 2008] Curt, A., Hedel, H. J. V., Klaus, D., and Dietz, V. (2008). Recovery from a spinal cord injury: Significance of compensation, neural plasticity, and repair. *Journal of Neurotrauma*.
- [Curtis et al., 1999] Curtis, K. A., Drysdale, G. A., Lanza, R. D., Kolber, M., Vitolo, R. S., and West, R. (1999). Shoulder pain in wheelchair users with tetraplegia and paraplegia. *Archives of Physical Medicine and Rehabilitation*.
- [Cuturi and Blondel, 2017] Cuturi, M. and Blondel, M. (2017). Soft-dtw: A differentiable loss function for time-series. *34th International Conference on Machine Learning, ICML 2017*.

Bibliography

- [Czech et al., 2020] Czech, M. D., Psaltos, D., Zhang, H., Adamusiak, T., Calicchio, M., Kelekar, A., Messere, A., Dijk, K. R. V., Ramos, V., Demanuele, C., Cai, X., Santamaria, M., Patel, S., and Karahanoglu, F. I. (2020). Age and environment-related differences in gait in healthy adults using wearables. *npj Digital Medicine*.
- [Dalyan et al., 1999] Dalyan, M., Cardenas, D. D., and Gerard, B. (1999). Upper extremity pain after spinal cord injury. *Spinal Cord*.
- [Dandu et al., 2018] Dandu, S. R., Engelhard, M. M., Qureshi, A., Gong, J., Lach, J. C., Brandt-Pearce, M., and Goldman, M. D. (2018). Understanding the physiological significance of four inertial gait features in multiple sclerosis. *IEEE Journal of Biomedical and Health Informatics*.
- [Davidoff et al., 1991] Davidoff, G., Werner, R., and Waring, W. (1991). Compressive mononeuropathies of the upper extremity in chronic paraplegia. *Spinal Cord*.
- [de Vries et al., 2009] de Vries, W. H., Veeger, H. E., Baten, C. T., and van der Helm, F. C. (2009). Magnetic distortion in motion labs, implications for validating inertial magnetic sensors. *Gait and Posture*.
- [Demers and Levin, 2017] Demers, M. and Levin, M. F. (2017). Do activity level outcome measures commonly used in neurological practice assess upper-limb movement quality? *Neurorehabilitation and Neural Repair*.
- [Dewan et al., 2019] Dewan, M. C., Rattani, A., Gupta, S., Baticulon, R. E., Hung, Y. C., Punchak, M., Agrawal, A., Adeleye, A. O., Shrimel, M. G., Rubiano, A. M., Rosenfeld, J. V., and Park, K. B. (2019). Estimating the global incidence of traumatic brain injury. *Journal of Neurosurgery*.
- [Deyo et al., 1991] Deyo, R. A., Diehr, P., and Patrick, D. L. (1991). Reproducibility and responsiveness of health status measures statistics and strategies for evaluation. *Controlled Clinical Trials*.
- [Dietz and Fouad, 2014] Dietz, V. and Fouad, K. (2014). Restoration of sensorimotor functions after spinal cord injury. *Brain*.
- [Dobkin, 2013] Dobkin, B. H. (2013). Wearable motion sensors to continuously measure real-world physical activities. *Current Opinion in Neurology*.
- [Engelhard et al., 2016] Engelhard, M. M., Dandu, S. R., Patek, S. D., Lach, J. C., and Goldman, M. D. (2016). Quantifying six-minute walk induced gait deterioration with inertial sensors in multiple sclerosis subjects. *Gait and Posture*.
- [Eriks-Hoogland et al., 2012] Eriks-Hoogland, I., Engisch, R., Brinkhof, M., and Drongelen, S. V. (2012). Acromioclavicular joint arthritis in persons with spinal cord injury compared to able-bodied persons. *Topics in Spinal Cord Injury Rehabilitation*.
- [Eriks-Hoogland et al., 2011] Eriks-Hoogland, I. E., Groot, S. D., Post, M. W., and Woude, L. H. V. D. (2011). Correlation of shoulder range of motion limitations at discharge with limitations in activities and participation one year later in persons with spinal cord injury. *Journal of Rehabilitation Medicine*, 43.
- [Eriks-Hoogland et al., 2014] Eriks-Hoogland, I. E., Hoekstra, T., Groot, S. D., Stucki, G., Post, M. W., and Woude, L. H. V. D. (2014). Trajectories of musculoskeletal shoulder pain after spinal cord injury: Identification and predictors. *Journal of Spinal Cord Medicine*.
- [Feigin et al., 2017] Feigin, V. L., Krishnamurthi, R. V., Theadom, A. M., Abajobir, A. A., Mishra, S. R., Ahmed, M. B., Abate, K. H., Mengistie, M. A., Wakayo, T., Abd-Allah, F., Abdulle, A. M., Abera, S. E., Mohammed, K. E., Abyu, G. Y., Asgedom, S. W., Atey, T. M., Betsu, B. D., Mezgebe, H. B., Tuem, K. B.,

- Woldu, M. A., Aichour, A. N., Aichour, I., Aichour, M. T., Akinyemi, R. O., Alabed, S., Al-Raddadi, R., Alvis-Guzman, N., Amare, A. T., Ansari, H., Anwari, P., Ärnlöv, J., Fereshtehnejad, S., Weiderpass, E., Havmoeller, R., Asayesh, H., Avila-Burgos, L., Avokpaho, E. E., Afrique, L. E., Azarpazhooh, M. R., Barac, A., Barboza, M., Barker-Collo, S. L., Bärnighausen, T., Farvid, M. S., Mohammed, S., Bedi, N., Beghi, E., Giussani, G., Bennett, D. A., Hay, S. I., Goulart, A. C., Santos, I. S., Bensenor, I. M., Lotufo, P. A., Berhane, A., Jeemon, P., Bhaumik, S., Dandona, L., Dandona, R., Kumar, G. A., Birlık, S. M., Biryukov, S., Casey, D., Foreman, K. J., Goldberg, E. M., Khalil, I. A., Kyu, H. H., Manhertz, T., Mokdad, A. H., Naghavi, M., Nguyen, G., Nichols, E., Smith, M., Murray, C. J., Roth, G. A., Stanaway, J. D., Vos, T., Ellenbogen, R. G., Jakovljevic, M., Tirschwell, D. L., Zunt, J. R., Boneya, D. J., Hambisa, M., Bullo, L. N., Carabin, H., Castañeda-Orjuela, C. A., Catalá-López, F., Tabarés-Seisdedos, R., Chen, H., Chitheer, A. A., Chowdhury, R., Christensen, H., Deveber, G. A., Dharmaratne, S. D., Do, H. P., Nguyen, C. T., Nguyen, Q. L., Nguyen, T. H., Nong, V. M., Dokova, K., Dorsey, E. R., Eskandarieh, S., Fischer, E., Majeed, A., Steiner, T. J., Rawaf, S., Shakir, R., Shoman, H., Geleijnse, J. M., Gillum, R. F., Gona, P. N., Gughani, H. C., Gupta, R., Hachinski, V., Hamadeh, R. R., Hankey, G. J., Hareri, H. A., Heydarpour, P., Sahraian, M. A., Kasaeian, A., Malekzadeh, R., Roshandel, G., Sepanlou, S. G., Hotez, P. J., Javanbakht, M., Jonas, J. B., Kalkonde, Y., Kandel, A., Karch, A., Kastor, A., Rahman, M., Keiyoro, P. N., Khader, Y. S., Khan, E. A., Khang, Y., Khoja, A. T., Tran, B. X., Khubchandani, J., Kim, D., Kim, Y. J., Kivimaki, M., Kokubo, Y., Kosen, S., Kravchenko, M., Piradov, M. A., Varakin, Y. Y., Defo, B. K., Kulkarni, C., Kumar, R., Larsson, A., Lavados, P. M., Li, Y., Liang, X., Liben, M. L., Lo, W. D., Logroscino, G., Loy, C. T., Mackay, M. T., Meretoja, A., Szoeki, C. E., Razek, H. M. A. E., Mantovani, L. G., Massano, J., Mazidi, M., McAlinden, C., Mehata, S., Mehndiratta, M. M., Memish, Z. A., Mendoza, W., Mensah, G. A., Wijeratne, T., Miller, T. R., Ibrahim, N. M., Mohammadi, A., Moradi-Lakeh, M., Velasquez, I. M., Musa, K. I., Ngunjiri, J. W., Ningrum, D. N., Norrving, B., Stein, D. J., Noubiap, J. J., Ogbo, F. A., Renzaho, A. M., Owolabi, M. O., Pandian, J. D., Parmar, P. G., Pereira, D. M., Petzold, M., Phillips, M. R., Poulton, R. G., Pourmalek, F., Qorbani, M., Rafay, A., Rai, R. K., Rajsic, S., Ranta, A., Rezai, M. S., Rubagotti, E., Sachdev, P., Safiri, S., Sahathevan, R., Samy, A. M., Santalucia, P., Sartorius, B., Satpathy, M., Sawhney, M., Saylan, M. I., Shaikh, M. A., Shamsizadeh, M., Sheth, K. N., Shigematsu, M., Silva, D. A., Sobngwi, E., Sposato, L. A., Stovner, L. J., Stovner, L. J., Abdulkader, R. S., Tanne, D., Thrift, A. G., Topor-Madry, R., Truelsen, T., Ukwaja, K. N., Uthman, O. A., Vasankari, T., Venketasubramanian, N., Vlassov, V. V., Wadilo, E., Wallin, M. T., Westerman, R., Wiysonge, C. S., Wolfe, C. D., Xavier, D., Xu, G., Yano, Y., Yimam, H. H., Yonemoto, N., Yu, C., Zaidi, Z., and Zaki, M. E. (2017). Global, regional, and national burden of neurological disorders during 1990–2015: a systematic analysis for the global burden of disease study 2015. *The Lancet Neurology*.
- [Field-Fote and Tepavac, 2002] Field-Fote, E. C. and Tepavac, D. (2002). Improved intralimb coordination in people with incomplete spinal cord injury following training with body weight support and electrical stimulation. *Physical Therapy*.
- [Formstone et al., 2021] Formstone, L., Huo, W., Wilson, S., McGregor, A., Bentley, P., and Vaidyanathan, R. (2021). Quantification of motor function post-stroke using novel combination of wearable inertial and mechanomyographic sensors. *IEEE Transactions on Neural Systems and Rehabilitation Engineering*.
- [Forrest et al., 2014] Forrest, G. F., Hutchinson, K., Lorenz, D. J., Buehner, J. J., VanHiel, L. R., Sisto, S. A., and Basso, D. M. (2014). Are the 10 meter and 6 minute walk tests redundant in patients with spinal cord injury? *PLoS ONE*.
- [Frank and Hall, 2001] Frank, E. and Hall, M. (2001). A simple approach to ordinal classification. *Lecture Notes in Computer Science (including subseries Lecture Notes in Artificial Intelligence and Lecture Notes in Bioinformatics)*.

Bibliography

- [Frykberg et al., 2021] Frykberg, G. E., Grip, H., and Murphy, M. A. (2021). How many trials are needed in kinematic analysis of reach-to-grasp?—a study of the drinking task in persons with stroke and non-disabled controls. *Journal of NeuroEngineering and Rehabilitation*.
- [Garofalo, 2012] Garofalo, P. (2012). Healthcare applications based on mems technology. *Advancing Microelectronics*.
- [Gilmore and Jog, 2017] Gilmore, G. and Jog, M. (2017). Future perspectives: Assessment tools and rehabilitation in the new age. *Movement Disorders Rehabilitation*.
- [Gironda et al., 2004] Gironda, R. J., Clark, M. E., Neugaard, B., and Nelson, A. (2004). Upper limb pain in a national sample of veterans with paraplegia. *Journal of Spinal Cord Medicine*.
- [Gladstone et al., 2002] Gladstone, D. J., Danells, C. J., and Black, S. E. (2002). The fugl-meyer assessment of motor recovery after stroke: A critical review of its measurement properties. *Neurorehabilitation and Neural Repair*.
- [Goldsack et al., 2020] Goldsack, J. C., Coravos, A., Bakker, J. P., Bent, B., Dowling, A. V., Fitzer-Attas, C., Godfrey, A., Godino, J. G., Gujar, N., Izmailova, E., Manta, C., Peterson, B., Vandendriessche, B., Wood, W. A., Wang, K. W., and Dunn, J. (2020). Verification, analytical validation, and clinical validation (v3): the foundation of determining fit-for-purpose for biometric monitoring technologies (biomets). *npj Digital Medicine*.
- [Gong et al., 2016] Gong, J., Qi, Y., Goldman, M. D., and Lach, J. (2016). Causality analysis of inertial body sensors for multiple sclerosis diagnostic enhancement. *IEEE Journal of Biomedical and Health Informatics*.
- [Gooch et al., 2017] Gooch, C. L., Pracht, E., and Borenstein, A. R. (2017). The burden of neurological disease in the united states: A summary report and call to action. *Annals of Neurology*.
- [Groot et al., 2005] Groot, S. D., Dallmeijer, A. J., Kilkens, O. J., Asbeck, F. W. V., Nene, A. V., Angenot, E. L., Post, M. W., and Woude, L. H. V. D. (2005). Course of gross mechanical efficiency in handrim wheelchair propulsion during rehabilitation of people with spinal cord injury: A prospective cohort study. *Archives of Physical Medicine and Rehabilitation*.
- [Groot et al., 2002] Groot, S. D., Veeger, D. H., Hollander, A. P., and Lucas, L. H. (2002). Wheelchair propulsion technique and mechanical efficiency after 3 wk of practice. *Medicine and Science in Sports and Exercise*.
- [Groot et al., 2004] Groot, S. D., Veeger, H. E., Hollander, A. P., and Woude, L. H. V. D. (2004). Effect of wheelchair stroke pattern on mechanical efficiency. *American Journal of Physical Medicine and Rehabilitation*.
- [Gutierrez et al., 2007] Gutierrez, D. D., Thompson, L., Kemp, B., Mulroy, S. J., Winstein, C. J., Gordon, J., Brown, D. A., Knutson, L., Fowler, E., DeMuth, S., Kulig, K., and Sullivan, K. (2007). The relationship of shoulder pain intensity to quality of life, physical activity, and community participation in persons with paraplegia. *Journal of Spinal Cord Medicine*.
- [Hedel, 2009] Hedel, H. J. V. (2009). Gait speed in relation to categories of functional ambulation after spinal cord injury. *Neurorehabilitation and Neural Repair*.
- [Hedel et al., 2009] Hedel, H. J. V., Dietz, V., Meiners, T., Benito, J., Abel, R., Meindl, R., Marcus, O., Röhl, K., Thietje, R., Gerner, H. J., Harms, J., Potulski, M., Maier, D., Duysens, J., Bussel, B., Kriz, J., Al-Khodairy, A., Kaps, H. P., and Kalke, Y. B. (2009). Walking during daily life can be validly and responsively assessed in subjects with a spinal cord injury. *Neurorehabilitation and Neural Repair*.

- [Hedel et al., 2006] Hedel, H. J. V., Wirz, M., and Curt, A. (2006). Improving walking assessment in subjects with an incomplete spinal cord injury: Responsiveness. *Spinal Cord*.
- [Hedel et al., 2005] Hedel, H. J. V., Wirz, M., and Dietz, V. (2005). Assessing walking ability in subjects with spinal cord injury: Validity and reliability of 3 walking tests. *Archives of Physical Medicine and Rehabilitation*.
- [Hendricks et al., 2002] Hendricks, H. T., Limbeek, J. V., Geurts, A. C., and Zwarts, M. J. (2002). Motor recovery after stroke: A systematic review of the literature. *Archives of Physical Medicine and Rehabilitation*.
- [Hillen et al., 2013] Hillen, B. K., Abbas, J. J., and Jung, R. (2013). Accelerating locomotor recovery after incomplete spinal injury. *Annals of the New York Academy of Sciences*.
- [Hollman et al., 2016] Hollman, J. H., Watkins, M. K., Imhoff, A. C., Braun, C. E., Akervik, K. A., and Ness, D. K. (2016). A comparison of variability in spatiotemporal gait parameters between treadmill and overground walking conditions. *Gait and Posture*.
- [Hosseini et al., 2012] Hosseini, S. M., Oyster, M. L., Kirby, R. L., Harrington, A. L., and Boninger, M. L. (2012). Manual wheelchair skills capacity predicts quality of life and community integration in persons with spinal cord injury. *Archives of Physical Medicine and Rehabilitation*.
- [Hundza et al., 2014] Hundza, S. R., Hook, W. R., Harris, C. R., Mahajan, S. V., Leslie, P. A., Spani, C. A., Spalteholz, L. G., Birch, B. J., Commandeur, D. T., and Livingston, N. J. (2014). Accurate and reliable gait cycle detection in parkinson's disease. *IEEE Transactions on Neural Systems and Rehabilitation Engineering*.
- [Hussey and Stauffer, 1973] Hussey, R. W. and Stauffer, E. S. (1973). Spinal cord injury: Requirements for ambulation. *Archives of Physical Medicine and Rehabilitation*.
- [Iolanda et al., 2018] Iolanda, P., Marcella, M., Federica, T., Luigi, T. N., Giorgio, S., Armin, C., and Marco, M. (2018). The nisci project. antibodies against nogo-a to enhance plasticity, regeneration and functional recovery after acute spinal cord injury, a multicenter european clinical proof of concept trial. *SCHOOL AND SYMPOSIUM ON ADVANCED NEUROREHABILITATION (SSNR2018)*.
- [Itzkovich et al., 2007] Itzkovich, M., Gelernter, I., Biering-Sorensen, F., Weeks, C., Laramee, M. T., Craven, B. C., Tonack, M., Hitzig, S. L., Glaser, E., Zeilig, G., Aito, S., Scivoletto, G., Mecci, M., Chadwick, R. J., Masry, W. S. E., Osman, A., Glass, C. A., Silva, P., Soni, B. M., Gardner, B. P., Savic, G., Bergström, E. M., Bluvshstein, V., Ronen, J., and Catz, A. (2007). The spinal cord independence measure (scim) version iii: Reliability and validity in a multi-center international study. *Disability and Rehabilitation*.
- [Jahanian et al., 2022] Jahanian, O., Straaten, M. G. V., Goodwin, B. M., Lennon, R. J., Barlow, J. D., Murthy, N. S., and Morrow, M. M. (2022). Shoulder magnetic resonance imaging findings in manual wheelchair users with spinal cord injury. *Journal of Spinal Cord Medicine*.
- [Jalloul, 2018] Jalloul, N. (2018). Wearable sensors for the monitoring of movement disorders. *Biomedical Journal*.
- [Jasiewicz et al., 2006] Jasiewicz, J. M., Allum, J. H. J., Middleton, J. W., Barriskill, A., Condie, P., Purcell, B., and Li, R. C. T. (2006). Gait event detection using linear accelerometers or angular velocity transducers in able-bodied and spinal-cord injured individuals. *Gait & posture*.
- [Jensen et al., 2005] Jensen, M. P., Hoffman, A. J., and Cardenas, D. D. (2005). Chronic pain in individuals with spinal cord injury: A survey and longitudinal study. *Spinal Cord*.

Bibliography

- [Johansson et al., 2018] Johansson, D., Malmgren, K., and Murphy, M. A. (2018). Wearable sensors for clinical applications in epilepsy, parkinson's disease, and stroke: a mixed-methods systematic review. *Journal of Neurology*.
- [Jones, 2017] Jones, T. A. (2017). Motor compensation and its effects on neural reorganization after stroke. *Nature Reviews Neuroscience*.
- [Kanzler et al., 2022] Kanzler, C. M., Lamers, I., Feys, P., Gassert, R., and Lambercy, O. (2022). Personalized prediction of rehabilitation outcomes in multiple sclerosis: a proof-of-concept using clinical data, digital health metrics, and machine learning. *Medical and Biological Engineering and Computing*.
- [Kanzler et al., 2020] Kanzler, C. M., Schwarz, A., Held, J. P., Luft, A. R., Gassert, R., and Lambercy, O. (2020). Technology-aided assessment of functionally relevant sensorimotor impairments in arm and hand of post-stroke individuals. *Journal of NeuroEngineering and Rehabilitation*.
- [Katan and Luft, 2018] Katan, M. and Luft, A. (2018). Global burden of stroke. *Seminars in Neurology*.
- [Katz et al., 1998] Katz, D. I., Alexander, M. P., and Klein, R. B. (1998). Recovery of arm function in patients with paresis after traumatic brain injury. *Archives of Physical Medicine and Rehabilitation*.
- [Kim et al., 2004] Kim, C. M., Eng, J. J., and Whittaker, M. W. (2004). Level walking and ambulatory capacity in persons with incomplete spinal cord injury: Relationship with muscle strength. *Spinal Cord*.
- [Kim et al., 2021] Kim, G. J., Parnandi, A., Eva, S., and Schambra, H. (2021). The use of wearable sensors to assess and treat the upper extremity after stroke: a scoping review. *Disability and Rehabilitation*.
- [Kim et al., 2016] Kim, W. S., Cho, S., Baek, D., Bang, H., and Paik, N. J. (2016). Upper extremity functional evaluation by fugl-meyer assessment scoring using depth-sensing camera in hemiplegic stroke patients. *PLoS ONE*.
- [Kirshblum et al., 2011] Kirshblum, S. C., Waring, W., Biering-Sorensen, F., Burns, S. P., Johansen, M., Schmidt-Read, M., Donovan, W., Graves, D., Jha, A., Jones, L., Mulcahey, M. J., and Krassioukov, A. (2011). Reference for the 2011 revision of the international standards for neurological classification of spinal cord injury. *Journal of Spinal Cord Medicine*.
- [Kirtley et al., 1985] Kirtley, C., Whittle, M. W., and Jefferson, R. J. (1985). Influence of walking speed on gait parameters. *Journal of Biomedical Engineering*.
- [Kister et al., 2013] Kister, I., Bacon, T. E., Chamot, E., Salter, A. R., Cutter, G. R., Kalina, J. T., and Herbert, J. (2013). Natural history of multiple sclerosis symptoms. *International Journal of MS Care*.
- [Kooijmans et al., 2014] Kooijmans, H., Horemans, H. L., Stam, H. J., and Bussmann, J. B. (2014). Valid detection of self-propelled wheelchair driving with two accelerometers. *Physiological Measurement*.
- [Krawetz and Nance, 1996] Krawetz, P. and Nance, P. (1996). Gait analysis of spinal cord injured subjects: Effects of injury level and spasticity. *Archives of Physical Medicine and Rehabilitation*.
- [Kressler et al., 2018] Kressler, J., Koeplin-Day, J., Muendle, B., Rosby, B., Santo, E., and Domingo, A. (2018). Accuracy and precision of consumer-level activity monitors for stroke detection during wheelchair propulsion and arm ergometry. *PLoS ONE*.
- [Kwakkel et al., 2003] Kwakkel, G., Kollen, B. J., der Grond, J. V. V., and Prevo, A. J. (2003). Probability of regaining dexterity in the flaccid upper limb: Impact of severity of paresis and time since onset in acute stroke. *Stroke*.

- [Kwakkel et al., 2017] Kwakkel, G., Lannin, N. A., Borschmann, K., English, C., Ali, M., Churilov, L., Saposnik, G., Winstein, C., van Wegen, E. E., Wolf, S. L., Krakauer, J. W., and Bernhardt, J. (2017). Standardized measurement of sensorimotor recovery in stroke trials: Consensus-based core recommendations from the stroke recovery and rehabilitation roundtable. *International Journal of Stroke*.
- [Kwakkel et al., 2019] Kwakkel, G., Wegen, E. E. V., Burridge, J. H., Winstein, C. J., van Dokkum, L. E., Murphy, M. A., Levin, M. F., and Krakauer, J. W. (2019). Standardized measurement of quality of upper limb movement after stroke: Consensus-based core recommendations from the second stroke recovery and rehabilitation roundtable. *International Journal of Stroke*.
- [Kwarciak et al., 2009] Kwarciak, A. M., Sisto, S. A., Yarossi, M., Price, R., Komaroff, E., and Boninger, M. L. (2009). Redefining the manual wheelchair stroke cycle: Identification and impact of non-propulsive pushrim contact. *Archives of Physical Medicine and Rehabilitation*.
- [Kwarciak et al., 2012] Kwarciak, A. M., Turner, J. T., Guo, L., and Richter, W. M. (2012). The effects of four different stroke patterns on manual wheelchair propulsion and upper limb muscle strain. *Disability and Rehabilitation: Assistive Technology*.
- [Laidig et al., 2019] Laidig, D., Lehmann, D., Begin, M. A., and Seel, T. (2019). Magnetometer-free realtime inertial motion tracking by exploitation of kinematic constraints in 2-dof joints. *Proceedings of the Annual International Conference of the IEEE Engineering in Medicine and Biology Society, EMBS*.
- [Lam et al., 2008] Lam, T., Noonan, V. K., and Eng, J. J. (2008). A systematic review of functional ambulation outcome measures in spinal cord injury. *Spinal Cord*.
- [Lambercy et al., 2021] Lambercy, O., Lehner, R., Chua, K., Wee, S. K., Rajeswaran, D. K., Kuah, C. W. K., Ang, W. T., Liang, P., Campolo, D., Hussain, A., Aguirre-Ollinger, G., Guan, C., Kanzler, C. M., Wenderoth, N., and Gassert, R. (2021). Neurorehabilitation from a distance: Can intelligent technology support decentralized access to quality therapy? *Frontiers in Robotics and AI*.
- [Lambercy et al., 2016] Lambercy, O., Maggioni, S., Lünenburger, L., Gassert, R., and Bolliger, M. (2016). Robotic and wearable sensor technologies for measurements/clinical assessments. *Neurorehabilitation Technology, Second Edition*.
- [Lawrence et al., 2001] Lawrence, E. S., Coshall, C., Dundas, R., Stewart, J., Rudd, A. G., Howard, R., and Wolfe, C. D. (2001). Estimates of the prevalence of acute stroke impairments and disability in a multiethnic population. *Stroke*.
- [Lee et al., 2001] Lee, J. H. V. D., Beckerman, H., Lankhorst, G. J., and Bouter, L. M. (2001). The responsiveness of the action research arm test and the fugl-meyer assessment scale in chronic stroke patients. *Journal of Rehabilitation Medicine*.
- [Lee et al., 2019] Lee, S. I., Liu, X., Rajan, S., Ramasarma, N., Choe, E. K., and Bonato, P. (2019). A novel upper-limb function measure derived from finger-worn sensor data collected in a free-living setting. *PLoS ONE*.
- [Lemmens et al., 2012] Lemmens, R. J., Timmermans, A. A., Janssen-Potten, Y. J., Smeets, R. J., and Seelen, H. A. (2012). Valid and reliable instruments for arm-hand assessment at icf activity level in persons with hemiplegia: A systematic review. *BMC Neurology*.
- [Lenton et al., 2008] Lenton, J. P., Fowler, N. E., Woude, L. V. D., and Goosey-Tolfrey, V. L. (2008). Wheelchair propulsion: Effects of experience and push strategy on efficiency and perceived exertion. *Applied Physiology, Nutrition and Metabolism*.

Bibliography

- [Levin et al., 2009] Levin, M. F., Kleim, J. A., and Wolf, S. L. (2009). What do motor "recovery" and "compensation" mean in patients following stroke? *Neurorehabilitation and Neural Repair*.
- [Lewis et al., 2018] Lewis, A. R., Phillips, E. J., Robertson, W. S. P., Grimshaw, P. N., and Portus, M. (2018). Intra-stroke profiling of wheelchair propulsion using inertial measurement units. *proceedings*.
- [Li et al., 2010] Li, Q., Young, M., Naing, V., and Donelan, J. M. (2010). Walking speed estimation using a shank-mounted inertial measurement unit. *Journal of Biomechanics*.
- [Lindsay et al., 2019] Lindsay, M. P., Norrving, B., Sacco, R. L., Brainin, M., Hacke, W., Martins, S., Pandian, J., and Feigin, V. (2019). World stroke organization (wso): Global stroke fact sheet 2019. *International Journal of Stroke*.
- [Lord et al., 2013] Lord, S., Galna, B., Verghese, J., Coleman, S., Burn, D., and Rochester, L. (2013). Independent domains of gait in older adults and associated motor and nonmotor attributes: Validation of a factor analysis approach. *Journals of Gerontology - Series A Biological Sciences and Medical Sciences*.
- [Lyle, 1981] Lyle, R. C. (1981). A performance test for assessment of upper limb function in physical rehabilitation treatment and research. *International Journal of Rehabilitation Research*.
- [Ma et al., 2014] Ma, V. Y., Chan, L., and Carruthers, K. J. (2014). Incidence, prevalence, costs, and impact on disability of common conditions requiring rehabilitation in the united states: Stroke, spinal cord injury, traumatic brain injury, multiple sclerosis, osteoarthritis, rheumatoid arthritis, limb loss, and back pain. *Archives of Physical Medicine and Rehabilitation*.
- [MacDuff et al., 2022] MacDuff, H., Armstrong, E., and Ferguson-Pell, M. (2022). Technologies measuring manual wheelchair propulsion metrics: a scoping review. *Assistive Technology*.
- [Madgwick et al., 2011] Madgwick, S. O., Harrison, A. J., and Vaidyanathan, R. (2011). Estimation of imu and marg orientation using a gradient descent algorithm. *IEEE International Conference on Rehabilitation Robotics*.
- [Maetzler et al., 2013] Maetzler, W., Domingos, J., Srulijes, K., Ferreira, J. J., and Bloem, B. R. (2013). Quantitative wearable sensors for objective assessment of parkinson's disease. *Movement Disorders*.
- [Mansour et al., 2015] Mansour, K. B., Rezzoug, N., and Gorce, P. (2015). Analysis of several methods and inertial sensors locations to assess gait parameters in able-bodied subjects. *Gait and Posture*.
- [Marco-Ahulló et al., 2021] Marco-Ahulló, A., Montesinos-Magraner, L., Gonzalez, L. M., Llorens, R., Segura-Navarro, X., and García-Massó, X. (2021). Validation of using smartphone built-in accelerometers to estimate the active energy expenditures of full-time manual wheelchair users with spinal cord injury. *Sensors*.
- [Maynard et al., 1997] Maynard, F. M., Bracken, M. B., Creasey, G., Ditunno, J. F., Donovan, W. H., Ducker, T. B., Garber, S. L., Marino, R. J., Stover, S. L., Tator, C. H., Waters, R. L., Wilberger, J. E., and Young, W. (1997). International standards for neurological and functional classification of spinal cord injury. *Spinal Cord*.
- [Meyer et al., 2019] Meyer, C., Killeen, T., Easthope, C. S., Curt, A., Bolliger, M., Linnebank, M., Zörner, B., and Filli, L. (2019). Familiarization with treadmill walking: How much is enough? *Scientific Reports*.
- [Meyer et al., 2022] Meyer, J. T., Werner, C., Hermann, S., Demkó, L., Lambercy, O., and Gassert, R. (2022). Understanding technology-induced compensation: Effects of a wrist-constrained robotic hand orthosis on grasping kinematics. *Biosystems and Biorobotics*.

- [Moreno et al., 2020] Moreno, D., Glasheen, E., Domingo, A., Panaligan, V. B., Penaflor, T., Rioveros, A., and Kressler, J. (2020). Validity of caloric expenditure measured from a wheelchair user smartwatch. *International Journal of Sports Medicine*.
- [Morganti et al., 2005] Morganti, B., Scivoletto, G., Ditunno, P., Ditunno, J. E., and Molinari, M. (2005). Walking index for spinal cord injury (wisci): Criterion validation. *Spinal Cord*.
- [Murphy et al., 2018] Murphy, M. A., Murphy, S., Persson, H. C., Bergström, U. B., and Sunnerhagen, K. S. (2018). Kinematic analysis using 3d motion capture of drinking task in people with and without upper-extremity impairments. *Journal of Visualized Experiments*, 2018.
- [Murphy et al., 2015] Murphy, M. A., Resteghini, C., Feys, P., and Lamers, I. (2015). An overview of systematic reviews on upper extremity outcome measures after stroke. *BMC Neurology*.
- [Murphy et al., 2011] Murphy, M. A., Willén, C., and Sunnerhagen, K. S. (2011). Kinematic variables quantifying upper-extremity performance after stroke during reaching and drinking from a glass. *Neurorehabilitation and Neural Repair*.
- [Murphy et al., 2012] Murphy, M. A., Willén, C., and Sunnerhagen, K. S. (2012). Movement kinematics during a drinking task are associated with the activity capacity level after stroke. *Neurorehabilitation and Neural Repair*, 26.
- [Nas, 2015] Nas, K. (2015). Rehabilitation of spinal cord injuries. *World Journal of Orthopedics*.
- [Nightingale et al., 2015] Nightingale, T. E., Walhin, J. P., Thompson, D., and Bilzon, J. L. J. (2015). Influence of accelerometer type and placement on physical activity energy expenditure prediction in manual wheelchair users. *PLoS ONE*.
- [Nilsson et al., 2014] Nilsson, J. O., Gupta, A. K., and Handel, P. (2014). Foot-mounted inertial navigation made easy. *IPIN 2014 - 2014 International Conference on Indoor Positioning and Indoor Navigation*.
- [Olesh et al., 2014] Olesh, E. V., Yakovenko, S., and Gritsenko, V. (2014). Automated assessment of upper extremity movement impairment due to stroke. *PLoS ONE*.
- [Oung et al., 2015] Oung, Q. W., Muthusamy, H., Lee, H. L., Basah, S. N., Yaacob, S., Sarillee, M., and Lee, C. H. (2015). Technologies for assessment of motor disorders in parkinson's disease: A review. *Sensors (Switzerland)*.
- [Panebianco et al., 2018] Panebianco, G. P., Bisi, M. C., Stagni, R., and Fantozzi, S. (2018). Analysis of the performance of 17 algorithms from a systematic review: Influence of sensor position, analysed variable and computational approach in gait timing estimation from imu measurements. *Gait and Posture*.
- [Patel et al., 2010] Patel, S., Hughes, R., Hester, T., Stein, J., Akay, M., Dy, J., and Bonato, P. (2010). Tracking motor recovery in stroke survivors undergoing rehabilitation using wearable technology. *2010 Annual International Conference of the IEEE Engineering in Medicine and Biology Society, EMBC'10*.
- [Patrick, 2003] Patrick, J. H. (2003). Case for gait analysis as part of the management of incomplete spinal cord injury. *Spinal Cord*.
- [Pike et al., 2018] Pike, S., Lannin, N. A., Wales, K., and Cusick, A. (2018). A systematic review of the psychometric properties of the action research arm test in neurorehabilitation. *Australian Occupational Therapy Journal*.

Bibliography

- [Pohl et al., 2020] Pohl, J., Held, J. P. O., Verheyden, G., Murphy, M. A., Engelter, S., Flöel, A., Keller, T., Kwakkel, G., Nef, T., Ward, N., Luft, A. R., and Veerbeek, J. M. (2020). Consensus-based core set of outcome measures for clinical motor rehabilitation after stroke—a delphi study. *Frontiers in Neurology*.
- [Pollock et al., 2014] Pollock, A., Farmer, S. E., Brady, M. C., Langhorne, P., Mead, G. E., Mehrholz, J., and van Wijck, F. (2014). Interventions for improving upper limb function after stroke. *Cochrane Database of Systematic Reviews*.
- [Popp et al., 2018] Popp, W. L., Richner, L., Brogioli, M., Wilms, B., Spengler, C. M., Curt, A. E., Starkey, M. L., and Gassert, R. (2018). Estimation of energy expenditure in wheelchair-bound spinal cord injured individuals using inertial measurement units. *Frontiers in Neurology*.
- [Popp et al., 2019] Popp, W. L., Schneider, S., Bär, J., Bösch, P., Spengler, C. M., Gassert, R., and Curt, A. (2019). Wearable sensors in ambulatory individuals with a spinal cord injury: From energy expenditure estimation to activity recommendations. *Frontiers in Neurology*.
- [Prange-Lasonder et al., 2021] Prange-Lasonder, G. B., Murphy, M. A., Lamers, I., Hughes, A. M., Bururke, J. H., Feys, P., Keller, T., Klamroth-Marganska, V., Tarkka, I. M., Timmermans, A., and Burridge, J. H. (2021). European evidence-based recommendations for clinical assessment of upper limb in neurorehabilitation (caulin): data synthesis from systematic reviews, clinical practice guidelines and expert consensus. *Journal of NeuroEngineering and Rehabilitation*.
- [Ramer et al., 2014] Ramer, L. M., Ramer, M. S., and Bradbury, E. J. (2014). Restoring function after spinal cord injury: Towards clinical translation of experimental strategies. *The Lancet Neurology*.
- [Rampp et al., 2015] Rampp, A., Barth, J., Schüle, S., Gaßmann, K. G., Klucken, J., and Eskofier, B. M. (2015). Inertial sensor-based stride parameter calculation from gait sequences in geriatric patients. *IEEE Transactions on Biomedical Engineering*.
- [Rast et al., 2022] Rast, F. M., Aschwanden, S., Werner, C., Demkó, L., and Labruyère, R. (2022). Accuracy and comparison of sensor-based gait speed estimations under standardized and daily life conditions in children undergoing rehabilitation. *Journal of NeuroEngineering and Rehabilitation*.
- [Rast and Labruyère, 2020] Rast, F. M. and Labruyère, R. (2020). Systematic review on the application of wearable inertial sensors to quantify everyday life motor activity in people with mobility impairments. *Journal of NeuroEngineering and Rehabilitation*.
- [Repnik et al., 2018] Repnik, E., Puh, U., Goljar, N., Munih, M., and Mihelj, M. (2018). Using inertial measurement units and electromyography to quantify movement during action research arm test execution. *Sensors (Switzerland)*.
- [Requejo et al., 2008] Requejo, P. S., Mulroy, S. J., Haubert, L. L., Newsam, C. J., Gronley, J. A. K., and Perry, J. (2008). Evidence-based strategies to preserve shoulder function in manual wheelchair users with spinal cord injury. *Topics in Spinal Cord Injury Rehabilitation*.
- [Richter et al., 2007] Richter, W. M., Rodriguez, R., Woods, K. R., and Axelson, P. W. (2007). Stroke pattern and handrim biomechanics for level and uphill wheelchair propulsion at self-selected speeds. *Archives of Physical Medicine and Rehabilitation*.
- [Ryerson, 2009] Ryerson, S. (2009). Neurological assessment: The basis of clinical decision making. *Pocketbook of Neurological Physiotherapy*.
- [Sabatini et al., 2005] Sabatini, A. M., Martelloni, C., Scapellato, S., and Cavallo, F. (2005). Assessment of walking features from foot inertial sensing. *IEEE Transactions on Biomedical Engineering*.

- [Saes et al., 2022] Saes, M., Refai, M. I. M., van Beijnum, B. J. F., Bussmann, J. B. J., Jansma, E. P., Veltink, P. H., Buurke, J. H., van Wegen, E. E. H., Meskers, C. G. M., Krakauer, J. W., and Kwakkel, G. (2022). Quantifying quality of reaching movements longitudinally post-stroke: A systematic review. *Neurorehabilitation and neural repair*.
- [Salarian et al., 2004] Salarian, A., Russmann, H., Vingerhoets, F. J., Dehollain, C., Blanc, Y., Burkhard, P. R., and Aminian, K. (2004). Gait assessment in parkinson's disease: Toward an ambulatory system for long-term monitoring. *IEEE Transactions on Biomedical Engineering*.
- [Salter et al., 2005] Salter, K., Jutai, J. W., Teasell, R., Foley, N. C., Bitensky, J., and Bayley, M. (2005). Issues for selection of outcome measures in stroke rehabilitation: Icf participation. *Disability and Rehabilitation*.
- [Samuel et al., 2017] Samuel, G. S., Oey, N. E., Choo, M., Ju, H., Chan, W. Y., Kok, S., Ge, Y., Dongen, A. M. V., and Ng, Y. S. (2017). Combining levodopa and virtual reality-based therapy for rehabilitation of the upper limb after acute stroke: Pilot study part ii. *Singapore Medical Journal*.
- [Sapienza et al., 2017] Sapienza, S., Adans-Dester, C., O'Brien, A., Vergara-Diaz, G., Lee, S., Patel, S., Black-Schaffer, R., Zafonte, R., Bonato, P., Meagher, C., Hughes, A. M., Burrige, J., and Demarchi, D. (2017). Using a minimum set of wearable sensors to assess quality of movement in stroke survivors. *Proceedings - 2017 IEEE 2nd International Conference on Connected Health: Applications, Systems and Engineering Technologies, CHASE 2017*.
- [Sasaki et al., 2017] Sasaki, J. E., Sandroff, B., Bamman, M., and Motl, R. W. (2017). Motion sensors in multiple sclerosis: Narrative review and update of applications. *Expert Review of Medical Devices*.
- [Schneider et al., 2019] Schneider, S., Popp, W. L., Brogioli, M., Albisser, U., Ortmann, S., Velstra, I. M., Demko, L., Gassert, R., and Curt, A. (2019). Predicting upper limb compensation during prehension tasks in tetraplegic spinal cord injured patients using a single wearable sensor. *IEEE International Conference on Rehabilitation Robotics*.
- [Schwarz et al., 2019] Schwarz, A., Kanzler, C. M., Lambercy, O., Luft, A. R., and Veerbeek, J. M. (2019). Systematic review on kinematic assessments of upper limb movements after stroke. *Stroke*.
- [Scivoletto et al., 2007] Scivoletto, G., Ivanenko, Y., Morganti, B., Grasso, R., Zago, M., Lacquaniti, F., Ditunno, J., and Molinari, M. (2007). Review article: Plasticity of spinal centers in spinal cord injury patients: New concepts for gait evaluation and training. *Neurorehabilitation and Neural Repair*.
- [Seel and Ruppel, 2017] Seel, T. and Ruppel, S. (2017). Eliminating the effect of magnetic disturbances on the inclination estimates of inertial sensors. *IFAC-PapersOnLine*.
- [Shema-Shiratzky et al., 2019] Shema-Shiratzky, S., Gazit, E., Sun, R., Regev, K., Karni, A., Sosnoff, J. J., Herman, T., Mirelman, A., and Hausdorff, J. M. (2019). Deterioration of specific aspects of gait during the instrumented 6-min walk test among people with multiple sclerosis. *Journal of Neurology*.
- [Shin et al., 2013] Shin, J. C., Kim, D. H., Yu, S. J., Yang, H. E., and Yoon, S. Y. (2013). Epidemiologic change of patients with spinal cord injury. *Annals of Rehabilitation Medicine*.
- [Shirota et al., 2019] Shirota, C., Balasubramanian, S., and Melendez-Calderon, A. (2019). Technology-aided assessments of sensorimotor function: Current use, barriers and future directions in the view of different stakeholders. *Journal of NeuroEngineering and Rehabilitation*.
- [Simbaña et al., 2019] Simbaña, E. D. O., Baeza, P. S.-H., Huete, A. J., and Balaguer, C. (2019). Review of automated systems for upper limbs functional assessment in neurorehabilitation. *IEEE Access*.

Bibliography

- [Simpson and Eng, 2013] Simpson, L. A. and Eng, J. J. (2013). Functional recovery following stroke: Capturing changes in upper-extremity function. *Neurorehabilitation and Neural Repair*.
- [Song, 2012] Song, C. S. (2012). Intrarater reliability of the action research arm test for individuals with parkinson's disease. *Journal of Physical Therapy Science*.
- [Song and Hidler, 2008] Song, J. L. and Hidler, J. (2008). Biomechanics of overground vs. treadmill walking in healthy individuals. *Journal of Applied Physiology*.
- [Steinert et al., 2020] Steinert, A., Sattler, I., Otte, K., Röhling, H., Mansow-Model, S., and Müller-Werdan, U. (2020). Using new camera-based technologies for gait analysis in older adults in comparison to the established gaitrite system. *Sensors*.
- [Steitz et al., 2022] Steitz, M. K., Renzel, R., Schönhammer, J., Valladares, B., Schreiner, S. J., Widmer, M., Rasch, B., Luft, A. R., and Baumann, C. R. (2022). Improved Motor Learning after Stroke using Auditory Targeted Memory Reactivation. *in prep*.
- [Stieglitz et al., 2021] Stieglitz, L. H., Hofer, A. S., Bolliger, M., Oertel, M. F., Filli, L., Willi, R., Cathomen, A., Meyer, C., Schubert, M., Hubli, M., Kessler, T. M., Baumann, C. R., Imbach, L., Krüsi, I., Prusse, A., Schwab, M. E., Regli, L., and Curt, A. (2021). Deep brain stimulation for locomotion in incomplete human spinal cord injury (dbs-sci): Protocol of a prospective one-armed multi-centre study. *BMJ Open*.
- [Storm et al., 2020] Storm, F. A., Cesareo, A., Reni, G., and Biffi, E. (2020). Wearable inertial sensors to assess gait during the 6-minute walk test: A systematic review. *Sensors (Switzerland)*.
- [Suto et al., 2017] Suto, J., Oniga, S., and Sitar, P. P. (2017). Feature analysis to human activity recognition. *International Journal of Computers, Communications and Control*.
- [Tang et al., 2020] Tang, L., Halloran, S., Shi, J. Q., Guan, Y., Cao, C., and Eyre, J. (2020). Evaluating upper limb function after stroke using the free-living accelerometer data. *Statistical Methods in Medical Research*.
- [Tator, 1995] Tator, C. H. (1995). Update on the pathophysiology and pathology of acute spinal cord injury. *Brain Pathology*.
- [Thrane et al., 2020] Thrane, G., Thrane, G., Sunnerhagen, K. S., and Murphy, M. A. (2020). Upper limb kinematics during the first year after stroke: The stroke arm longitudinal study at the university of gothenburg (salgot). *Journal of NeuroEngineering and Rehabilitation*.
- [Tong and Granat, 1999] Tong, K. and Granat, M. H. (1999). A practical gait analysis system using gyroscopes. *Medical Engineering and Physics*.
- [Trojaniello et al., 2014a] Trojaniello, D., Cereatti, A., and Croce, U. D. (2014a). Gait direction of progression estimate using shank worn mimus. *Gnb2014*.
- [Trojaniello et al., 2014b] Trojaniello, D., Cereatti, A., Pelosin, E., Avanzino, L., Mirelman, A., Hausdorff, J. M., and Croce, U. D. (2014b). Estimation of step-by-step spatio-temporal parameters of normal and impaired gait using shank-mounted magneto-inertial sensors: application to elderly, hemiparetic, parkinsonian and choreic gait. *J Neuroeng Rehabil*.
- [Trojaniello et al., 2014c] Trojaniello, D., Cereatti, A., Ravaschio, A., Bandettini, M., and Croce, U. D. (2014c). Assessment of gait direction changes during straight-ahead walking in healthy elderly and huntington disease patients using a shank worn mimu. *2014 36th Annual International Conference of the IEEE Engineering in Medicine and Biology Society, EMBC 2014*.

- [Tunca et al., 2017] Tunca, C., Pehlivan, N., Ak, N., Arnrich, B., Salur, G., and Ersoy, C. (2017). Inertial sensor-based robust gait analysis in non-hospital settings for neurological disorders. *Sensors (Switzerland)*.
- [Turner et al., 2001] Turner, J. A., Cardenas, D. D., Warms, C. A., and McClellan, C. B. (2001). Chronic pain associated with spinal cord injuries: A community survey. *Archives of Physical Medicine and Rehabilitation*.
- [van Middendorp et al., 2011] van Middendorp, J. J., Goss, B., Urquhart, S., Atresh, S., Williams, R. P., and Schuetz, M. (2011). Diagnosis and prognosis of traumatic spinal cord injury. *Global Spine Journal*.
- [Vasudevan et al., 2022] Vasudevan, S., Saha, A., Tarver, M. E., and Patel, B. (2022). Digital biomarkers: Convergence of digital health technologies and biomarkers. *npj Digital Medicine*.
- [Vienne et al., 2017] Vienne, A., Barrois, R. P., Buffat, S., Ricard, D., and Vidal, P. P. (2017). Inertial sensors to assess gait quality in patients with neurological disorders: A systematic review of technical and analytical challenges. *Frontiers in Psychology*.
- [Wahlstrom and Skog, 2021] Wahlstrom, J. and Skog, I. (2021). Fifteen years of progress at zero velocity: A review. *IEEE Sensors Journal*.
- [Werner et al., 2021] Werner, C., Easthope, C. A., Curt, A., and Demkó, L. (2021). Towards a mobile gait analysis for patients with a spinal cord injury: A robust algorithm validated for slow walking speeds. *Sensors*.
- [WHO, 2001] WHO, W. H. O. (2001). International classification of functioning, disability and health (icf). *World Health Organization*.
- [WHO, 2006] WHO, W. H. O. (2006). Neurological disorders: public health challenges. *World Health Organization*.
- [WHO, 2013] WHO, W. H. O. (2013). International perspectives on spinal cord injury. *World Health Organization*.
- [Wirz and van Hedel, 2018] Wirz, M. and van Hedel, H. J. (2018). Balance, gait, and falls in spinal cord injury. *Handbook of Clinical Neurology*.
- [Wirz et al., 2006] Wirz, M., van Hedel, H. J., Rupp, R., Curt, A., and Dietz, V. (2006). Muscle force and gait performance: Relationships after spinal cord injury. *Archives of Physical Medicine and Rehabilitation*.
- [Wolf et al., 2021] Wolf, S., Gerloff, C., and Backhaus, W. (2021). Predictive value of upper extremity outcome measures after stroke—a systematic review and metaregression analysis. *Frontiers in Neurology*.
- [Wyndaele and Wyndaele, 2006] Wyndaele, M. and Wyndaele, J. J. (2006). Incidence, prevalence and epidemiology of spinal cord injury: What learns a worldwide literature survey? *Spinal Cord*.
- [Yang and Li, 2012] Yang, S. and Li, Q. (2012). Inertial sensor-based methods in walking speed estimation: A systematic review. *Sensors (Switzerland)*.
- [Yozbatiran et al., 2008] Yozbatiran, N., Der-Yeghiaian, L., and Cramer, S. C. (2008). A standardized approach to performing the action research arm test. *Neurorehabilitation and Neural Repair*.
- [Zhang et al., 2018] Zhang, W., Smuck, M., Legault, C., Ith, M. A., Muaremi, A., and Aminian, K. (2018). Gait symmetry assessment with a low back 3d accelerometer in post-stroke patients. *Sensors (Switzerland)*.

Complete List of Publications

Journal Papers

- (1) **C. Werner**, C. Awai Easthope, A. Curt, and L. Demkó, "Towards a mobile gait analysis for patients with a spinal cord injury: a robust algorithm validated for slow walking speeds", in *Sensors*, 2021
- (2) **C. Werner***, J. G Schönhammer*, M. K. Steitz, O. Lambercy, A. R. Luft, L. Demkó, and C. Awai Easthope, "Using Wearable Inertial Sensors to Estimate Clinical Scores of Upper Limb Movement Quality in Stroke", in *Frontiers in Physiology*, 2022
- (3) R. Femiano, **C. Werner**, M. Wilhelm, and P. Eser, "Validation of open-source step-counting algorithms for wrist-worn tri-axial accelerometers in cardiovascular patients", in *Gait & posture*, 2022
- (4) P. Eser, N. Gonzalez-Jaramillo, S. Weber, R. Femiano, **C. Werner**, F. Casanova, A. Bano, O.H. Franco, and M. Wilhelm "Comparison of the 2010 and 2020 World Health Organization guidelines on physical activity in patients with percutaneous coronary interventions early after hospital discharge", in *European Journal of Preventive Cardiology*, 2022
- (5) P. Eser, N. Gonzalez-Jaramillo, S. Weber, J. Fritsche, R. Femiano, **C. Werner**, F. Casanova, A. Bano, O. D. Franco, and M. Wilhelm "Objectively measured adherence to physical activity among patients with coronary artery disease: Comparison of the 2010 and 2020 World Health Organization guidelines and daily steps.", in *Frontiers in Cardiovascular Medicine*, 2022
- (6) F. M. Rast, S. Aschwanden, **C. Werner**, L. Demkó, and R. Labruyère, "Accuracy and comparison of sensor-based gait speed estimations under standardized and daily life conditions in children undergoing rehabilitation", in *Journal of NeuroEngineering and Rehabilitation*, 2022
- (7) **C. Werner***, M. Gönel*, I. Lerch, A. Curt, and L. Demkó, "Data-driven characterization of walking after a spinal cord injury using inertial sensors", *under evaluation*
- (8) S. Amrein, **C. Werner**, U. Arnet, and W. de Vries, "Machine learning based methodology for estimation of shoulder load in wheelchair-related activities using wearables", *under evaluation*
- (9) **C. Werner**, A. Linke, W. de Vries, A. Curt, and L. Demkó, "Determining wheeling propulsion patterns using a sparse inertial sensor setup", *in preparation*

Conference Contributions

- (1) **C. Werner**, S. Schneider, R. Gassert, A. Curt, and L. Demkó, "Complementing Clinical Gait Assessments of Spinal Cord Injured Individuals using Wearable Movement Sensors", in *2020 42nd Annual International Conference of the IEEE Engineering in Medicine & Biology Society (EMBC)*, 2020
- (2) J. T. Meyer*, **C. Werner***, S. Hermann, L. Demkó, O. Lambercy, and R. Gassert, "Understanding Technology-Induced Compensation: Effects of a Wrist-Constrained Robotic Hand Orthosis on Grasping Kinematics", in *International Symposium on Wearable Robotics*, 2020
- (3) **C. Werner**, A. Linke, A. Curt, and L. Demkó, "Assessing wheeling performance in patients with a spinal cord injury using wearable inertial sensors ", presented as a poster at *RehabWeek*, 2022

* authors share first authorship